Investigation into Pathological Responses of Two Phenotypes of the Scleractinian Coral, *Montastraea faveolata*, to Putative Marine *Vibrio* Pathogens

A Thesis Presented

by

Angela Richards Donà

to

The Graduate School

in Partial Fulfillment of the

Requirements

for the Degree of

Master of Science

in

Marine and Atmospheric Science

Stony Brook University

August 2012

Stony Brook University

The Graduate School

Angela Richards Donà

We, the thesis committee for the above candidate for the

Master of Science degree, hereby recommend

acceptance of this thesis.

Dr. Gordon T. Taylor – Thesis Advisor
Professor, Marine and Atmospheric Sciences

Dr. Glenn Lopez – Second Reader
Professor, Marine and Atmospheric Sciences

Dr. Bassem Allam – Third Reader
Associate Professor, Marine and Atmospheric Sciences

Dr. Esther Peters – Fourth Reader
Assistant Professor (Term), Environmental Science and Policy, George Mason University

Dr. James Cervino – Fifth Reader
Guest Investigator, Woods Hole Oceanographic Institution

This thesis is accepted by the Graduate School

Charles Taber
Interim Dean of the Graduate School

Abstract of the Thesis

Investigation into the Pathological Responses of Two Phenotypes of the Scleractinian Coral, *Montastraea faveolata*, to Putative Marine *Vibrio* Pathogens

by

Angela Richards Donà

Master of Science

in

Marine and Atmospheric Science

Stony Brook University

2012

Corals of the genus *Montastraea* in the Caribbean are highly susceptible to disease, although not all neighboring colonies appear to be affected on the same time scales. Stressed corals are unable to function optimally and are less likely to be reproductively successful than those that are not stressed. *Montastraea* spp. corals, like all corals from the order Scleractinia, are adapted to the narrow ranges in temperature and irradiance found in tropical waters. These environmental factors play an important role in a coral colony's ability to maintain homeostasis and excursions from their normal ranges for extended periods of time can trigger coral stress responses. Experiments using specimens from two *M. faveolata* colonies exposed to *Vibrio* spp. bacteria, at normal and elevated temperatures, provided a means by which presumed physiological differences between these colonies could be identified and tested under acutely stressful conditions. Two strains of *Vibrio harveyi* and one strain of *Vibrio parahaemolyticus* were used separately and in combination to induce Caribbean yellow band disease (CYBD)-like lesions. At the conclusion of the challenge experiments (34 days), all specimens except one lacked lesions or other gross morphological changes generally recognized as signs of disease. The tissue sections, however, showed notable and often severe increase in pathological changes in all treated specimens. Pathological changes are defined as any alterations in the function, structure or appearance of tissues from normal that impair the coral.

Severity scores corresponding to the frequency with which a pathological change was observed were assigned for 33 criteria (0% = no change). Exposed specimens scored consistently high for certain criteria, i.e., karyolysis of the nuclei in the gastrodermis, changes to nuclei of symbiotic algae (zooxanthellae), and loss of integrity of the epidermis (with average severity scores 3.9, 3.5, and 3.2, respectively). A severity score of 3.2 corresponds to approximately 55% frequency of the observed pathological change per section of tissue, and 3.9 corresponds to roughly 70% frequency, clearly suggesting coral stress. Kruskal-Wallis H test analyses of the histopathological indices failed to find statistically significant differences in responses of the two phenotypes and their overall responses to elevated temperature (27 vs. 32°C). Control specimens were generally found to be in better condition than the bacteria-exposed counterparts but the condition of the treated corals appeared to improve after the exposure period, while the controls' condition worsened. Notable morphological differences at the light microscopic level exist between the phenotypes but acute exposure to putative pathogenic bacteria resulted in similar pathological changes to the coral epithelia and mesenteries despite colony dissimilarities. Large numbers of degenerating zooxanthellae were observed associated with lysosomes in the deep gastrodermis of the basal body wall in what is believed to be the first reported case of symbiophagy in *Montastraea* spp. corals resulting in the digestion of the symbionts *in situ*. Another novel finding is the presence of clusters of suspect bacteria in the coral skeleton lining the calicodermis and in close association with the endolithic communities. Field-collected samples from CYBD-infected colonies were compared to the experimental specimens to determine whether the *Vibrio* spp. used as inocula caused similar pathology to that occurring in the natural environment. Histological analysis of these CYBD samples showed that the pathological signs were observably different from those experimentally induced and may result from chronic exposures that cause lesions when additional environmental factors provide conditions that favor the opportunistic microbes.

Table of Contents

List of Figures

List of Tables

List of Abbreviations

(CYBD)	Caribbean yellow band disease
(H&E)	Hematoxylin and eosin
(P1)	Phenotype 1
(P2)	Phenotype 2
(SBW)	Surface body wall
(BBW)	Basal body wall
(DIH_2O)	Deionized water
(LKDS)	Field-collected Looe Key CYBD Lesion Samples
(LKHS)	Field-collected Looe Key Presumed Healthy Samples
(FISH)	Fluorescence in situ hybridization

Acknowledgments

Special thanks go to: Thomas Plant/Plant Family Environmental Foundation for partial funding of the challenge experiment component of this research; Erich Bartels of Mote Marine Laboratory for the many tasks that were essential to the success of the challenge experiment; Dr. Konrad Hughen of Woods Hole Oceanographic Institution (WHOI) for partial funding of the challenge experiment and sharing field samples from Looe Key; Dr. Gary Vora of the U.S. Navy for providing the *Vibrio* spp. used for the challenge experiments; Dr. David Allen of the National Institute of Standards and Technology (NIST) for measurements of the daily PAR values at Mote, assistance during the challenge experiments, and with Dr. Jeeseong Hwang from NIST for instruction on and help with all aspects of the spectral imaging of slides prepared for FISH; Dr. Thomas J. Goreau for his generous advice and for the use of his father's beautiful coral illustration; Dr. Yee Ean Ong for statistics and pathology advice; and Alessandro Donà for the field photography and assistance during the field work. Many thanks also go to Sara Cernadas Martin and Agnieszka Podlaska for help in the lab, to Emmanuelle Pales-Espinosa for her excellent instruction in FISH protocol, and to Briana Hauff for editing my first draft.

I would like to thank my advisor Dr. Taylor, for taking me into his lab, for superior instruction in microbiology, for the patience he has shown me, and especially for edits to this thesis that greatly improved it. I also truly appreciate his high standards, although at times I felt the bar was so high I'd never be able to reach it. I am hugely grateful to Dr. Cervino, without whom I would not be here writing this thesis. He did not let the little thing of my art background get in the way of helping get into grad school to research coral disease. Hearty thanks go to Dr. Lopez for peerless instruction in class, hugely interesting conversation (on and off topic), and his well-pointed advice, and to Dr. Allam who has been a great resource for questions about pathology and whose advice improved many aspects of my research. Deep gratitude goes to Dr. Peters for incredible generosity with her time and her knowledge. I am also very grateful for her friendship. I feel so fortunate to have such a brilliant, and multi-faceted group of scientists on my side and I have learned so much from all of them.

Introduction

Coral reefs are among the most diverse ecosystems in the world and are of enormous value as a natural resource as well as a source of natural beauty. They provide protection to coastal areas, employment, food, and are of growing importance to the tourism industry. Many coastal communities rely on the health and bounty of the coral reefs for their very existence. Despite their importance, coral reefs are currently under attack by a myriad of stressors: thermal stress, pollution, overfishing, sedimentation and pathogenic microorganisms (Glynn 1991; Goreau et al. 1998; Harvell et al. 1999; Cervino et al. 2001; Bruno et al. 2003; Weil et al. 2006), to name a few. In 1973, the first coral disease was recorded and since then diseases such as Caribbean yellow band disease (CYBD), white band disease, white plague, bacterial and thermal bleaching, and black band disease have become common sightings on Caribbean reefs. Most current evidence shows that microbial pathogens play a major role in most "band" diseases (Santavy and Peters 1997) as well as bleaching in the Mediterranean Sea (Kushmaro et al. 1997), Indian Ocean and Red Sea (Ben-Haim et al. 2003). This investigation was undertaken to elucidate potential causes of coral colony disease vulnerability by challenging two distinct phenotypes of an important and threatened coral species, *Montastraea faveolata*, known to be susceptible to the putative bacterial pathogens of CYBD.

Coral anatomy, physiology and histology

Scleractinian corals are members of the phylum Cnidaria and as such have a very simple body plan and possess epithelial, muscle, connective, and nervous tissues. They are diploblastic Eumetazoans at the tissue grade of construction (Hyman 1940) and have tentacles with cnidae, adhesive or stinging cells. They exhibit primary hexamerous, radial symmetry (from fertilized egg to adult) with polyps that arrange themselves around an oral-aboral axis inside a corallite—the cup-like skeleton in which each polyp is fixed. The incomplete gastrovascular cavity has one opening at the oral disk, and is derived from one of only two embryonic germ layers: the endoderm. The ectoderm forms the middle layer mesoglea—the fibrous connective tissue that

supports the epithelia—and the epidermis. Externally, polyps are connected by the coenenchyme, whereas internally, gastrovascular cavities are connected by various gastrovascular canals. These canals allow the colonial corals to share resources among polyps. The gastrovascular cavity is partitioned by vertical walls of tissue in multiples of six, called mesenteries, that either extend entirely to the tubular actinopharynx or are incomplete. Greatly folded mesenteries provide the gastrovascular cavity with supporting structure—via longitudinal retractor and transverse mesenterial muscles—and increased surface area for nutrient uptake. The free inner edges of the mesenteries are mesenterial filaments (Figure 1), the thick rounded margin of which is the cnidoglandular band, and the site of a battery of nematocysts and lysozyme-containing cells. The mesenteries help protect corals from attack by other organisms and fend off competitors for viable reef substrate by extending out of the mouth or cinclides (temporary apertures or pores) in the tissue and discharging their nematocysts or digesting the intruder by release of hydrolytic enzymes stored in the acidophilic granular gland cells (Goreau 1956, Galloway et al. 2006).

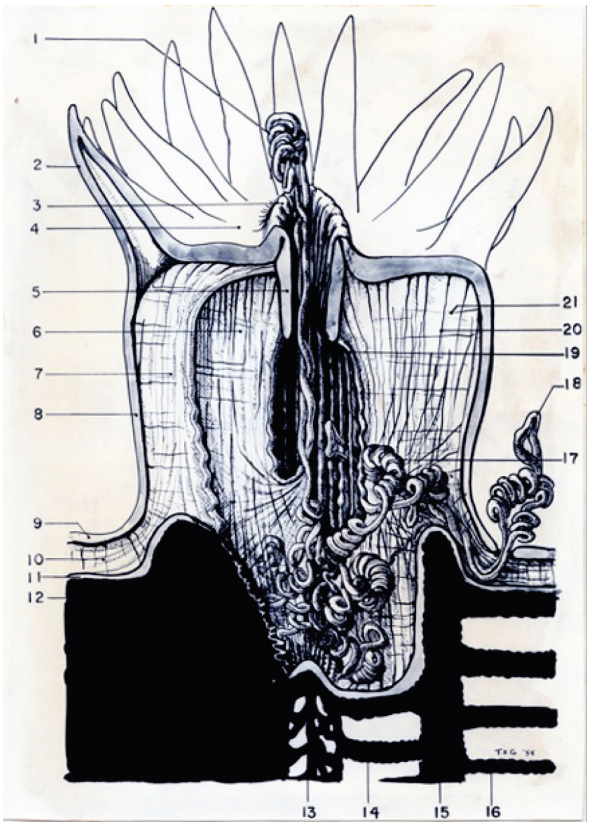

1. Mesenterial filament (through mouth)
2. Tentacle
3. Mouth
4. Oral disk
5. Actinopharynx
6. Complete mesentery
7. Incomplete mesentery
8. Surface body wall
9. Edge zone or coenenchyme
10. Gastrovascular canal
11. Basal body wall
12. Costa and septum
13. Columella
14. Endotheca
15. Theca
16. Peritheca
17. Mesenterial filament (pars convoluta)
18. Mesenterial filament (through cinclide)
19. Mesenterial filament (pars recta)
20. Longitudinal retractor muscle fibers in mesentery
21. Radial muscle fibers in mesentery

Figure 1. Anatomy of a scleractinian coral. Illustration by T.F. Goreau, 1956.

Animals at the tissue grade of construction have epithelia but no formation of organs. Scleractinian coral bodies consist of two basic strata of epithelia; the surface body wall (SBW) consisting of the epidermis, mesoglea, and gastrodermis (Figure 2); and the basal body wall (BBW) consisting of gastrodermis, mesoglea, and calicodermis. The epidermis is the outermost layer with cilia on the free surface in contact with seawater. The calicodermis is the site of actively accreting aragonite and where the coral tissue attaches to the exoskeleton or "corallum." It is the presence of the corallum that inspired the common name "stony corals" and defines their sessile lifestyle. The gastrodermis of the SBW and BBW that enclose the gastrovascular cavities and canals of the colonial polyps contain intracellular symbiotic dinoflagellates also known as zooxanthellae. These photosynthetic algae take up residence inside membrane-bound vacuoles of gastrodermal cells and provide the coral host their photosynthate for nutrition.

Stony corals, including *Montastraea faveolata*, have the fewest cell types of all animals with the exception of sponges and mesozoans. The epidermis of the surface body wall is pseudostratified and consists primarily of ciliated columnar epitheliomuscular and supporting cells with a negligible amount of extracellular matrix. Columnar mucocytes are fairly evenly interspersed along the epidermis, actively secreting mucus and releasing it through an apical pore (Figure 2). This mucopolysaccharide layer is critical for the optimal functioning and protection of the coral colony. All cells are attached to the basal lamina but not all reach the surface and are therefore not in contact with seawater. The nuclei of the epidermis are oblong or ovoid. Contractile tentacles that extend from the oral disk aid the coral in capturing food, removal of settling organisms and sediment, and defense. The epidermis (including tentacles) of *M. faveolata* may also contain spirocysts—tightly coiled tubules of sticky microfibrillae inside a single-walled capsule—other nematocysts also produced by cnidocytes, and sensory, interstitial, and pigment cells. The mesoglea is a highly fibrous connective tissue made up of various cells and collagenous fibers in an abundant, hydrated, amorphous protein and polysaccharide matrix or "ground substance." This thin layer provides the epidermis and gastrodermis with structural stability and a medium for transport between them. The gastrodermal epithelia of the surface and basal body walls form the inner lining of the gastrovascular cavity and are important for the digestion of food particles, absorption of nutrients and discharge of waste products. They are made up primarily of cuboidal or columnar nutritive-muscular cells and membrane-bound vacuoles occupied by zooxanthellae (Figure 2).

Zooxanthellae are typically present in areal densities of approximately one million cells per square centimeter of coral tissue and have unique nuclei with permanently condensed chromatin (Muller-Parker and D'Elia 1997). In addition, granular gland cells, supporting cells, cnidocytes, mucocytes, amoebocytes and sensory cells can be found in the gastrodermal epithelia. The calicodermis (formerly calicoblastic epithelium) is made up of mostly cuboidal cells modified to produce and discharge an organic matrix in which calcium carbonate crystals condense to form the aragonite skeleton. Near the surface and along the septa and costae, these cells may become fairly elongated and threadlike. Desmocytes are anchor cells present in the calicodermis that are modified via fingerlike extensions on the proximal surface that weave into the collagen fibers of the mesoglea. On their distal surface, filaments extend out and attach to the skeleton (Muscatine et al. 1997; Peters 2011).

Montastraea faveolata

Montastraea faveolata corals found between the 0 and 25 m depth range are mostly large, boulder-like structures that are wide at their bases and taper upwards in the water column to a rounded or flattened apex. Most have knobby protrusions or ridges that run, often in straight lines, longitudinally along the colony surface and have free edges at the base of the colony and slopes that resemble flared skirts. *M. faveolata* colonies may also form plate-like structures where sunlight penetration is less intense, i.e., below 15 m or under or alongside structures such as natural overhangs, docks or seawalls (pers. observ.; Szmant et al. 1997). Zooxanthellae that form symbioses with these corals possess diadinoxanthin and peridinin—characteristic brown or yellow-brown pigments—in addition to chlorophylls *a* and *c* (Muller-Parker and D'Elia 1997). These pigments are responsible for the yellow-brown pigmentation of many *M. faveolata* colonies. *Montastraea* spp. corals form partnerships with a number of zooxanthellae clades, simultaneously, and the location of each clade depends on the irradiance levels (Rowan et al. 1997; Knowlton and Rohwer 2003). In addition to brown hues, *M. faveolata* display colors such as beige, dark orange-brown, and iridescent pale green and lilac (Figure 3).

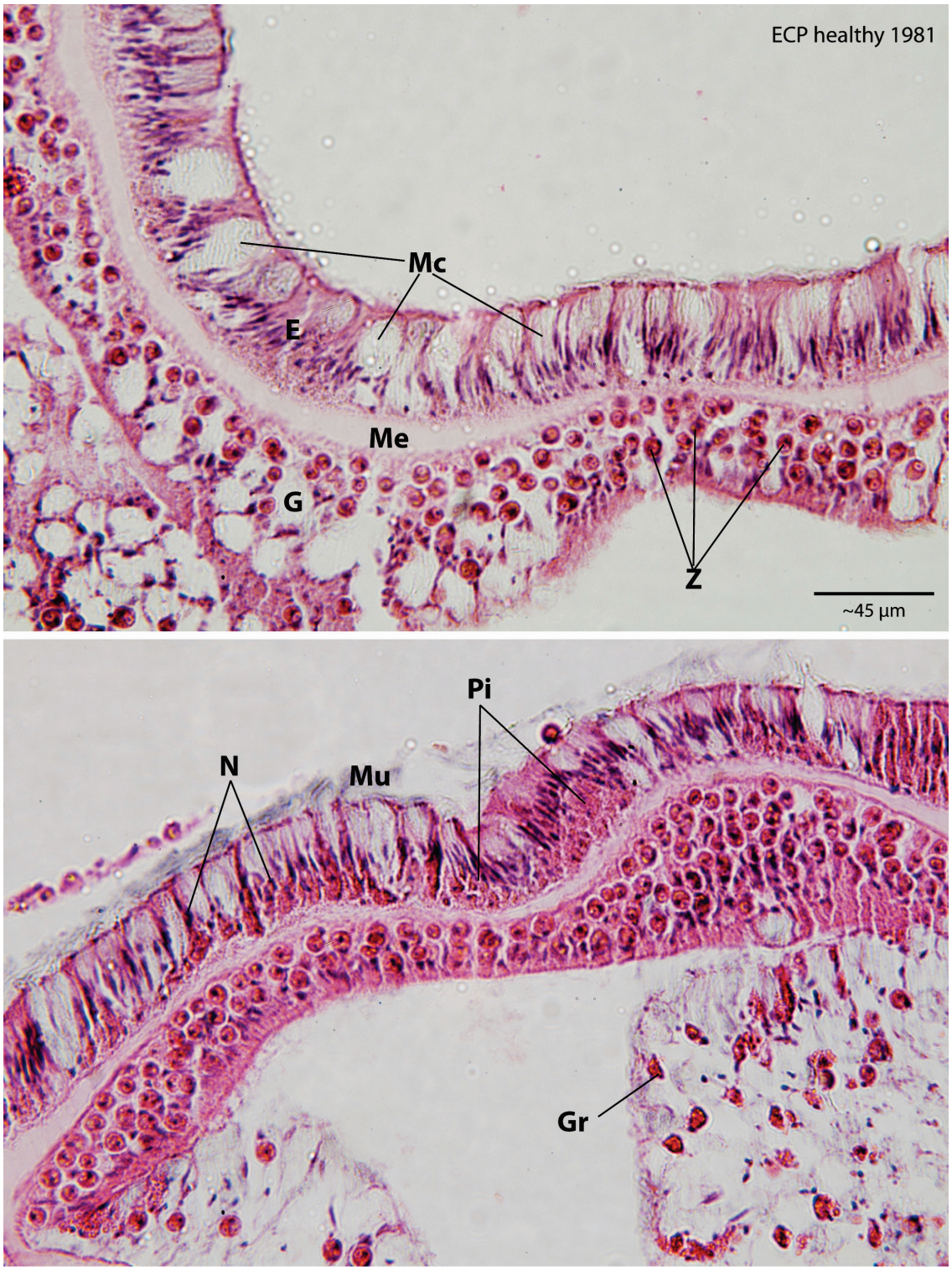

Figure 2. Healthy *M. faveolata* specimens from Dr. Esther Peters, collected and processed in 1981. E = epidermis, G = gastrodermis, Me = mesoglea, Z = zooxanthellae, Mc = mucocytes, N = nuclei, Mu = mucus, Pi = pigment cells, Gr = granular gland cell. Scale bar for both photomicrographs.

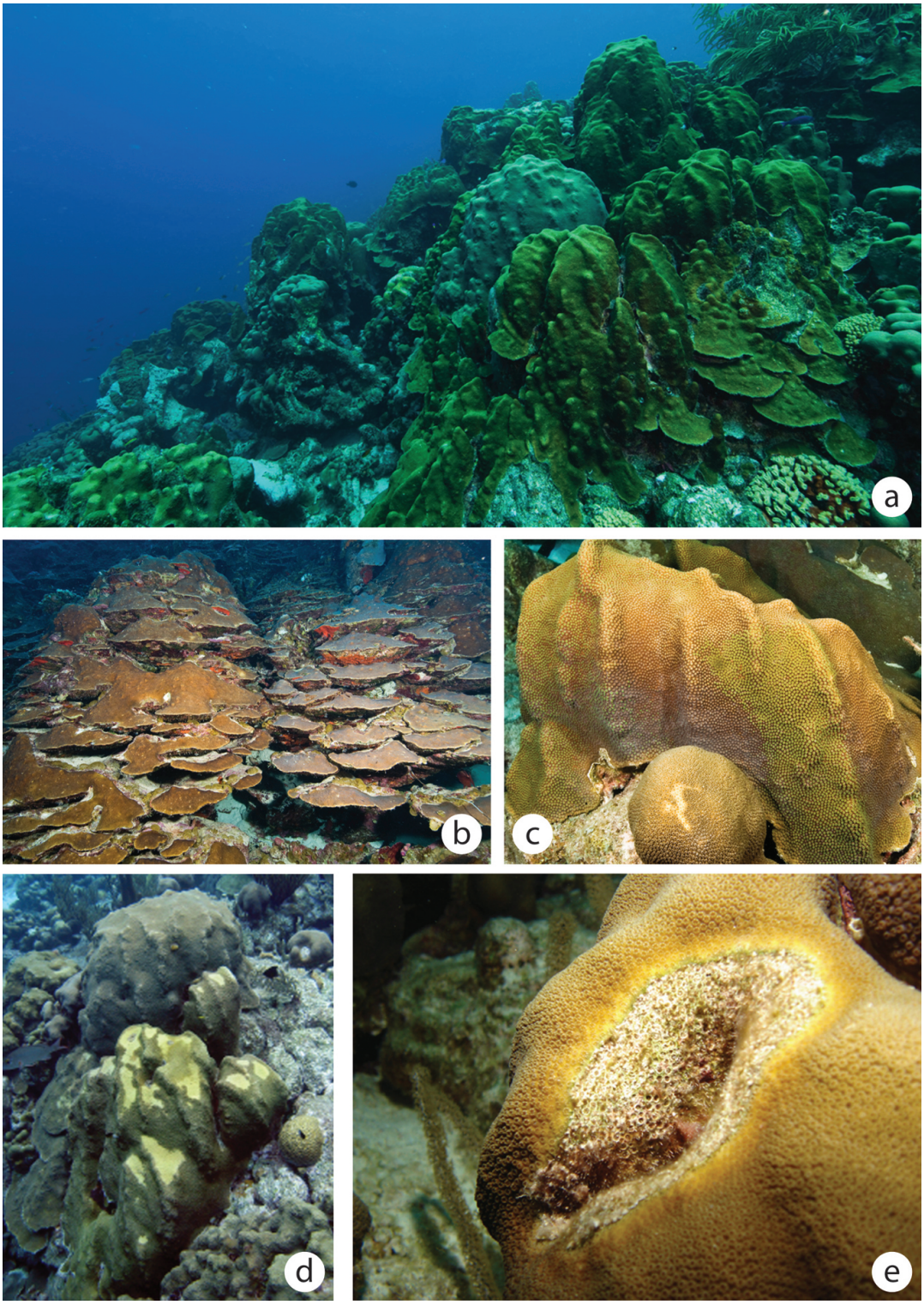

Figure 3. *Montastraea faveolata*. Pictorial examples of morphology, pigmentation, and disease. (*a*) Typical morphology at 5 to 15 m depth, (*b*) typical morphology below 15 m, (*c*) atypical display of various pigmentations on one colony, (*d*) colony in recovery phase after bleaching, (*e*) colony with signs of CYBD. Photos: Alessandro Donà, Bonaire, 2007-2011.

Microscopically, *M. faveolata* colonies are imperforate, which refers to the lack of openings in the aragonite theca (Figure 1) through which gastrovascular canals may run. Instead of *through* the walls of the corallite, the canals must run *over* them to form connections between polyps. Imperforate corals are distinguishable under the microscope having a well-defined polyp region connected by coenenchymal tissue that is continuous and just below the surface. The epidermis and the gastrodermis of the surface body wall should have approximately the same thickness, in contrast to their thinner mesogleal supporting layer (Figure 2). The layers of the BBW are more disparate with a very thin calicodermis and gastrodermis often many times thicker. An interesting characteristic of *M. faveolata* is the presence of assemblages of lightly golden, eosinophilic (pink) granular pigment cells (when stained with hematoxylin and eosin) often located at the base of the epidermis and in larger masses in the mesenteries (Figure 2). The appearance of clusters of brightly pink-stained granular gland cells (believed to contain lysozymes and zymogens) in the mesenteries—resembling individual raspberries, but different from those present in the cnidoglandular bands of the mesenterial filaments—is also among the unique characteristics of this genus (Figure 2). The lysosomes contained in these cells are also separate from those commonly found as normal constituents of all cells. *M. faveolata* is monoecious, therefore ova and spermaries develop in the same sac-like structures within the mesoglea along the mesenteries.

Each *M. faveolata* colony is uniquely situated in the water column upon a stretch of reef and each will be subject to the prevailing environmental conditions at its location. Theoretically, two colonies in close proximity to one another are very likely to experience the same environmental conditions. And yet, it is not uncommon to see one colony with lesions and another, directly adjacent, inexplicably without (pers. observ.). This may simply be a matter of a latent infection that has not yet formed gross visible lesions. But it is also possible that unique physiology between colonies may play a role. Whereas all *M. faveolata* colonies share the same general morphological, histological and ultrastructural characteristics, a wide range in variations of these shared characteristics is evident. Challenging two colonies/phenotypes harvested from neighboring locations provided experimental conditions to evaluate whether these colonies differed in their responses to the same acute microbial exposures.

Corals and coral disease

The obligate, symbiotic relationship reef-building corals form with zooxanthellae is an example of a mutualistic partnership. These photosynthetic unicellular algae are members of the genus *Symbiodinium*, which reside in the gastrodermis of the coral animal, provide between 63% and 95% of the products of photosynthesis to their host (Muscatine and Cernichiari 1969; Muscatine et al. 1981; Stat et al. 2006; Jones et al. 2008), and aid in the synthesis of the calcium carbonate skeleton underlying coral tissue (Pearse and Muscatine 1971; Goreau et al. 1979; Lajeunesse 2002). This union provides the symbiotic dinoflagellates with predation-free living conditions, carbon dioxide, and inorganic waste products of the host's metabolism (Pearse and Muscatine 1971; Goreau et al. 1979). In addition, corals use chemotaxis to detect particulate animal food in the surrounding water and either sweeps it into the mouth with tentacles, convey it via ciliary action into the gastrovascular cavity, or digests it extracellularly by extruding mesenterial filaments (Goreau et al. 1971, 1979). Polyp diameter determines the size of the particulate food, which may include small fish, and zooplankton, the digestion of which provides inorganic carbon and nitrogen to the zooxanthellae (Goreau et al. 1971). The tight nutrient cycling between coral and algae allows the sessile, mixotrophic holobiont to thrive in the oligotrophic waters of tropical oceans (Muller-Parker and D'Elia 1997; LaJeunesse 2002; Stat et al. 2006). The coral host regulates the population density of its symbionts by controlling their cell division or their growth, by digestion (symbiophagy), and/or by daily release into the water column (Jones and Yellowlees 1997; Stat et al. 2006). *Montastraea* spp. corals normally associate with a number of taxa of *Symbiodinium* (Rowan et al. 1997; Toller et al. 2001) that dynamically populate microniches corresponding to areas exposed to different levels of irradiance, but these associations may shift or change entirely when light intensity changes (Rowan et al. 1997; Toller et al. 2001). In context of the reef, decreases in irradiance may occur with increased sediment, pollutant or nutrient load in the water. Physical damage to corals, i.e., breaking or tipping over during storms or through contact with humans may cause local changes in irradiance.

Corals are adapted to the light intensity encountered within their preferred depth range (Iglesias-Prieto et al. 1992; Rowan et al. 1997; Baker 2001). The coral holobiont that effectively captures available light and converts it to biomass is able to grow large and occupy more space

on the reef, and thus capture more light (Goreau et al. 1979). Under optimal conditions, photosynthetic dinoflagellates can greatly increase a coral's ability to grow and lay down the skeleton it needs. Therefore, hermatypic corals rarely form reefs below 100 meters depth (Pearse & Muscatine 1971; Goreau et al. 1979). Thermal and other biotic or abiotic stressors can disrupt the important coral/symbiont biochemistry and impair the relatively slow-growing coral host. Compromised corals potentially become more susceptible to opportunistic pathogens that may be present in the water column (Santavy and Peters 1997).

Corals throughout the world have adapted to local temperature ranges. Reefs with high local temperature means are populated by taxa with high temperature thresholds (Iglesias-Prieto et al. 1992; Goreau and Hayes 1994; Rowan et al. 1997; Baker et al. 2008). Although zooxanthellate scleractinians inhabit well-defined tropical to sub-tropical latitudes, the oceanic and atmospheric processes that affect each individual reef can be quite different and remarkable (LaJeunesse 2002; Baker et al. 2008). On the local scale it would seem that individual neighboring colonies are exposed to the same conditions with little variability.

Montastraea spp. corals—one of the most important reef-building genera in the tropical western Atlantic and Caribbean (Van Veghel 1994; Knowlton et al. 1997; Szmant et al. 1997)—are highly susceptible to CYBD. Previous studies have implicated a consortium of *Vibrio* spp. as the putative causes of CYBD (Cervino et al. 2004b; 2008). These *Vibrio* spp. directly target the symbiont, lysing the algae in the gastrodermis of the coral host (Cervino et al. 2001; 2004b). Without their symbionts, corals eventually die or lose biomass, impeding their ability to grow and reproduce (Antonius 1977, 1981; Peters 1984; Kojis and Quinn 1985; Szmant 1991; Santavy and Peters 1997; Goreau et al. 1998; Porter et al. 2001). Coral hosts experiencing even minimal levels of stress may divert energy expenditures from growth and reproduction to defensive or protective processes (Santavy and Peters 1997). As a result, the coral will become less capable of dealing with stressor(s) and may begin to show signs of disease (Peters 1997). It is unclear why or how many coral diseases begin and what factors render a particular coral species or individual colonies within that species vulnerable. It is clear however, that lesion formation and tissue loss due to microbial infection have caused great increases in reef degradation since 1973 (Santavy and Peters 1997). A primary objective of the present investigation was to identify possible mechanisms of infection and differences in responses between colonies to exposure to

opportunistic pathogens. Particular emphasis was given to coral host physiology playing a primary role in the defense of the holobiont.

Coral-associated microbes and *Vibrio* spp. bacteria

Corals have a complex relationship with bacteria. The mucopolysaccharide surface layer is inhabited by hundreds to thousands of species of microbes believed to be beneficial to the coral holobiont (Antonius 1981; Ritchie 2006). The surface mucus layer is the primary defense against attack from potentially destructive environmental forces such as desiccation, sedimentation, UV radiation, and opportunistic pathogenic bacteria (Ducklow and Mitchell 1979; Antonius 1981; Ritchie 2006). Coral mucus traps sediment and is able to remove it via ciliary action of the epidermal cells, although mucus production is not unlimited and cannot cope with continuous supplies of sediment beyond what it is accustomed to, without the coral eventually showing signs of stress (Antonius 1981; Peters and Pilson 1985). Interestingly, numerous bacterial species in coral-associated microbial communities associate specifically with certain coral species, often in microniches (Rosenberg et al. 2007a). Many have symbiotic relationships with the coral host, and it is believed that corals shelter microbes that are beneficial to them (Knowlton and Rohwer 2003). It has also been shown that corals exhibiting signs of disease have undergone shifts in their normal mucosal flora (Ritchie 2006; Bourne et al. 2007; Cunning et al. 2008). Thus, it seems that a potential point of entry for bacteria is through the coral mucus, where they may be able to overwhelm the natural flora. Cunning et al. (2008) found that the prevalence of *Vibrio harveyi* in the coral's mucus increased with disease to 45% of the total microbial community, whereas in healthy colonies, *V. harveyi* was < 31%. In contrast, populations of *Vibrio fortis*, whose percentage was found in healthy corals to be 69%, decreased in diseased specimens to 48%. Kushmaro et al. (1997) discovered that *Vibrio* AK-1 (later named *V. shiloi*) experimentally inoculated *in aquaria* onto healthy *Oculina patagonica* corals from the Mediterranean Sea, is able to penetrate coral tissue and cause coral bleaching. They demonstrated a close relationship between proliferation of *V. shiloi* around the coral's symbiotic algae and elevated temperature. Bacterial coral bleaching occurred at temperatures above 26°C but did not occur when temperatures were lowered to 16°C. They believed that higher seawater temperatures may lower a coral's natural resistance to infection, increase bacterial virulence or both. Banin et al. (2000; 2001) later showed that *Vibrio shiloi* attaches to the surface of *Oculina*

patagonica and subsequently penetrates the tissue. High concentrations of a proline-rich peptide "toxin P" are biosynthesized by the internalized bacteria and released to inhibit photosynthesis of the zooxanthellae in the presence of NH_3 (Banin et al. 2001; Rosenberg et al. 2007a).

Coral reefs that have undergone changes from very healthy to degraded have also experienced changes in the microbial communities associated with them (Nelson et al. 2011). Nelson and colleagues found that the microbial communities in seawater associated with near pristine reefs are similar to those of the oligotrophic open ocean, whereas diseased and algae-covered reefs are dominated by "super-heterotrophs" such as *Vibrio* spp., *Staphylococcus* spp., and *E. coli*. These changes provide bacteria with increased opportunity to infect coral tissue and cause disease and many of the virulence factors in *Vibrio* spp. are favored over coral host defenses in warmer-than-normal seawater temperatures (Owens and Busico-Salcedo 2006). Coral reefs around the world, particularly in the Caribbean, have experienced an increase in coral disease in recent decades (Santavy and Peters 1997; Peters 1993; McWilliams et al. 2005). Incidences of elevated sea surface temperatures have also increased in the Caribbean over the past few decades (McWilliams et al. 2005), providing a possible link between disease and temperature. *M. faveolata* colonies used for the present study were collected from NOAA facility waters in Key West, where they were presumed to be subjected to many of the same biotic and abiotic stressors as their counterparts at locations throughout the Florida Keys. CYBD is a known contributor to reef degradation in the Florida Keys since affected corals can be found even in the protected waters of Looe Key, a national marine sanctuary (pers. observ).

Gamma-proteobacteria from the genus *Vibrio* are common, opportunistic, marine microbes, often found to be pathogenic to many coral, fish, and shellfish species throughout the world (Colwell 2006). These Gram-negative, motile, curved rods have been implicated in numerous marine diseases. It is clear from field monitoring that *Montastraea* spp. colonies do not all become demonstrably affected by CYBD. Explanations for this may be temporal, as well as spatial, variations in exposure to the pathogenic bacteria and/or other environmental stressors that may render the coral vulnerable. Genetic differences among individual colonies and their symbionts may also contribute to these field observations. Additionally, it is possible that sublethal effects of exposure to pathogens occur within the apparently healthy corals resulting in latent infections that do not show visible signs of stress or disease.

Cervino et al. (2004b) performed challenge experiments with novel *Vibrio* strains isolated from CYBD-affected *M. faveolata* corals. These experiments yielded positive results when all four novel strains were introduced as a cocktail. However, when used separately, the individual bacterial strains did not cause lesions to form. It is unclear how all of the bacterial strains associated with CYBD gain access to the coral gastrodermis and symbionts, but it is possible that one opportunistic *Vibrio* strain may be able to infect the coral and weaken its defenses substantially to allow the remaining opportunists to enter and work synergistically. The lesion is the clear and unequivocal sign of disease, but it is not known how long the coral has been expending energy to resist infection or how long it takes for a lesion to emerge. The challenge experiments described in this thesis used acute exposures of *V. harveyi* and *V. parahaemolyticus* based on expectations that certain *Vibrios* may be able to weaken the host and lesions needn't be readily visible for a coral to be infected.

Coral pathology

Morphological alterations to cells refer to changes in the structure of cells that may be indicative of some pathological processes. Structural changes in cells lead to functional abnormalities, which in turn lead to tissue injury. The alterations can also be a result of genetic or biochemical changes in cells, but virtually all forms of disease begin with molecular or structural changes. Functional derangements in a coral, such as loss of symbiotic algal cells or inability to remove debris from its surface via ciliary action, often lead to development of lesions and signs of disease. Corals have a limited range of expression of stress and it is often difficult to determine at the gross morphological level, whether a coral is diseased if the telltale signs, i.e., a yellow band of discolored tissue or a black band of pathogens, are not present.

Normally functioning cells are able to acclimate to physiological or pathological stressors in order to maintain homeostasis. These adaptations are generally reversed when the harmful stimuli have been removed. Cells continue to function and survive changes in a number of ways; through hypertrophy, which is an increase in size and metabolic function of the affected cell(s); hyperplasia, or an increase in the *number* of cells in a tissue or organ; and atrophy, a decrease in metabolic activity and size of the cell in response to a reduction in nutrient availability. Hypertrophy and hyperplasia are uniquely different responses to cellular stress but can be triggered by the same stimuli such as increased demand for the function each cell performs.

When a cell reaches its capacity to function under stress or if it is further exposed to other abiotic or biotic stressors, it may undergo irreversible cell injury. Cells that experience acute or prolonged exposures to pathogenic bacteria or other harmful substances may respond through cellular swelling and lipid changes or irreversible injury that leads to apoptosis or necrosis. Finally, autophagic responses to reduction in available nutrients, changes in irradiance or temperature stress, may be triggered and lead to cell death. Coral host gastrodermal vacuolar membranes may become modified into autophagosomes able to fuse with the zooxanthellae and digest them. This process is termed "symbiophagy" and is an important process by which the coral host is able to rid itself of its symbionts during a stress event (Cervino et al. 2004a, 2008; Downs et al. 2009).

Metaplasia is another important reversible change that may occur as a coping mechanism for cells attempting to maintain homeostasis in the presence of harmful stimuli or lack of important resources (Kumar et al. 2010; Young et al. 2011). Metaplasia involves one differentiated cell type that is replaced by another type more adept at survival under the stressful conditions. For example, in coral epidermis, columnar cells may become cuboidal and vice versa. This type of response may occur in coral tissues experiencing a great reduction in nutrients, such as those in CYBD bands or in the tissues directly adjacent to the active infection however, it is impossible with light microscopy to make the determination between metaplasia and attenuation resulting from other cellular processes.

When the harmful stimulus that causes reversible cell injury is persistent and continues to cause damage, irreversible cell injury occurs, followed by cell death. Cell death in the coral host and its symbiotic algae can occur along two very separate pathways (Dunn et al. 2002). Necrosis, a strictly pathological process, is the result of severe damage to the cell membrane, digestion of cytoplasm and cellular components by lysosomes, and subsequent leakage of cell contents into the extracellular matrix. Microscopically, necrosis manifests through enlargement of the cell; pyknosis, karyorrhexis, or karyolysis of the nucleus (Figure 4); disrupted plasma membrane; and inflammatory response and infiltration of immune cells into adjacent tissues. Apoptosis, the second mode of cell death, generally occurs as a result of damage to DNA. Proteins within a cell will set off apoptotic processes, characterized by the dissolution of a cell's nucleus, cell fragmentation, and finally, its termination by phagocytosis of the various apoptotic bodies

(Kumar et al. 2010; Young et al. 2011). An intact plasma membrane, and shrinkage in cell size are notable microscopic features of an apoptotic cell. While the triggering of apoptosis may be a pathological response, it is also a very important normal function of healthy cells and may not necessarily be associated with cell injury. Biochemical and ultrastructural changes precede those that can be realistically viewed by light microscopy, at which point the cell damage is likely irreversible (Kumar et al. 2010; Young et al. 2011). Therefore, it is generally understood that recognizable pathological changes to tissues viewed microscopically are permanent and proceeding towards cell death (Figure 5). Unfortunately, many of the above-described changes may not be readily visible to the naked eye and with light microscopy one may be unable to differentiate between apoptosis and necrosis or changes manifested in metaplasia and attenuation.

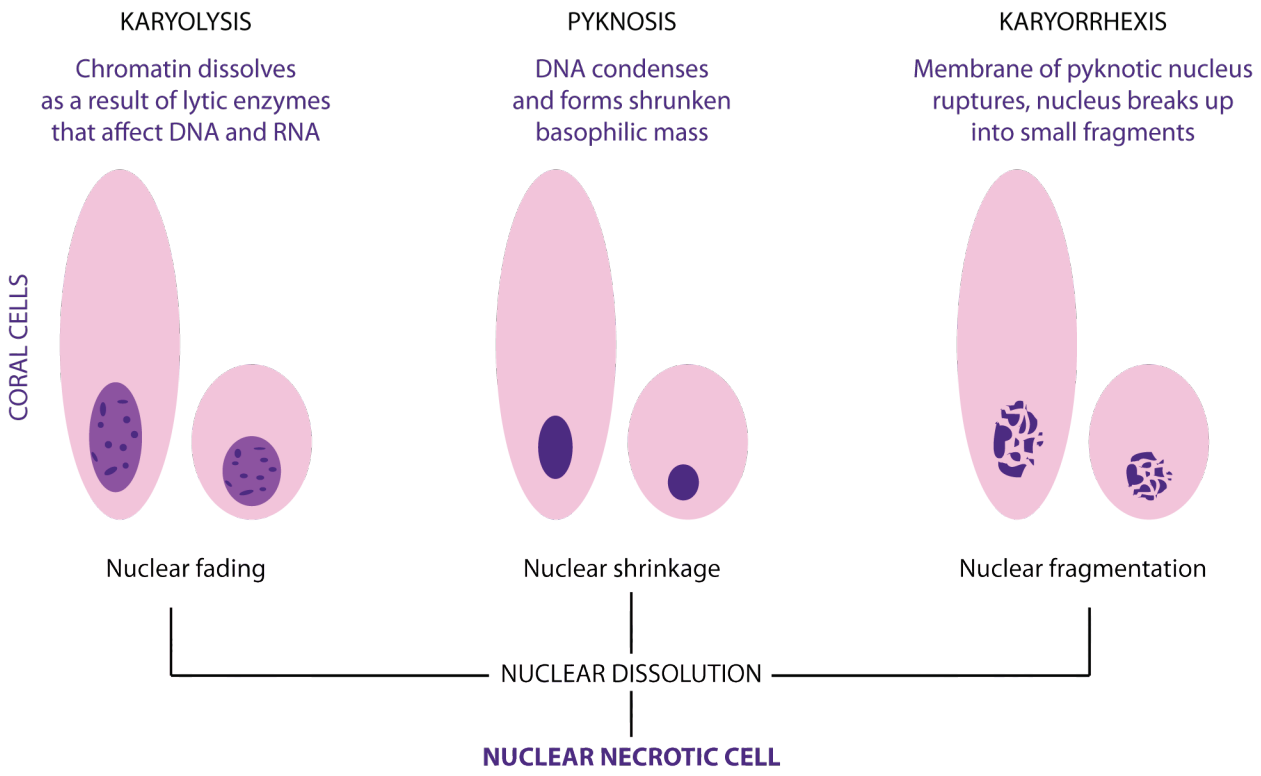

Figure 4. Pathological changes to the nucleus of a coral cell. Adapted from public domain material.

This investigation was designed to address the confounding observations in the field where neighboring colonies, although presumed subjected to the same environmental conditions, do not all show signs of disease on the same timescale. Alternatively, since corals have a very limited range of responses to stress, some colonies may be experiencing imperceptible latent infections while others succumb and become demonstrably diseased. It was thus hypothesized that *Montastraea faveolata* specimens obtained from phenotypically different colonies, fixed at the termination of acute bacterial challenge experiments and prepared for histological analysis will demonstrate that coral colonies respond to potentially pathogenic *Vibrio* spp. differently and that the responses may be affected by elevation in seawater temperature. The null hypothesis is that responses of the phenotypes to bacterial challenges at normal or at elevated temperatures are not different. This investigation is intended to elucidate whether a colony's susceptibility to infectious disease is a function of its physiology and if differences between phenotypes may render one more vulnerable than another. Pathological changes in cells and tissues prepared for histology can be detected by light microscopy before gross morphological changes, i.e., lesions, occur.

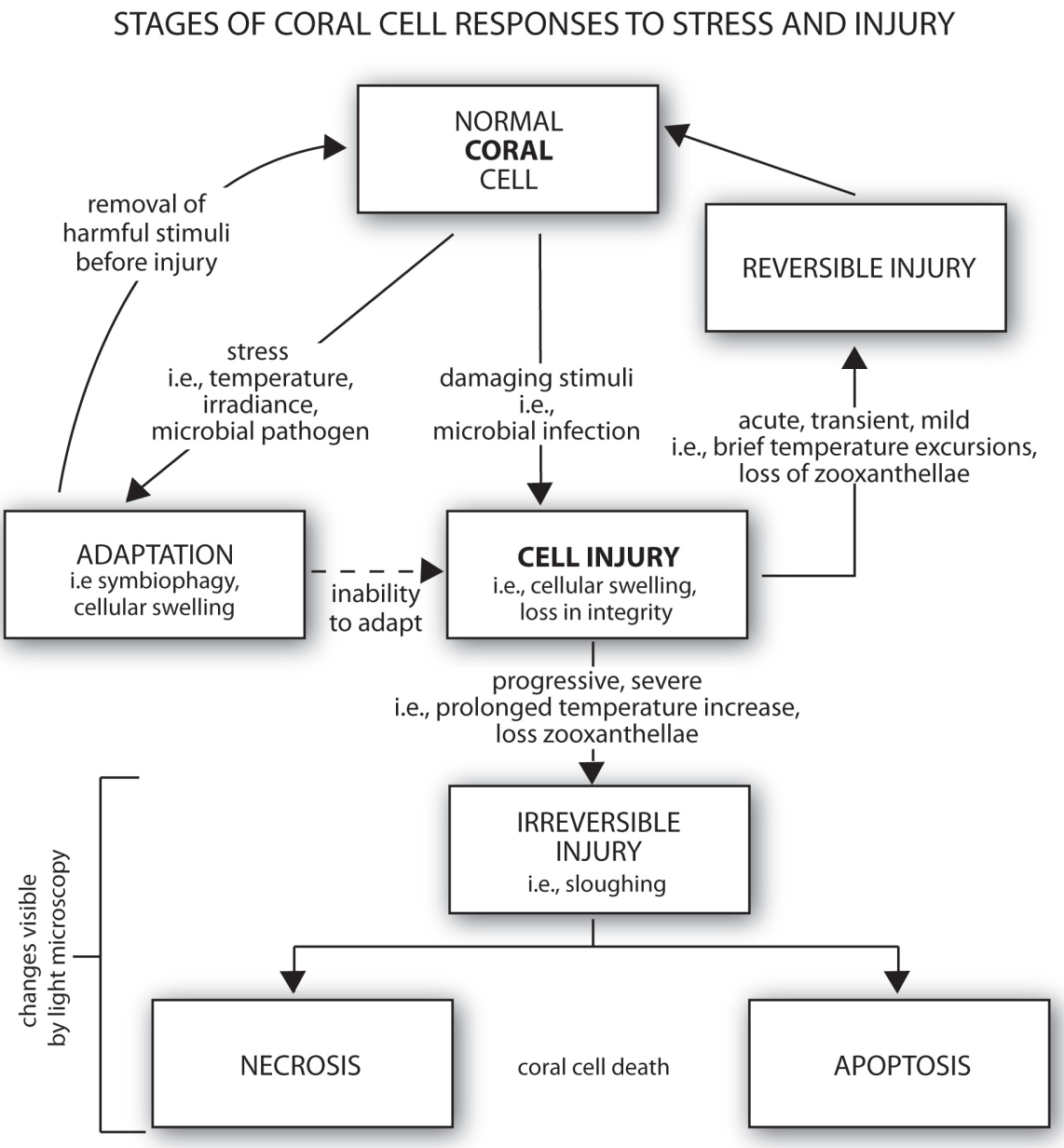

Figure 5. Coral cellular responses to stress. Adapted from Kumar et al. 2010.

Methods and Materials

To test the hypothesis that coral phenotypes respond to potentially pathogenic *Vibrio* spp. differently and that these differences may be affected by elevation in seawater temperature, a comprehensive bacterial challenge experiment was conducted at Mote Marine Laboratory's Tropical Research Laboratory (TRL) in Summerland Key, Florida followed by tissue sample processing for histopathological examination, conducted at George Mason University. An additional 27 days was added to the experiment after the exposure period when it became clear that the specimens were not developing lesions. This effectively added a time component to the experiment that allowed for the comparison of the specimens over the course of the 34 days. The hypothesis was tested with bacterial challenges, but the exposures were also intended to elucidate whether certain *Vibrio* species were able to jump-start the formation of yellow lesions similar to those associated with CYBD, and combinations of the *Vibrio* species were used to see if synergy between bacteria was an important component of bacterial virulence. Another added component to the research was the provision of field-collected CYBD-infected samples, which permitted histological comparisons between the experiment specimens and real diseased specimens.

Challenge Experiment

Coral collection, acclimation and tank set up

Two (2) large colonies of *Montastraea faveolata* were collected from the NOAA dockside nursery in Key West, Florida (Figure 6). These colonies, originally obtained from a seawall in the Key West area through rescue efforts to recover and use corals that would otherwise be impacted by marine construction projects, had been held *in situ* in a suspended rack system in 8–12 ft. of seawater and maintained for several years prior to harvest. The conditions at the NOAA dockside nursery in Key West provided water quality similar to the environment from which the corals originated, and corals remained apparently disease-free during the period

in which they were held prior to collection. The coral colonies were transported to the TRL in large coolers, and transferred to flow-through seawater tables under 70% reducing shade cloth. Within 24 h, the two colonies were cut into approximately 10 cm^2 squares using a MK Diamond Products 10-inch wet cutting tile saw. A small plastic color-coded square was attached to bare substrate on the side of each specimen using gel Super Glue™ providing a means by which each individual specimen could be recognized according to the corresponding parent colony. These newly fragmented and tagged corals were then held in shaded flow-through seawater tables for an additional 6 days to further recover from the fragmentation process. Prior to initiating the experiment, twenty 5-gallon aquaria were placed in the flow-through seawater tables under the 70% reducing shade cloth. The flow-through system prevented the water around the tanks from stagnating and overheating. Each tank was filled with 20 µm-filtered seawater—presumably allowing the smaller microplankton, including small diatoms and flagellates into the tanks. All tanks were fitted with 65 gallons per hour (gph) submersible power heads attached to the inside, to provide water movement, and clear Plexiglas® covers were placed on top of all tanks to avoid water evaporation and a resulting increase in salinity. A 200W submersible aquarium heater was also placed in ten of the twenty tanks and all these were kept in a separate flow-through seawater table. Six days after collection and fragmentation, two specimens from each of the two coral colonies were introduced into the aquaria, where temperatures were 26.5 to 27.5°C, similar to the ambient temperature of the surrounding water bath. The thermostat on the submersible heaters started at 27°C and settings were increased by 0.5 to 1°C every 24 h until a maximum setting of 32°C was reached seven days later. In addition, four specimens—two from each phenotype—were added to both temperature tanks. These four "time zero" (T_0) control specimens were collected and fixed at the beginning of the experiment.

Figure 6. NOAA Dockside Nursery, Key West, Florida. Site of *M. faveolata* colony collection. Note light and turbidity conditions. Photos: Erich Bartels taken in May 2010, 12:00 pm.

Temperature and salinity were monitored daily, and 10%–50% water changes with small additions of deionized water (DIH_2O) were done to maintain correct salinity levels during the acclimation period. On day one of the challenge experiments, each specimen was observed to possess obvious paling edges and a significant accumulation of filamentous macroalgae on all four sides of the freshly cut skeleton. A selection was therefore made from the remaining unused specimens whereby those that appeared healthier were exchanged for those more visibly stressed specimens originally selected for the tanks. The experiment therefore began using specimens that were the least compromised by their handling and environmental conditions. All edges of the specimens were then scrubbed free of macroalgae with a small wire brush and rinsed in filtered seawater before being returned to their tanks. Particular care was taken to avoid scrubbing coral tissue.

Challenge experiment set up

Given the large number of tanks required for all replicated treatments (20), each tank was labeled according to a color-coded system, as were all utensils, tubs and any tool or laboratory item that would come in contact with the corals or seawater in which they were kept (Figure 7). This was deemed necessary to avoid any cross contamination of bacteria from one treatment to the next and to serve as a visual aid for the correct placement of corals into tubs for exposures and back into tanks after exposures.

Vibrio spp. inocula

Montastraea faveolata specimens were exposed to various combinations of suspensions of two strains of the marine pathogenic bacterium *V. harveyi* (Collection of Aquatic Important Organisms–CAIM 1792; h^1, CAIM 1075; h^2), and one strain of *V. parahaemolyticus* (CAIM 29; P) obtained from Dr. Gary Vora, of the U.S. Naval Research Laboratory in Washington, D.C. These strains were isolated from diseased shrimp *Litopenaeus* sp. (CAIM 1792, CAIM 29) and the oyster *Crassostrea gigas* (CAIM 1075) though they have not been proven to be the etiological agents in the abovementioned diseased organisms. The choice of *Vibrio* species for the experiment was made primarily based on availability and the known association of *V. harveyi* with healthy and diseased corals (Cunning et al. 2008).

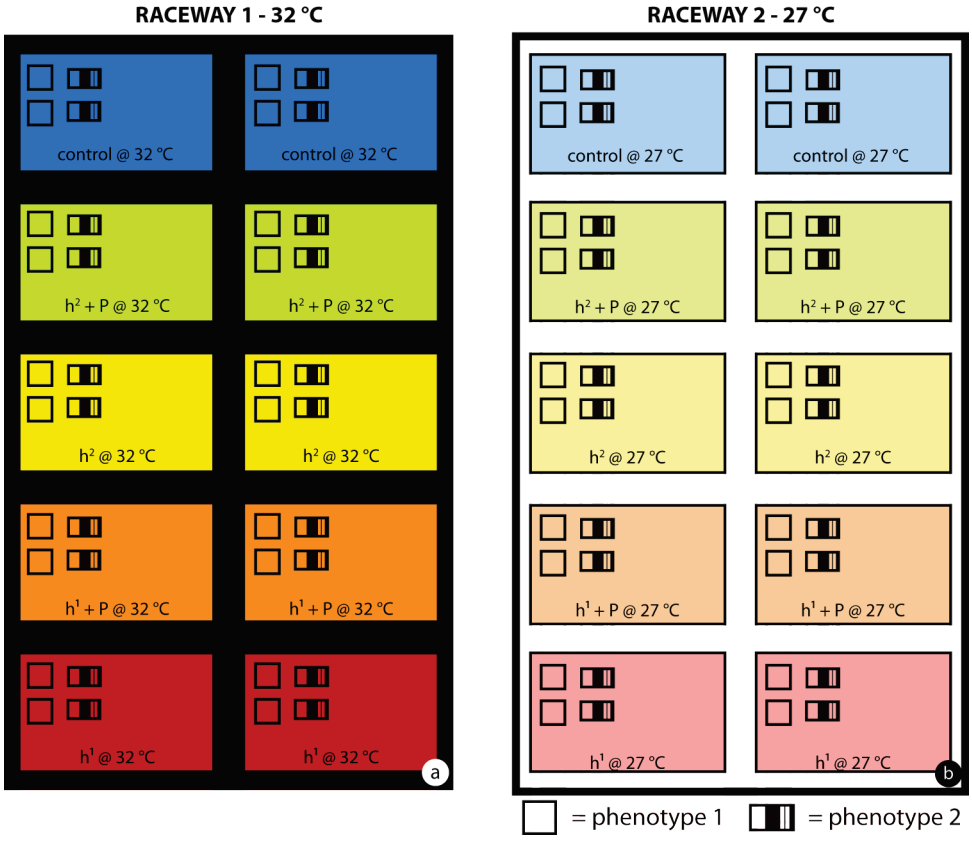

Figure 7. Challenge experiment design. Four different bacterial treatments in separate tanks, using *V. parahaemolyticus* (P) and *V. harveyi* (h^1 and h^2) plus controls were as follows: red = h^1; orange = h^1 + P; yellow = h^2; green = h^2 + P; blue = control. Heated (32°C; *a*) and ambient tanks (27°C; *b*) were kept in separate raceways.

At TRL, the *Vibrio* isolates were grown on glycerol artificial seawater agar plates (GASWA; 20.8 g NaCl, 0.56 g KCl, 4.8 g Mg_2SO_4, 4 g MgCl, 0.009 g K_2PO_4, 2 g Ria Salt, 4 g Peptone, 2 g Yeast, 2 mL Glycerol/Glycine, 15 g Agar 0.56 g Tris, 1 L Deionized H_2O; Smith and Hayasaka 1982) and incubated for approximately 24 h at ~35°C. Bacterial cells were resuspended from lawns on each plate with 8 mL sterile artificial seawater and poured into individual 50-mL sterile Falcon tubes (BD Biosciences, Franklin, NJ) in the following combinations: h^1, h^1+P, h^2, h^2+P (Table 1). For the first exposure, plates were visually inspected and chosen based on what was judged to be approximately similar growth. Two (2) agar plates per treatment were liquefied with a glass "hockey stick" after the addition of 8mL of sterile artificial seawater per plate, combined into Falcon tubes and diluted with 24 mL of sterile seawater (40 mL total). In treatments where only one strain was used, two plates of that strain were liquefied. In the combination treatments, one plate of each strain was liquefied and poured into the Falcon tube. Three (3) plates of bacteria were liquefied for each treatment for the second exposure and four plates were liquefied per treatment for the third exposure. As in the first exposure, combination treatments employed approximately equal bacterial concentrations of both strains (Figure 8). Every effort was made to have equal concentrations of bacteria for each treatment (number of harvested plates). However, cell yields among plates undoubtedly varied leading to difference in bacterial concentrations among treatments.

Bacterial exposures

To begin, four specimens—two from each phenotype—were removed from the tanks and immediately fixed in a 1:4 Z-Fix Concentrate (buffered zinc formalin fixative, Anatech, Ltd., USA): sterile artificial seawater solution before the bacterial challenges were conducted. These T_0 specimens provided the baseline condition of the corals before the exposure experiment began.

Table 1. Bacterial strains and assigned names used for the challenge experiment.

Bacteria	Strain	GenBank accession number	Assigned name
Vibrio harveyi	CAIM 1792	AHHQ0000000	h^1
Vibrio harveyi	CAIM 1075	GQ428229	h^2
Vibrio parahaemolyticus	CAIM 29	GQ428218	P

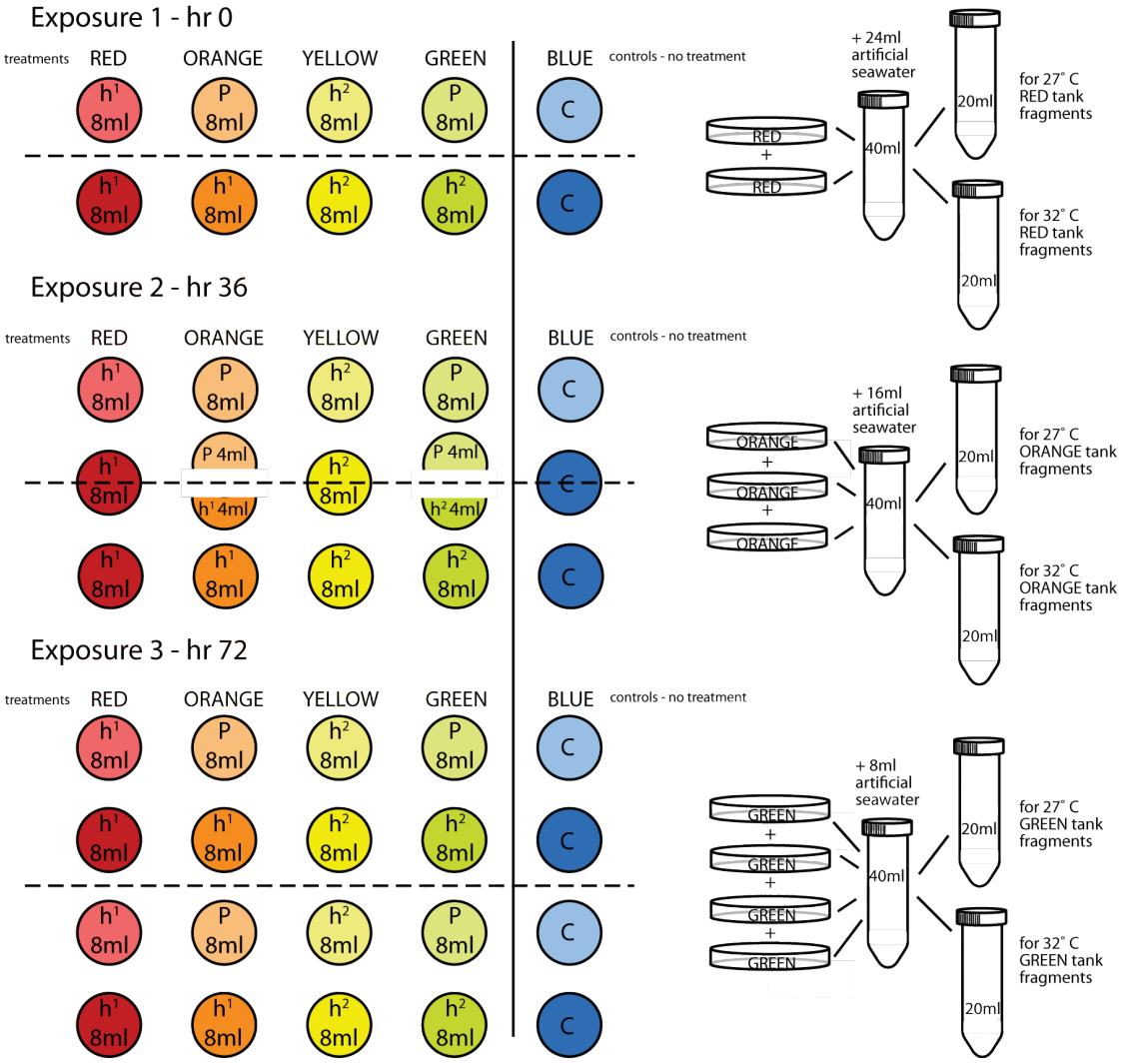

Figure 8. Colored circles represent bacterial plates and correspond to tank treatments. To maintain similar concentrations of bacteria between treatments for exposure 2, ORANGE and GREEN treatment plates were liquefied with 8mL sterile artificial seawater and 4mL of each suspension added to inoculum for a total of 12mL of each bacterial strain.

Coral specimens were removed from their tanks and placed in 1 L plastic tubs with ambient seawater. The inocula were then poured directly over the coral specimens. Tubs were then agitated lightly to mix bacterial suspensions throughout the tub. The specimens were exposed to each inoculum for periods of 4 h (exposure 1), 8 h (exposure 2), and 12 h (exposure 3) separated by periods of 36 h in their respective tanks without exposure. Tubs were covered loosely, allowing gas exchange, but not cross-contamination. Bacterial inocula were made fresh for each exposure.

During exposures, eight (8) coral specimens (four each from two tanks) occupied the tubs with approximately 630 mL of seawater from their respective tanks in an attempt to avoid stress from water or temperature change. Optical density measurements were performed on subsamples from the exposure tubs by turbidometry at 600 nm using a Spectronic 21 (Milton Roy) spectrophotometer. The 36-hour exposure hiatuses allowed for two nighttime exposures when corals generally extend their polyps to feed, as well as one daytime exposure. This strategy increased the probability of bacteria gaining entrance into the coral gastrovascular cavity and thus inner tissue layers.

Physical evidence, such as differences in colony color, polyp size and shape, showed that P1 and P2 were distinct phenotypes, but evidence of genetic differences was lacking. During the first exposure, two control specimens from P1 and P2 were mistakenly placed too close to one another in the exposure tub (Figure 9). Both specimens were later found with extruded mesenterial filaments attached to the other. Interestingly, this did not occur in any of the treatment tubs. *Montastraea* spp. corals are known interspecies aggressors on the reef (Lang 1973; Ferriz-Dominguez 2001; Sutherland et al. 2004) but little is known regarding intraspecies reactions. Due to the discovery of this aggressive behavior, specimens from each phenotype were subsequently isolated each to one side of the tub during exposures and no further aggressive behavior was observed.

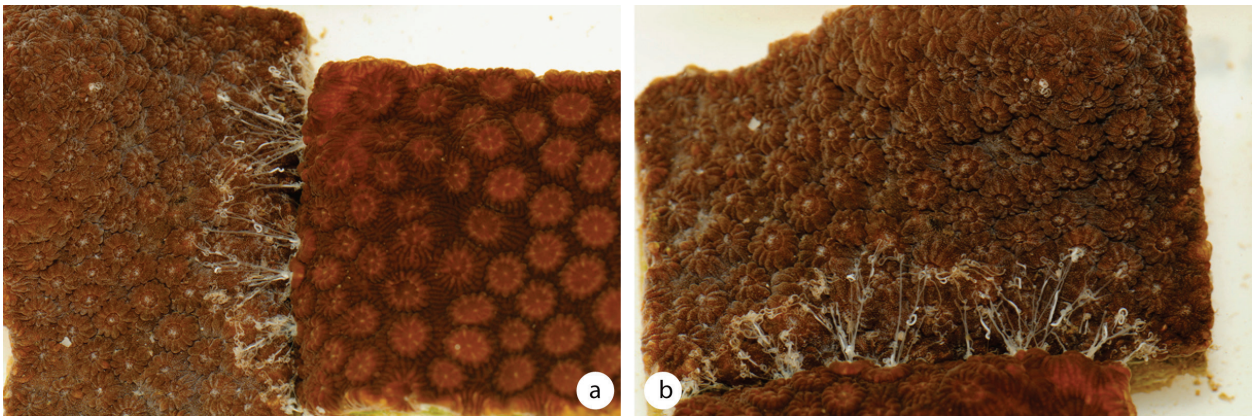

Figure 9. Control specimens from phenotype 1 (*a left, b top*) and phenotype 2 (*a right, b bottom*) during the first exposure. Recognition of non-self between the specimens suggests genetic uniqueness.

Bacterial concentrations

To derive suspended microbe counts in the experiments all three *Vibrio* species were serially diluted to produce a standard curve comparing turbidity and cell concentration. As with the exposure experiment, each *Vibrio* species was grown on GASWA media and incubated at ~35°C for 24 h. Eight mL of 0.2 µm-filtered seawater was added to each plate to liquefy. The suspension was preserved with formaldehyde at a 2% final concentration. Decimal dilutions were performed on the preserved suspension down to a final dilution of 10^{-8}. Spectrophotometer readings were taken with a Spectronic 21 spectrophotometer for each dilution at 600 nm. In parallel, subsamples of selected dilutions were subjected to standard epifluorescent direct cell counts (AODC) after staining with acridine orange on 0.2 µm membrane filters (Hobbie et al. 1977).

A 10^{-3} dilution was empirically found to provide optimal cell densities for AODC for each *Vibrio* species. Counts were done on epifluorescence microscope (Zeiss Axioskop) with oil immersion 100x objective lens and blue excitation. At least ten grids with a target number of ~30 bacterial cells per grid and a minimum of 300 cells were counted. Using a spreadsheet macro in Microsoft Excel (NewCount©) provided by the Taylor Lab, the concentration and counting statistics for the 10^{-3} dilution were calculated. Blank-corrected AODC cell concentrations were regressed against their corresponding transmittance (%) readings and were plotted for each

Vibrio species. These slopes were then used to estimate cell concentrations that corresponded to the transmittance readings gathered at TRL at the time of the exposure experiments (Table 2).

Table 2. Estimated bacterial concentrations used during the challenge experiments.

BACTERIAL CONCENTRATIONS		
MOTE READINGS	**Measured Transmittance**	**Estimated Concentration**
Challenge 1 - treatment	%	cells/mL
CAIM 1792	70	7.20×10^8
CAIM 1792 + CAIM 29	N/A	N/A
CAIM 1075	72	1.00×10^9
CAIM 1075 + CAIM 29	N/A	N/A
Challenge 2 - treatment		
CAIM 1792	47	1.50×10^9
CAIM 1792 + CAIM 29	43	2.15×10^9
CAIM 1075	53	2.00×10^9
CAIM 1075 + CAIM 29	46	2.30×10^9
Challenge 3 - treatment		
CAIM 1792	43	1.70×10^9
CAIM 1792 + CAIM 29	42	2.15×10^9
CAIM 1075	52	2.00×10^9
CAIM 1075 + CAIM 29	46	2.30×10^9

Tank monitoring

Tanks were monitored daily for salinity and temperature, and every two days for NO_3^-, NO_2^-, NH_4^+, and alkalinity. Water changes (removal of 20–100% of tank water and replacement with 20 µm-filtered sea water) were made daily and adequate shading was provided to avoid

algal accumulation on the exposed skeleton of coral specimens in distress and potentially impact the results of the bacterial exposures. Daily PAR values taken under the shades during the exposure period measured in the 30–100 µmol m^{-2} s^{-1} range at 12:00 pm, whereas PAR values for direct sunlight outside the shaded area measured ~2000 µmol m^{-2} s^{-1} (Figure 10*a, b*). After 7 days, daily tank monitoring and 10–20% water changes, continued but NO_3^-, NO_2^-, NH_4^+, and alkalinity were only tested on days 32 and 33. All 84 coral specimens were photographed at T_0 and every subsequent 24 h until the end of the exposure period, and on d 34.

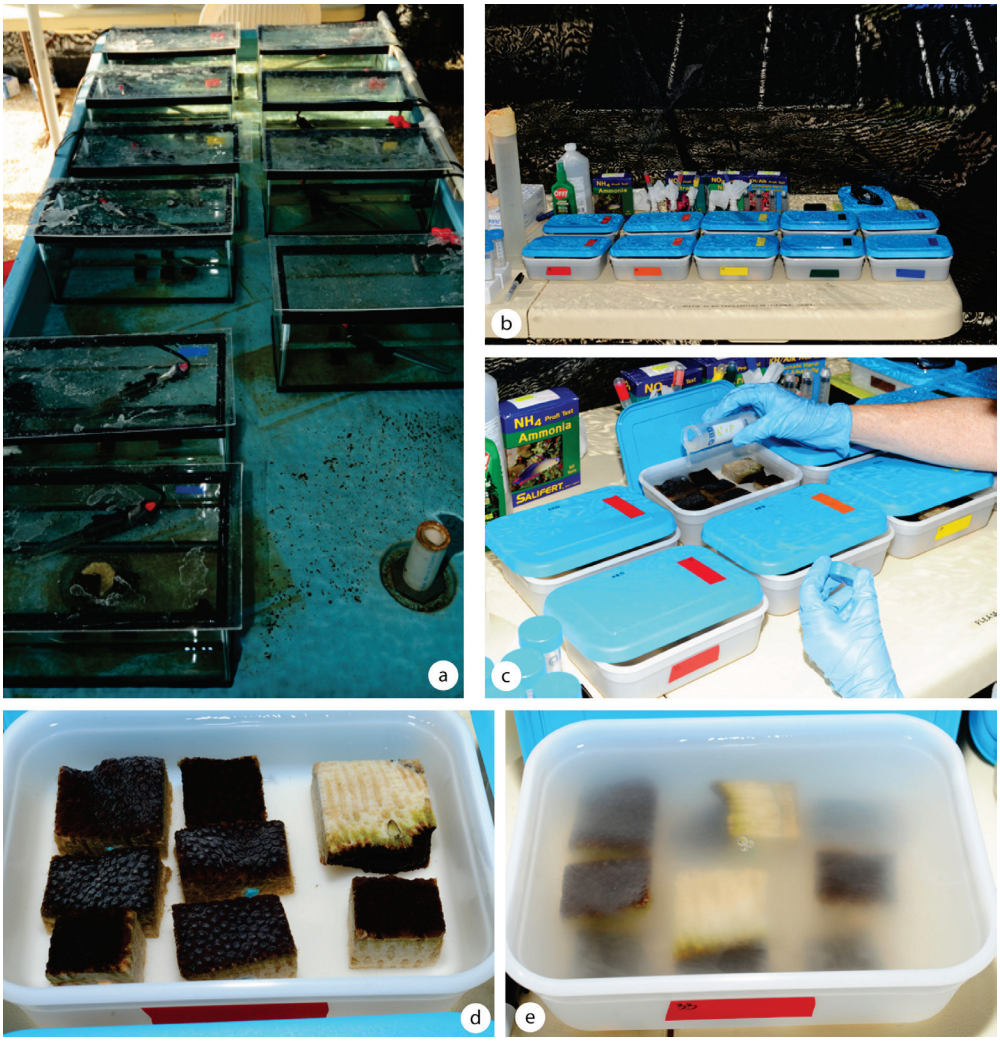

Figure 10. Photos taken at TRL during the challenge experiments. Photo (*a*) elevated temperature (32°C) raceway with heated tanks, (*b*) exposure station, shading for raceways visible, (*c*) pouring bacteria into tub over coral specimens during first exposure, (*d*) coral specimens moments before first exposure, (*e*) turbid inoculum "soup."

Post-exposure sampling

After 7 d exposures, all specimens were photographed and one set (one specimen chosen randomly from each phenotype) was fixed in 1:4 Z-Fix solution while the remaining specimens were left in their tanks for an additional 27 days. After 27 days, the experiment concluded and all remaining coral specimens were photographed and sampled as described below.

Coral specimens were removed from their respective tanks and split in half with hammer and chisel. One half of each specimen was placed in a liquid nitrogen Dewar flask for lipid biochemistry and bacterial phylogenetic analysis at the Woods Hole Oceanographic Institution (WHOI) by Dr. Konrad Hughen, Dr. James Cervino and Jessie Kneeland. The remaining halves were placed back in the collection tub for approximately one minute to allow the coral specimen to produce more mucus after it was divided. Mucus was collected by tipping each specimen on its side and dripping approximately four drops of seawater and mucus into a cryotube. The mucus sample was then placed in the liquid nitrogen Dewar as previously described. The specimen was then placed in a 125-mL screw-cap plastic container and fixed in 1:4 Z-Fix solution for histology.

Histology

Histoslide preparation

Preparation of all specimens for histology was performed at Dr. Esther Peters' laboratory at George Mason University under her supervision. In addition, some microtomy was done at SoMAS. The coral specimens remained in 1:4 Z-Fix/filtered seawater solution for approximately 6 months. They were rinsed in DIH_2O and photographed with histology lab log sample numbers and scale bars. Excess skeleton was removed with a hand-held rotary tool and the specimen was again rinsed in DI to remove any excess calcium carbonate residue. Each specimen was immersed in double its height of Immunocal™ (Decal Chemical Corporation, Tallman, NY) a mild, formic acid decalcifying solution, and decalcified for up to 48 h, as necessary. Some specimens required fresh Immunocal™ solution after 24 h. To allow off-gassing of CO_2 and prevent tissue dessication, Kimwipes were spread out onto the surface of the solution. After

visual verification of total decalcification specimens were rinsed in fresh DIH_2O for 10 min three times. The entire DIH_2O was discarded and 70% undenatured ethanol (EtOH) was added to the residual tissue for a minimum of 1 hour.

Tissue was trimmed with razor blades on a sterile cutting board in approximately 0.5 cm x 4 cm saggital sections (longitudinal section bisecting the tissue from the oral surface to the aboral plane). Cut locations were recorded on the photograph for each sample. Specific locations were noted to provide a "roadmap" for later locating the sample area viewed microscopically. Saggital tissue strips were placed in disposable tissue processing/embedding cassettes (Tissue Path IV, Fisher Scientific). The order and orientation in which each was placed was recorded on the sample's photograph and the cassettes were returned to the 70% EtOH where the majority of its pigments bled off. Tissue cassettes were then transferred to a clean bin of 70% EtOH overnight to further dehydrate the samples before processing and to remove any excess pigment before running them through the processor. In a Ventana RMC 1530 tissue processor, cassettes were run through a graded series of EtOH immersions; 85%, 95% and 100%, 15 min each, to dehydrate the tissue. These steps were followed by immersions in SafeClear™ xylene substitute clearing agent (Fisher Scientific Inc.), three changes of 15 min each, and finally in three changes of molten Paraplast Plus® Tissue Embedding Medium (Leica Microsystems), 30 min then two more changes at 15 min each with vacuum (15 mm Hg) applied during the last change. At the conclusion of the processor cycle, tissue cassettes were removed from the processor and placed in a heated (50°C) tissue-holding tank in the embedding station. Great care was taken in the transfer of the saggital tissue strips from the cassette to stainless steel embedding molds to keep each piece in the order and orientation in which they were placed in the cassettes. Newly embedded tissue molds were placed on 4°C cold plate to solidify and blocks were popped out of the molds when the paraffin was completely solid. Tissues were sectioned into 5-µm ribbons using Olympus CUT 4060 (George Mason University) and Leitz 1512 (SoMAS) microtomes. Tissue ribbons were removed from the microtome and floated in a Lab-Line Lo-Boy 26103 tissue water bath at 42°C and immediately mounted onto Thermo Scientific Super Up-Rite slides for histology, and Fisher Scientific, Tissue Path SuperFrost Plus slides for FISH.

Slides prepped for histology were stained with hematoxylin and eosin (H&E), one of the most common staining techniques in histology because the dyes stain various types of tissues and

elucidate morphological changes in tissues under stress. Slides stained with H&E show good cytoplasmic, nuclear, and extracellular matrix detail. Hematoxylin is a basic dye and stains nucleic acids and other basophilic substances purple, while eosin, an acidic dye, stains acidophilic cellular components, such as proteins, pink. The slides were stained following the procedures in Peters et al. (2005) and are outlined here. Up to 19 slides were placed in glass slide staining racks and dipped in glass staining dishes for each step of the staining procedure. See Figure 11 for the step-by-step process.

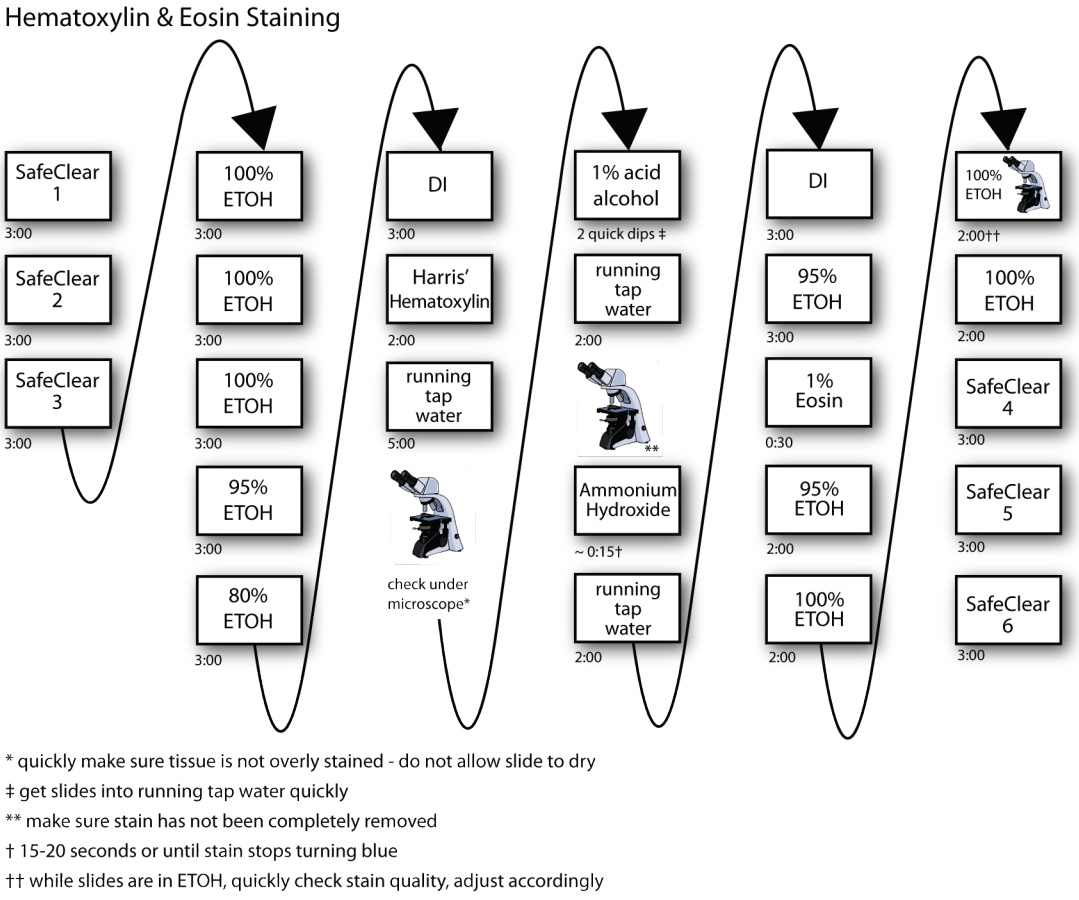

Figure 11. Staining procedure for hematoxylin and eosin (H&E) stains.

Following the final SafeClear rinse, drops of Permount™ mounting medium (Fisher Scientific) were added to the slide then a coverslip was applied and allowed to dry for several days before viewing under the microscope.

Histoslide analysis

Histoslides were examined on a Leica Diastar compound brightfield light microscope at six magnifications: 4x, 10x, 20x, 40x, 63x, and 100x with oil immersion. Each slide was examined at least twice: the first was done to gather first impressions and information on any abnormalities, changes in tissues and structures, presence of unfamiliar structures or any other observation deemed interesting or important. The second was done to score the state of the coral epithelia, mesenteries, and endosymbiotic algae in the sectioned specimens. Particular attention was given to the epidermis, gastrodermis, and the zooxanthellae of the surface body wall based on a working assumption that most of the changes would occur near or on the oral surface of the coral. This assumption was based on the nature of the exposure protocol and information regarding the formation of lesions or "yellow bands" in corals with CYBD. Criteria involving the deeper aboral regions of polyps were few, and this deep polyp tissue was evaluated mostly as a whole, rather than as individual criteria. Slides were assigned scores for **Severity**, which describes the frequency with which a pathological change occurs, and **Condition**, which describes the condition of the tissues and/or cells where that pathological change was found. The frequency of change is a measurement of how different a particular specimen is from a normal/healthy specimen. Healthy coral specimens from the collection of Dr. Esther Peters, processed in 1980, were analyzed and used as a standard from which all pathological changes were measured. These slides were used in lieu of the control specimens because they represented truly healthy specimens, whereas the control specimens did not (E.C. Peters, pers. comm.) Occurrence of a pathological change was averaged for the entire section being assessed, as was condition of tissues with those changes. Tallies were made and a score was assigned based on the percentage of tissue affected. The scoring protocol is further explained in Table 3.

Histology studies commonly involve acute exposure to toxicants, pollutants or as in this case, pathogenic organisms, in order to take advantage of what is often described as a highly qualitative and descriptive scientific method (Jagoe 1996). Histological analysis relies heavily on visual observation; therefore, visually observable changes must occur. To overcome the qualitative nature of some histological analyses, prevalence assessments corresponding to the amount of tissue affected were assigned to severity measurements effectively making the observed pathological changes semi-quantitative (Table 3). Quantitative (or semi-quantitative)

measurements are, in fact, an important requirement to address inter-colony variations in response to the bacterial challenges (Jagoe 1996). Additionally, evaluation of several sections per slide increased the probability of detecting verifiable differences among treatments (Jagoe 1996), and variation among specimens was addressed with replicates in separate tanks exposed to the same conditions. Areas of slides to be analyzed were chosen usually at random, unless tissue was scarce or appeared abraded (e.g., from rubbing against inside of jar, processing). In these cases, areas of tissue that could be more fairly evaluated were sought. Differentiation between effects of handling and effects potentially caused by the treatments was necessary to fairly assign values that represented pathological changes. The entire section was scanned and evaluated before a final judgment was made and score was assigned. A subset of the criteria was chosen at random (6 of 33) for evaluation of the replicates to gauge whether specimens of the same phenotype, exposed to the same conditions but in separate tanks responded similarly to their counterparts.

Table 3. Overview of scores for severity and condition. Slides were evaluated on 33 criteria and assigned scores for severity and condition for each of those criteria. Condition scores are a function of severity.

Severity Scores	**Condition Scores**
0 = No Change (0%)	0 = Excellent
0.5 (1 – 10%)	0.5
1 = Minimal (11 – 20%)	1 = Very Good
1.5 (21 – 30%)	1.5
2 = Mild (31 – 40%)	2 = Good
2.5 (41 – 50%)	2.5
3 = Moderate (51 – 60%)	3 = Fair
3.5 (61 – 70%)	3.5
4 = Marked (71 – 80%)	4 = Poor
4.5 (81 – 90%)	4.5
5 = Severe (91 – 100%)	5 = Very Poor

A score of (5) **Severe** reflects pathology that was in the worst possible condition (cells lysing or necrotic) and diffuse (found on 91% or more of the section). A score of (3) **Moderate** reflects multifocal pathology (found on 51%–60% of the section) and a score of (1) **Minimal** means the pathological change occurred but was focal, (found on 11%–20% of the section). It should be noted that no tissue sections were found 100% damaged. A score of (5) realistically reflects pathological change on ~ 91 - 95% of the tissue.

A secondary score was given for the condition of the tissue in question at the location(s) in question and represented judgment of the ability of the coral to function without impairment. A score of (0) **Excellent** is only given when the pathological change was not found at all. It is important to note that while a score of zero (0) for condition is possible, it does not mean the tissue was in excellent condition, it only reflects the fact that the severity score was zero (0) and thus the condition score was necessarily the same. The condition score was contingent upon finding a particular pathological change, therefore it is a function of the severity score and as such is considered less indicative of the overall health of the coral specimen than the severity score. A total of six criteria were used to evaluate the slides of specimens kept in replicate tanks at both temperatures and collection times. Replicate slides were scored for severity and condition, the results of which were compared to the scores for those same criteria of the primary set of slides. This comparison was done as a means to determine whether there were significant differences in responses of the same phenotypes to the same treatment but kept in separate tanks.

Criteria

The following criteria were evaluated and scored based on the types of pathological changes observed during the first review of the slides and changes commonly found in diseased corals. Provision of histoslides of healthy corals, field-collected from Puerto Rico in 1981 and prepared by Dr. Esther Peters, provided visual confirmation of healthy epithelia and mesenteries of *M. faveolata* (Figure 12). In addition, analyses of the T_0 specimens and their relatively high severity scores formed the basis for the decision to use the "1981 ECP healthy samples" as comparison specimens. Thus all criteria evaluated were compared and increases reflect the amount beyond that viewable in the comparison slides. All slides were evaluated first at lower magnification (4x, 10x, 20x) then higher magnification (40x) to see details of the changes evaluated. For complete details on how the criteria were evaluated see Appendix I.

Criteria used to evaluate changes to coral specimens	
Attenuation of epidermis	Suspect bacteria in/on epidermis
Attenuation of gastrodermis	Suspect bacteria in/on gastrodermis
Attenuation of calicodermis	Suspect bacteria in/on calicodermis
Attenuation of mesoglea	Suspect bacteria in/on endolithic organisms
Integrity of epidermis	Endolithic organisms adhesion to calicodermis
Integrity of gastrodermis	Endolithic organisms adhesion to gastrodermis
Integrity of calicodermis	Zooxanthellae shape/color/size changes
Integrity of mesoglea	Zooxanthellar nuclei shape changes
Increase/hypertrophy of mucocytes	Zooxanthellae yellowing
Mucus increase	Mesentery loss of integrity
Mucus/surface debris	Symbiophagy
Adhesion loss of epidermis	Karyorrhexis nuclei in epidermis
Adhesion loss of gastrodermis	Karyorrhexis nuclei in gastrodermis
Adhesion loss of calicodermis	Nuclei changes epidermis
Sloughing of epidermis	Nuclei changes gastrodermis
Sloughing of gastrodermis	Nuclei changes calicodermis
Sloughing of calicodermis	

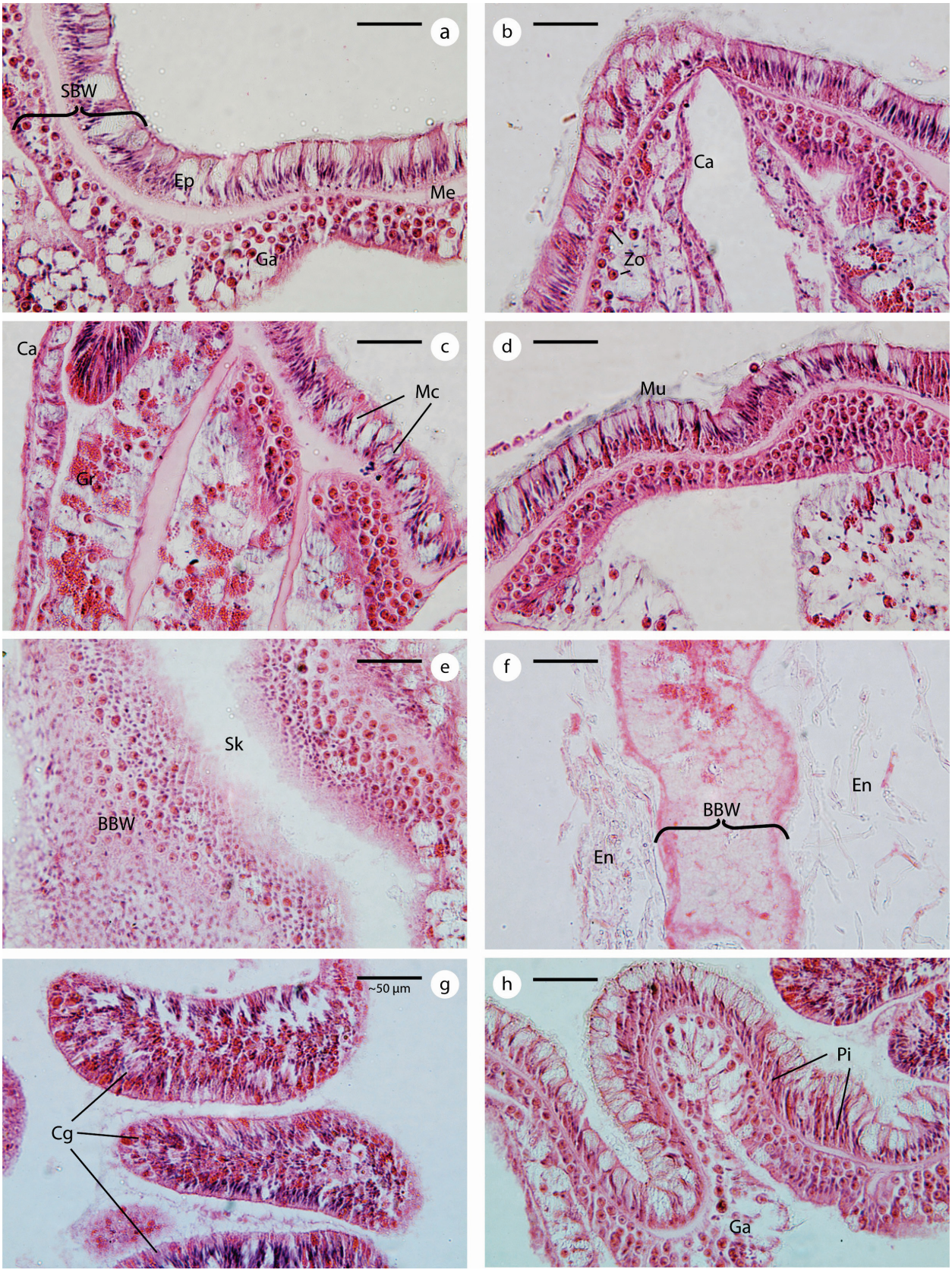
a
SBW
Ep
Me
Ga
b
Ca
Zo
c
Ca
Mc
Gr
d
Mu
e
Sk
BBW
f
En
BBW
En
g
~50 µm
Cg
h
Pi
Ga

Figure 12. Photomicrographs of field-collected, healthy samples from Puerto Rico, 1981. Slides from the collection of Dr. Esther Peters. The surface body wall, viewable in (*a, b, c, d, h*) and the basal body wall (*e, f*) were the primary foci of the investigation. Ep = epidermis, Ga = gastrodermis, Ca = calicodermis, Me = mesoglea, SBW = surface body wall, BBW = basal body wall, Cg = cnidoglandular band, Zo = zooxanthellae, Gr = large, raspberry-like granular gland cells, Mu = mucus, Mc = mucocytes, Pi = pigment cells, En = endolithic community, Sk = skeleton (no longer present). All scale bars ~50 µm.

Looe Key field-collected samples

Samples from three presumed healthy and two CYBD-infected *M. faveolata* colonies— one sample each from presumed-healthy *M. faveolata* colonies, and three samples from CYBD-affected colonies— were collected by SCUBA from the Looe Key National Marine Sanctuary, Florida. From diseased colonies, two samples were taken directly from yellow band lesions and one specimen from apparently healthy tissue far from the yellow band. Immediately following collection they were fixed in Z-fix solution for histological analysis. These specimens were prepared for histology with the experimental specimens. As an added precaution, the diseased samples were enrobed in agarose during processing, ensuring the pale band areas of the sample would not dissolve or tear away.

Data analysis

The Kruskal-Wallis H test was used for all analyses because it was able to compare three or more groups at a time. The semi-quantitative dataset comprised of the pooled severity scores (not normal) worked best with this non-parametric test, because it uses a distribution-free method that is not dependent on a given distribution of data (Sokal and Rohlf 2001). Usefulness of the Mann-Whitney test was also investigated but was not able to provide more accurate results from the dataset. A p-value of 0.05 was set as the threshold for statistical significance, meaning that a score with a p-value ≥ 0.05 would render the result non-significant (Ramsey and Schafer 2002). This assigned value is commonly used in pathology studies as the threshold (Renshaw and Gould 2006; Dr. Yee Ean Ong, M.D., pers. comm.)

All statistical analyses were done using Statistics Open For All (SOFA), version 1.1.3, open source software, free for download at http://www.sofastatistics.com/home.php. Figures were generated with SOFA and recreated with Adobe Illustrator CS4.

While individual criterion scores allow evaluation of each specimen based on a particular pathological change, it does not render a complete picture of the overall health of the coral specimen. To overcome this limitation, a simple mean of the total criteria scores was calculated. The mean score for each specimen was normalized to 100 and expressed as a percentage; 0% represents a specimen in perfect health whereas 100% represents a specimen in the worst possible condition. The use of the means of tallied scores has limited application, as it is understood that not all possible pathological changes to the coral were recorded and not all criteria analyzed influence the health of the coral equally. For example, the sloughing of epithelia is a strong indication of a major breakdown of cell adhesion, tissue integrity, and necrosis, whereas the importance of the presence of bacteria along the accreting surface of the calicodermis remains unclear. What *is* clear is that in the 1981 ECP healthy slides, suspect bacteria were not found using light microscopy. In summary, the mean of the tallied scores was used to give an overall picture of the amount of pathological changes observed based on the criteria chosen without assigning weight and is tabulated in the results section.

Results

Two phenotypes of the Caribbean coral *M. faveolata* were challenged with bacterial exposures to determine whether they respond differently to the same treatments and whether elevated temperatures affected their responses. First, gross morphology and condition of the specimens at T_0 will be described and compared. Then, the results from the bacterial exposures will be presented. The results will be laid out by phenotype at ambient temperature (27°C) with descriptions of the pathological changes observed, and how those changes compared between the phenotypes. The responses of each phenotype at elevated seawater temperatures (32°C) will be described, followed by a comparison of how the phenotypes responded to elevated temperature. Changes in the phenotypes over the course of the 34 d experiment will also be examined. Finally, comparisons of the histological observations between the experimental specimens and the field-collected Looe Key samples will be discussed. The field-collected CYBD evaluation is an important, albeit late, addition to the experiment because very little is known regarding coral cell and tissue changes that occur in infected specimens. Observations from Looe Key samples helped to determine whether the experimental exposures resulted in CYBD-like pathological changes to the cells and tissues. Pathological changes are defined as any alterations in the function, structure or appearance of tissues from normal that impair the coral.

Gross morphological description of phenotypes at T_0

At T_0—defined as the moment the experiment began and 16 days after the coral colonies were collected—the specimens were undergoing stress. This stress may have been the result of multiple factors, e.g., the acclimation period may have been too short, the fragmentation was too traumatic, or the new light regime change was too drastic. Specimens exhibited signs of stress from the fragmentation, believed to be limited to the margins, but none of the gross observations were interpreted as recognized signs of disease.

P1 specimens appeared dark brown in pigmentation with a superficial opaque, white filmy appearance (Figure 13*a, c*). This opaque white film appearance was caused by dense

communities of thraustochytrids (Kramarsky-Winter et al. 2006; Siboni et al. 2010), stramenopilan protists known to form symbiotic relationships with numerous marine organisms (Raghukumar 2002). Along the edges where the specimens had been cut, however, thraustochytrids were greatly diminished and tissue appeared shrunken. Some of the tissue on P1 specimens also appeared contracted at the center of the specimens (Figure 14*b*).

P2 specimens had a light brown to orange pigmentation, lacked the opaque, white film present in P1 specimens, were paling along the specimen margins, and some polyps seemed swollen. Thraustochytrids may have been present though not grossly visible (Figure 13*b, d*). In contrast to P1 specimens, P2 polyps often appeared hydropic (water-filled) at the margins and within the central regions of the specimens. Mesenterial filaments were seen extruding from the tissue not only at the recently cut margins but also internal to the edges, and polyps at the margins commonly appeared blistered, pale, and swollen (Figure 14*c, d, e*).

The average of severity scores for all histological criteria evaluated for the T_0 P1 specimens at 27°C and 32°C were both 34% (0% = perfectly healthy, 100% = in worst possible condition). The average of severity scores for the T_0 P2 specimen at 27°C was 38%, and at 32°C only slightly higher at 40%. These scores, like the gross observations, indicate all specimens were in less than optimal health at T_0. As these specimens served as the baseline for all treated and control specimens at both their respective temperatures, it was inferred that *all* specimens were somewhat impaired at the beginning of the *Vibrio* exposures. These and all subsequent severity scores indicate excursions from the healthy state shown and described in the ECP 1981 healthy samples.

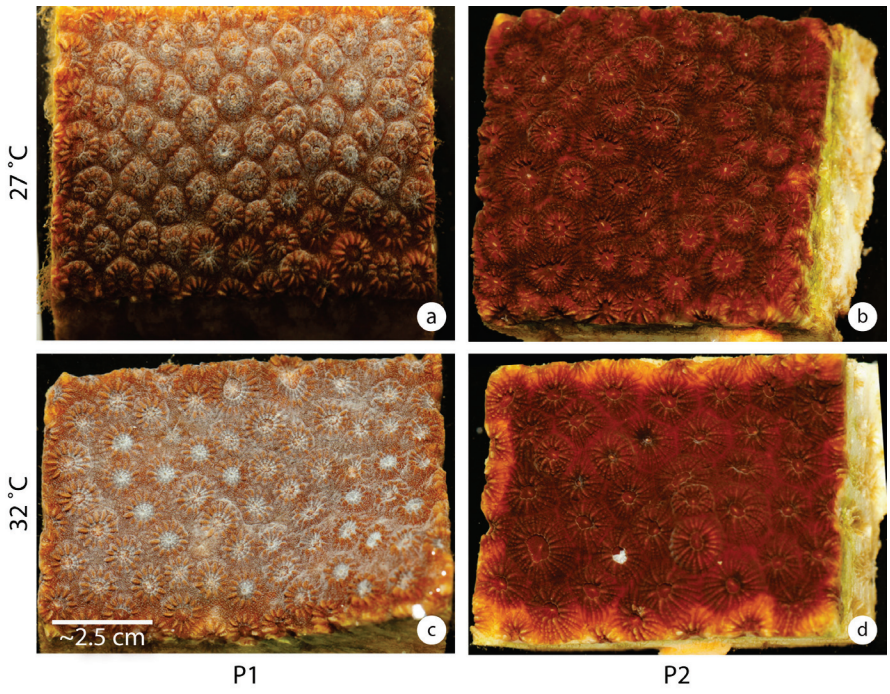

Figure 13. Photos of T_0 specimens from phenotypes 1 (*a, c*) and 2 (*b, d*) at 27 and 32°C.

Microscopically, P1 and P2 phenotypes were recognizably dissimilar. While they obviously shared the same basic coral body plan, there were a few very prominent differences. P1 epidermis contained the pigment cells characteristic of its genus, whereas P2 epidermis was virtually devoid of these cells. P1 morphology as viewed in the saggital sections was characterized by very steep septa and costae with correspondingly deep mesenteries inside deep elongated polyps. The slopes of P2 septa and costae were much more gradual with shallower mesenteries in shorter polyps. P1 had large, abundant, brightly eosinophilic granular gland cells scattered between the gastrodermal cells of the mesenteries toward the oral surface and some deeper in the gastrodermis of the basal body wall of the polyps (Figure 15*a, c, e*), whereas P2 did not (although eosinophilic granular gland cells containing small lysosomes were present on the cnidoglandular bands of the mesenterial filaments and some in the gastrodermis deeper in the polyp in both phenotypes, Figure 15*e, f*). Many oocytes were found in most P2 specimens, while in P1 gonads were almost completely absent (one mesentery with oocytes was observed in one specimen). In P1, the presence of epidermal pigment cells (containing green fluorescent proteins, E.C. Peters pers. comm.) is evident but these were rarely observed in P2 and reduced in size in those rare occurrences (Figure 15*a, b*) The grossly red portions of mesenterial filaments formed

by thin columnar cells packed with eosinophilic granules (which stain positively for iron, E.C. Peters pers. comm.) were present in P1 but not in P2 specimens. Thraustochytrids could not be positively identified in either phenotype microscopically, although it is clear they were present in great numbers in P1 specimens at the gross morphological level.

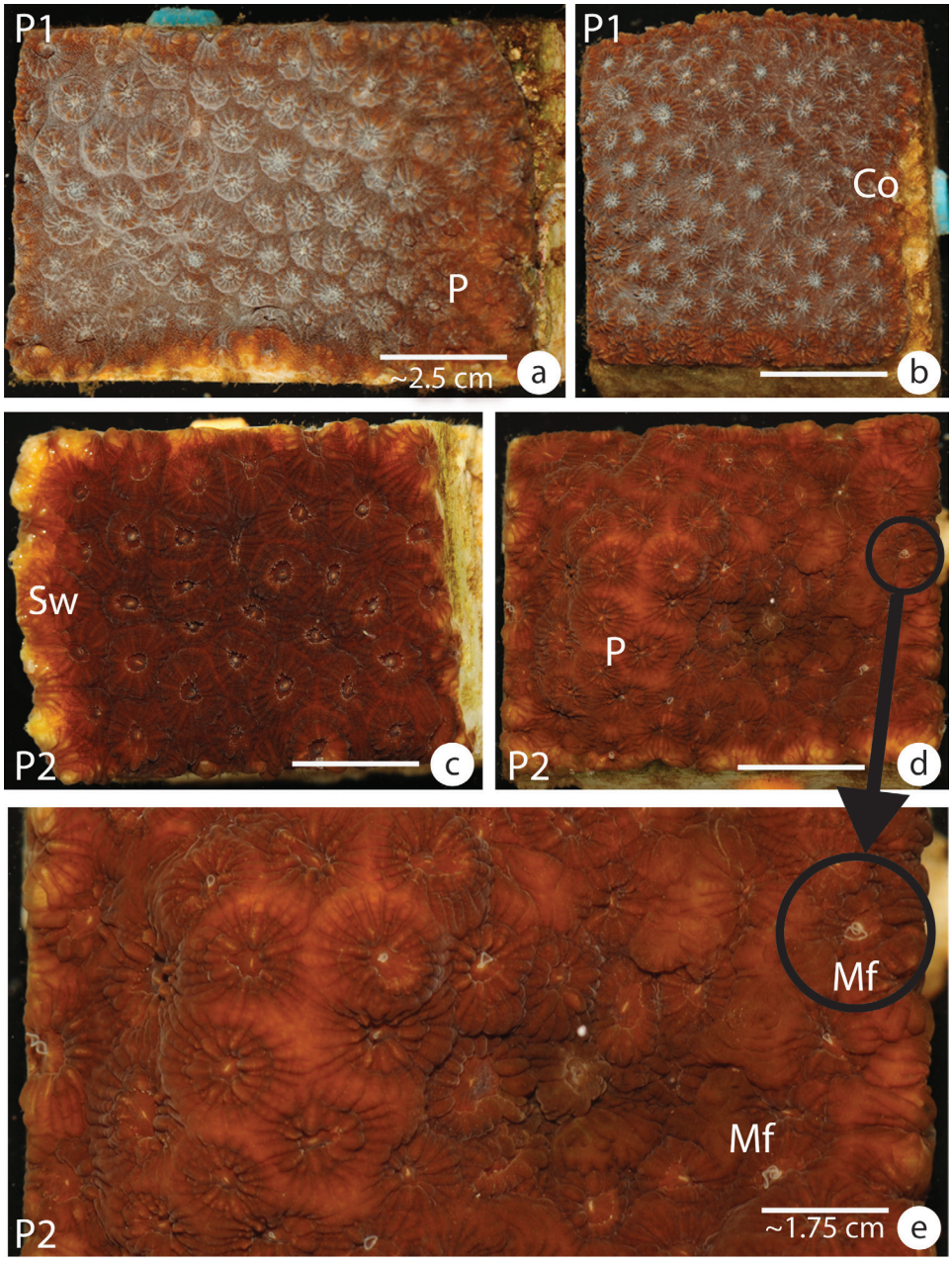

Figure 14. Photos at T_0 of coral phenotypes P1 (*a, b*), P2 (*c, d, e*) in 27°C tanks. P = paling, Co = contracted tissue, Sw = swelling, Mf = mesenterial filaments. Scale bars (*a, b, c, d*) ~2.5 cm.

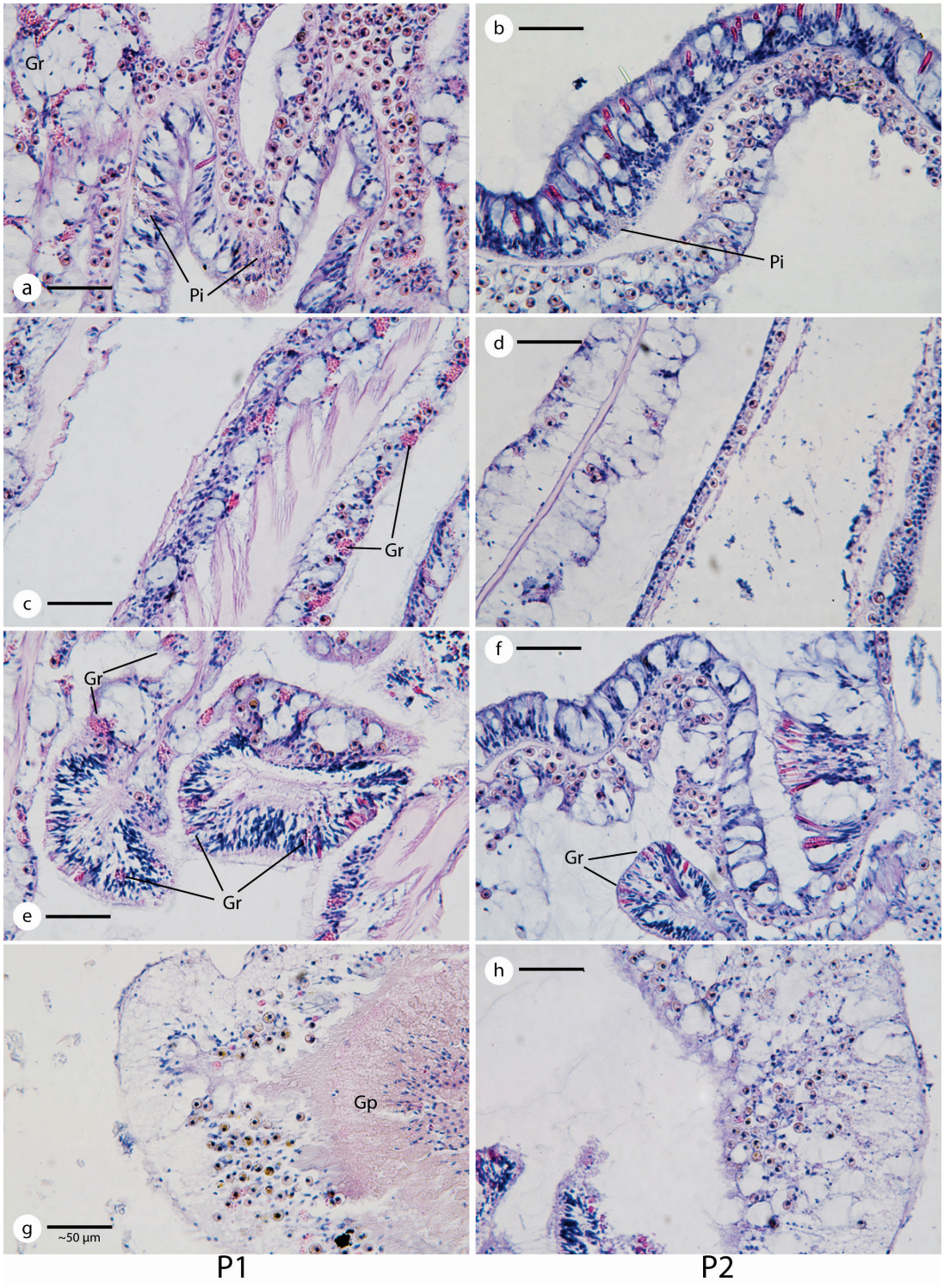

Figure 15. Photomicrographs at 40x of T_0 phenotypes P1 (left) and P2 (right) at 27°C. Photomicrographs (*a*, *b*) show surface body wall, (*c*, *d*) show calicodermis details, (*e*, *f)* show cnidoglandular bands and (*g*, *h*) show degenerating zooxanthellae. Acidophilic granular pigment and granular gland cells present in P1 but not in P2. Gr = large, raspberry-like granular gland cells, Gp = red granular pigment cells, Pi = pigment cells. All scale bars ~50 µm.

Differential responses of phenotypes to different *Vibrio* exposures

Severity and condition scores assigned to the experimental and control specimens were tabulated. Because the coral specimens were subjected to four different bacterial treatments (plus controls) at two different temperatures, the effects of the individual exposures were analyzed first to determine whether the scores for each were statistically different. If not, they could be designated as one exposure at a particular temperature. All bacterial exposures (h^1, h^1+P, h^2, h^2+P) had the same overall effects on all specimens exposed at a particular temperature. This conclusion is based on the Kruskal-Wallis H test performed on all pooled severity scores for the four specimens treated per temperature per time period (Table 4). The total number of data points (N) for each phenotype at a time and temperature is 132 (4 specimens x 33 criteria = 132 data points). Severity of pathological changes to the treated specimens can thus be described by group and temperature.

Table 4. Kruskal-Wallis H test for severity—measuring the frequency of pathological changes—to determine if there were significant differences for all 33 criteria between treatments within each phenotype.

P1

Treated **P1** fragments at 27 ˚C, day 7

Group	N	Median	Min	Max
h^1	33	4.0	0.0	5.0
h^1+P	33	3.0	0.0	5.0
h^2	33	3.0	0.0	5.0
h^2+P	33	2.0	0.0	5.0

p value: 0.145
Kruskal-Wallis H test statistic: 5.39
degrees of freedom: 3

Treated **P1** fragments at 32 ˚C, day 7

Group	N	Median	Min	Max
h^1	33	3.0	0.0	5.0
h^1+P	33	2.5	0.0	4.0
h^2	33	2.0	0.0	4.0
h^2+P	33	3.0	0.0	4.5

p value: 0.318
Kruskal-Wallis H test statistic: 3.524
degrees of freedom: 3

P2

Treated **P2** fragments at 27 ˚C, day 7

Group	N	Median	Min	Max
h^1	33	3.0	0.0	5.0
h^1+P	33	3.0	0.0	5.0
h^2	33	3.0	0.0	5.0
h^2+P	33	3.0	0.0	4.0

p value: 0.820
Kruskal-Wallis H test statistic: 0.923
degrees of freedom: 3

Treated **P2** fragments at 32 ˚C, day 7

Group	N	Median	Min	Max
h^1	33	3.5	0.0	5.0
h^1+P	33	3.0	0.0	5.0
h^2	33	3.0	0.0	4.0
h^2+P	33	3.0	0.0	4.0

p value: 0.221
Kruskal-Wallis H test statistic: 4.4
degrees of freedom: 3

Effects of exposures to *Vibrio* species on *M. faveolata* phenotypes (day 7)

Phenotype 1 at ambient temperature

Many prominent pathological changes to the coral cells and epithelia were observed, although grossly these were difficult to discern (Figure 16). No P1 specimens had visible lesions or areas with changes in pigmentation that appear in CYBD-infected corals in the field. Tissue appeared rather contracted at multiple foci, and the area covered by the opaque white film at T_0 appeared further contracted by d 7 towards the interior of the specimen and around the oral disks of polyps (Figure 16). Overall, all slides of exposed specimens at 27°C stained prominently basophilic (showing more uptake of hematoxylin), which would indicate breakdown of the eosinophilic proteins that would otherwise have stained pink. Control specimens instead stained evenly and brightly with both hematoxylin and eosin (Figure 17*d* compared to *e, f, g, h*).

The SBW of all exposed specimens showed epidermal cells that appeared to be sloughing away from the mesoglea at multiple foci. A large increase in the size and prevalence of hypertrophied mucocytes was evident (Figure 18*a*), many with numerous, sizeable ulcerations on the oral surface. Vacuolated epidermal cells, indistinguishable from enlarged mucocytes, may also have been present. Mucocytes appeared diffusely hypertrophied and vacuolated in the control as well, although they were smaller and fewer than in treated specimens.

Integrity of the epidermis was greatly compromised at numerous foci, with some areas terminating in total loss of the epithelia (or lacking cellular components that stain, rendering visualization impossible). SBW epithelia (epidermis and gastrodermis) at apices of septa (or costae) were extremely attenuated and often the site of sloughing. Control epithelia and symbiont conditions at septa were variable with some showing attenuation, loss of integrity (some ablation) and sloughing whereas other areas appeared mostly intact, although never as thick as in the 1981 ECP healthy samples (Figure 17*a* compared to *c, d;* Figure 19).

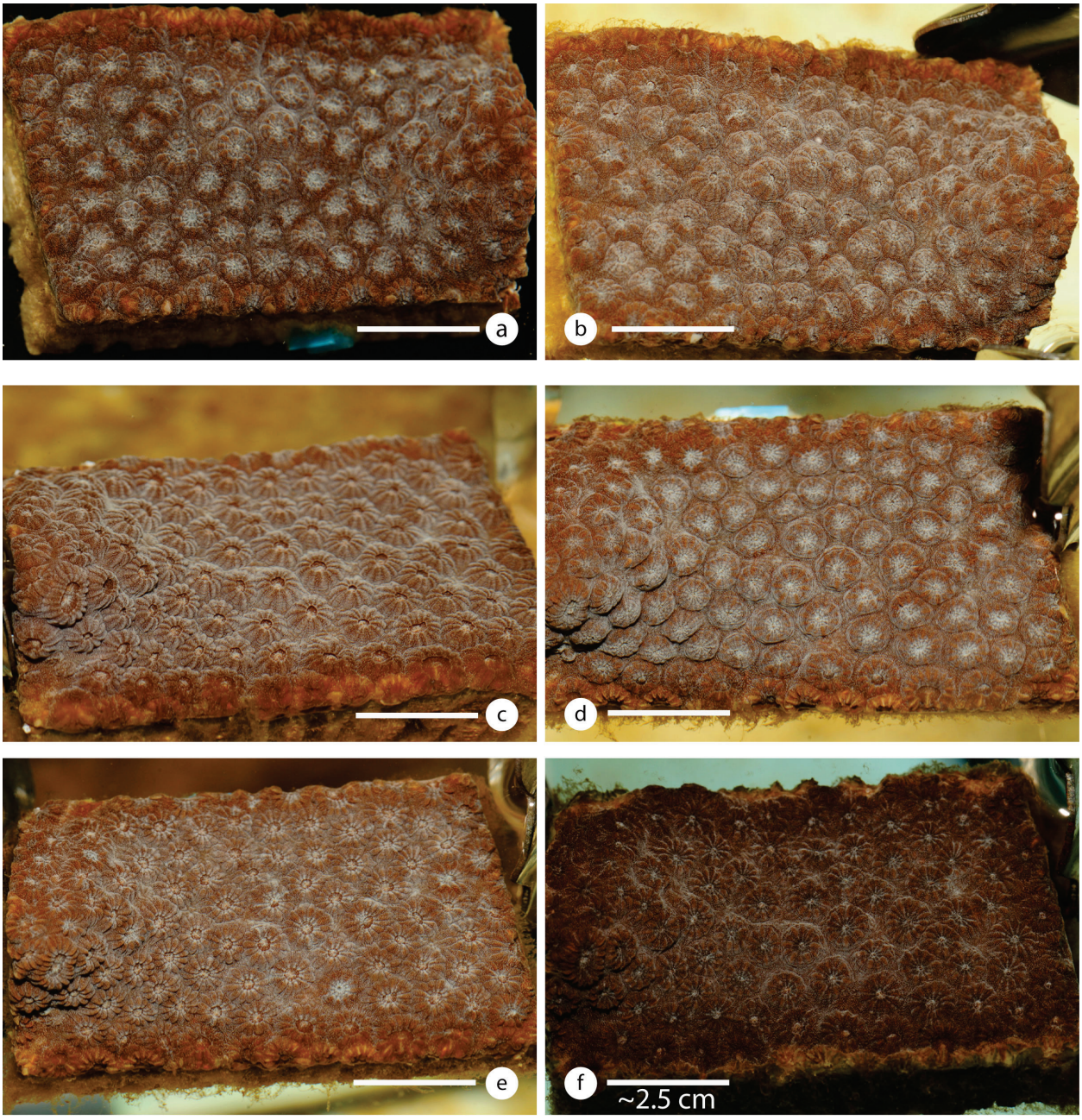

Figure 16. **P1** time series. Photographs taken every 24 h of same specimen at 27°C. Photomicrograph (*a*) T_0, (*b*) T_{24}, (*c*) T_{48}, (*d*) T_{72}, (*e*) T_{96}, (*f*) d 34. All photos were taken at approximately the same time of day with flash. Tissue found paling around the margins of the specimens at T_0, was lost by day 34 and was accompanied by filamentous and fuzzy macroalgae growth on all sides of the recently cut skeletons.

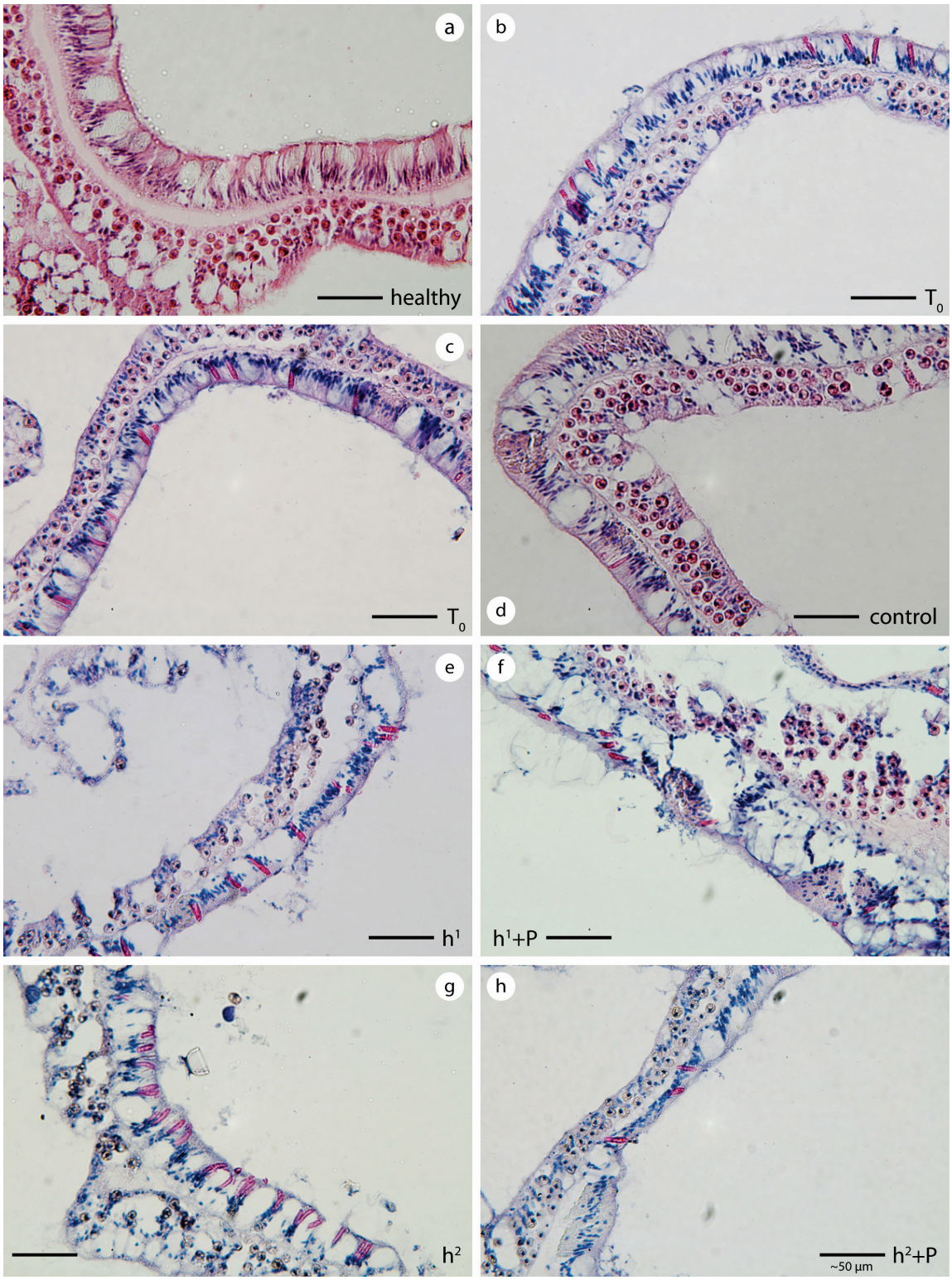

Figure 17. Photomicrographs at 40x of treated **P1** specimens kept in 27°C tanks and sacrificed at day 7 (*e, f, g, h*). To aid visual comparison, healthy *Montastraea faveolata* from 1981 and T_0 photomicrographs were included (*a, b, c, d*). Note clear changes from healthy/controls to treatments and similar responses to the different treatments. All scale bars ~50 µm.

In exposed specimens, feathery, basophilic, cellular extrusions were apparent at the oral surface, flowing into the lumen of the gastrovascular cavity, and in mesenteries. Pockets of debris, which included diatoms and other large particles, were obvious on the surface, presumably in the mucus layer. Cilia of the epidermis were not apparent, which may explain the accumulation of large particle debris. Similar to the epidermis, the gastrodermis exhibited signs of sloughing, loss of integrity, and multifocal attenuation, particularly at septa or costae. Instances of severe attenuation at tips of septa are believed to be abrasions in some instances and scores were given with great caution, reflecting this possibility. Nuclear fading in the epidermis was apparent, but to a much lesser degree than in the gastrodermis. The gastrodermis of the surface body wall and regions of the basal body wall closest to the surface were diffusely littered with karyorrhectic nuclei. These minute fragments of nuclei were also diffuse in the gastrodermis of the control specimen.

Refractile particles of unknown origin and composition were present throughout sections of some of the exposed corals in all layers of tissue including the mesoglea, in the mesogleal pleats, and in particular surrounding zooxanthellae. These particles might have been artifacts and were not included as criteria. They were not found in the control specimens. Very few foci of the epithelia appeared intact and free of pathological changes in exposed specimens (Figure 18). In contrast, epithelia of the control specimen were mildly changed.

The BBW exhibited extensive attenuation of the calicodermis, with severe loss of integrity and detachment of cells from the mesoglea, but not quite sloughing, in treated specimens. Karyolysis of the nuclei of the calicodermis was commonly seen and disorganized clumps of fine basophilic cells believed to be bacteria were found in abundance running along the calicodermis at multiple foci and among the endolithic organisms (filamentous algae, fungal hyphae, sponge tissue and spicules), many of which penetrated upwards into the skeleton and could be found directly below the surface body wall of septa and coenenchyme, often adhering to the tissue (Figure 18*c, g*). Karyolysis in the gastrodermis was also prevalent, and clusters of suspect bacteria were also present in the control along the calicodermis at multiple foci (Figure 17*g, h*) but rarely observed associated with the endolithic communities.

The majority of zooxanthellae exhibited structural deformity, paling and/or decrease in size. Subcellular anatomical features such as the starch collar and pyrenoid body were readily

visible and nuclei appeared stretched or trapezoidal in shape. Exocytosis did not appear to be occurring, although symbiophagy, as evidenced by a high density of zooxanthellae in advanced stages of necrosis found in the gastrodermis of the basal body wall, did appear to be more pronounced in the exposed samples than in controls (Figure 18*a, b, c*). Zooxanthellae of the control stained brightly eosinophilic with overall moderate changes to their shape and size. They exhibited very little of the yellowish-green tint observed in the exposed specimens, although the permanently condensed chromatin of the nuclei did not appear normal in the majority of the cells (Figure 19*c, d, e, f*).

No gonads were present in the mesenteries of any of the specimens except one, and some regions were entirely missing, although none had a ripped or torn appearance indicating artifacts of histological preparation. Cells of the cnidoglandular bands were highly vacuolated and enlarged and were found lacking integrity at multiple foci (Figure 18*d, e*). The bacterial treatments appear to have caused extensive pathological changes to the coral at the tissue and cellular level that were irreversible and presumably impaired function (Figure 5). The control specimens, while clearly responding to stress, appeared to be less impaired, the changes less severe and possibly reversible.

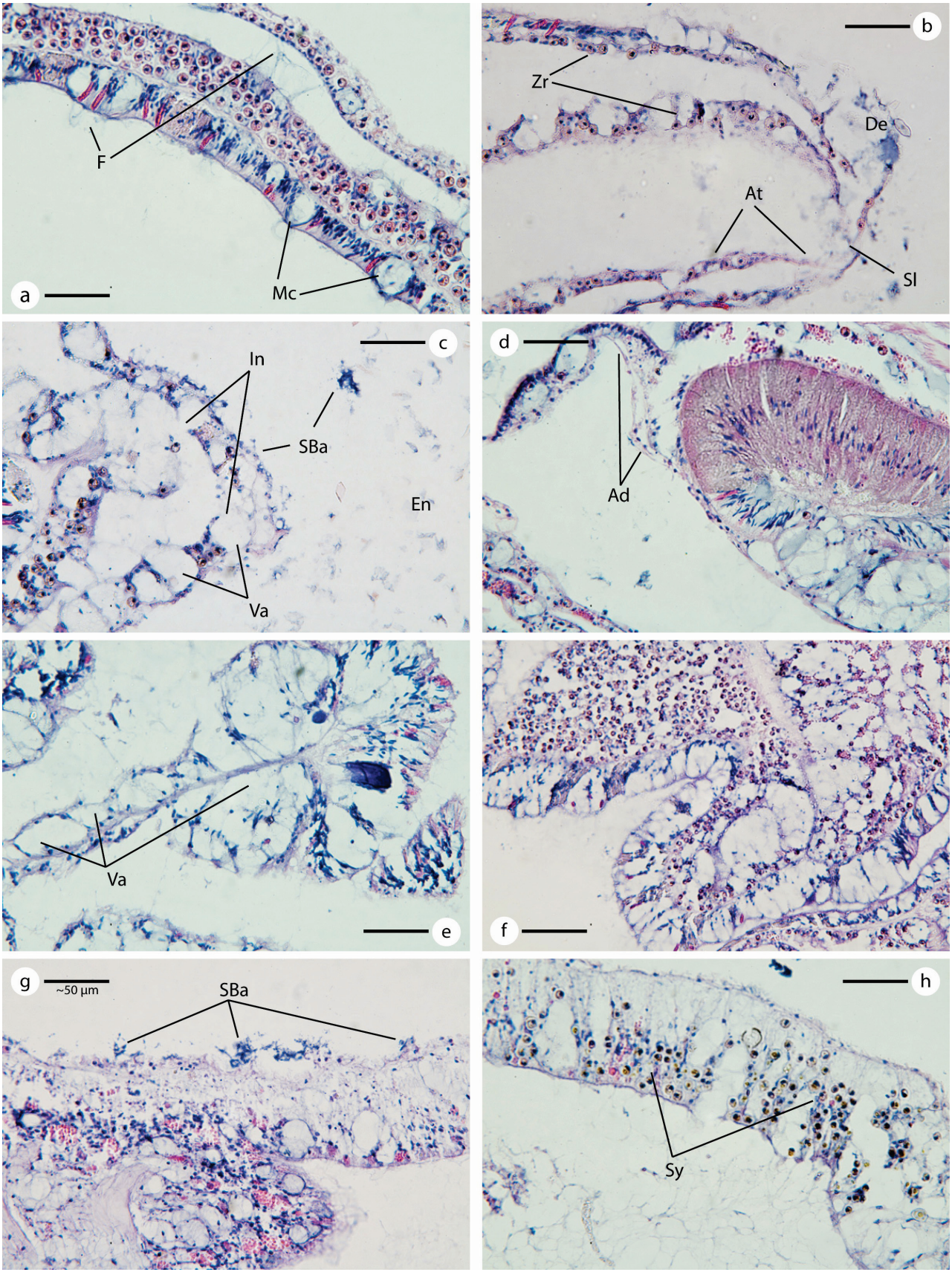
a
F
Mc
b
Zr
De
At
Sl
c
In
SBa
En
Va
d
Ad
e
Va
f
g
~50 µm
SBa
h
Sy

Figure 18. Photomicrographs at 40x of **P1** specimens, held at 27°C, sacrificed day 7. (*a*) changes to SBW, (*b*) sloughing of epidermis, reduction in zooxanthellae, (*c*) BBW with necrotic tissue and suspect bacteria, (*d*) loss of adhesion of the calicodermis, (*e*) cnidoglandular bands with hypertrophied, vacuolated cells, (*f*) vacuolated cells of SBW, (*g*) clumps of suspect bacteria and (*h*) degenerating zooxanthellae in BBW. Mc = mucocytes hypertrophy, F = feathery mucus strands, Va = vacuolated (or hypertrophied) cells, De = debris in mucus, Ad = loss of adhesion, In = integrity loss, En = endolithic organisms, SBa = suspect bacteria, Zr = reduction in zooxanthellae, Sl = sloughing, Sy = symbiophagy. All scale bars ~50 µm.

Observations of the histoslides showed real pathological changes in the specimens with apparent differences between treated and control. Analysis of the severity scores confirmed the differences were statistically significant ($p = 0.002$) with treated scores higher (more severe, median 3.0) than control scores (median 1.0; Table 5).

Table 5. Kruskal-Wallis H test comparing **P1** control specimen severity scores to treated specimen severity scores.

All **P1** at 27 ˚C, day 7

Group	N	Median	Min	Max
Control	33	1.0	0.0	5.0
Treated	132	3.0	0.0	5.0

p value: 0.002
Kruskal-Wallis H test statistic: 9.674
degrees of freedom: 1

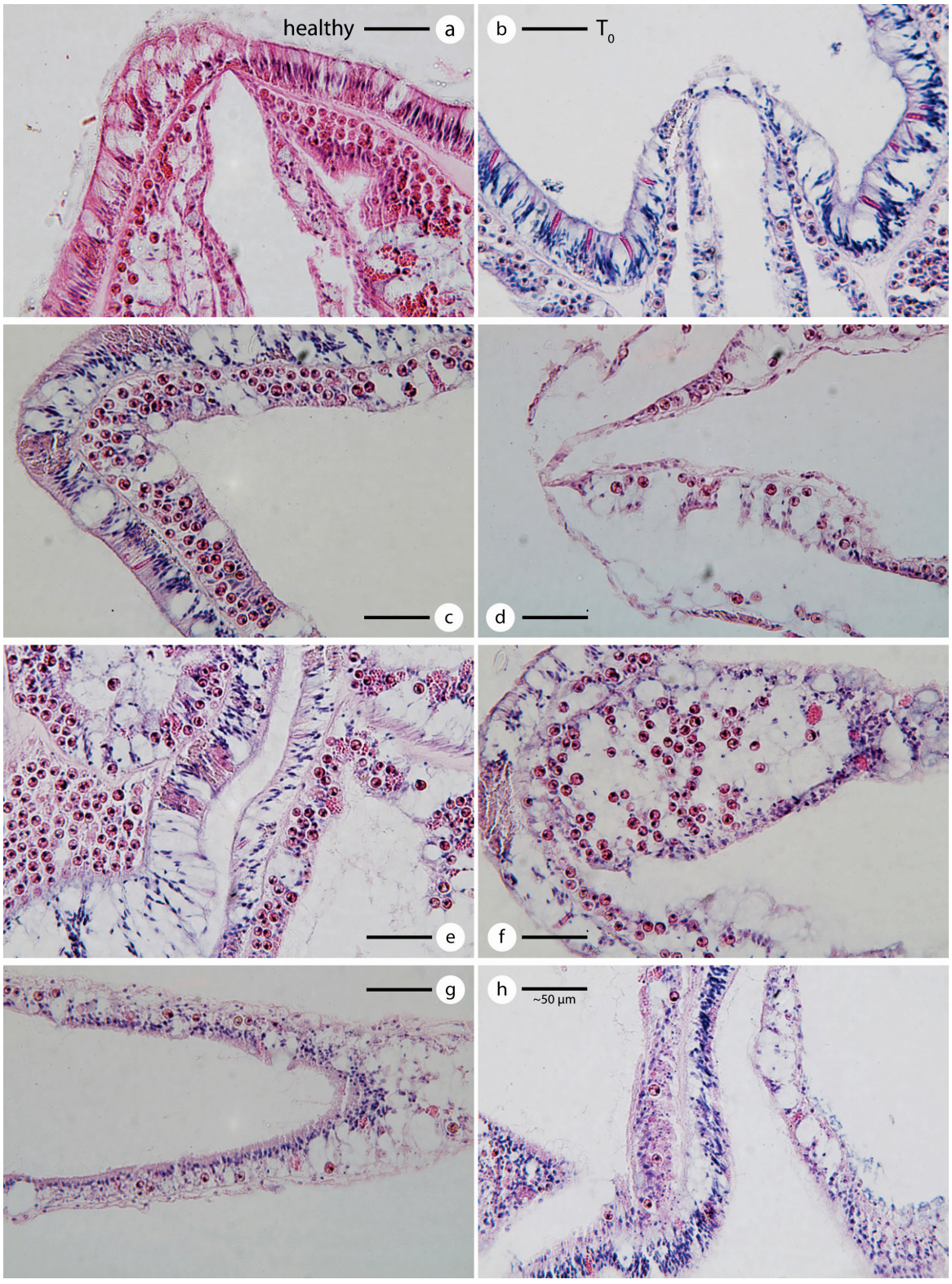

Figure 19. Photomicrographs at 40x of **P1** control specimen at 27°C, sacrificed on day 7. Photomicrograph (*a*) healthy specimen from 1981, (*b*) T_0 specimen. Photomicrographs (*c, d e, f*) show details of SBW and, (*g, h*) BBW of 7 d controls. All scale bars ~50 µm.

Phenotype 2 at ambient temperature

Most of the grossly visible changes that occurred in P2 specimens were only noticeable directly after the exposures (blistered polyps, pale oral disk; Figure 20*b*). Gross morphological changes over the course of the 7 d experiment were subtle to none, but by 34 d multifocal bleaching could be observed on a few specimens and shrunken tissue could be observed on most (Figure 20). No CYBD-like lesions were observed and the opaque white appearance of the P1 specimens was unperceivable in P2 (Figure 21). Microscopically, all exposed P2 slides appeared to have been slightly overstained with hematoxylin. Concurrently, the eosinophilic components (proteins) stained lightly, giving the slides an overall blue/purple quality. As in the P1 slides at 27°C, the cnidocysts stained consistently very brightly indicating that the lack of eosinophilic staining throughout was not an artifact of the staining process, rather an indication of degrading proteins in the tissues. In contrast, the P2 control specimen stained brightly and evenly with both stains (Figure 22; Figure 24).

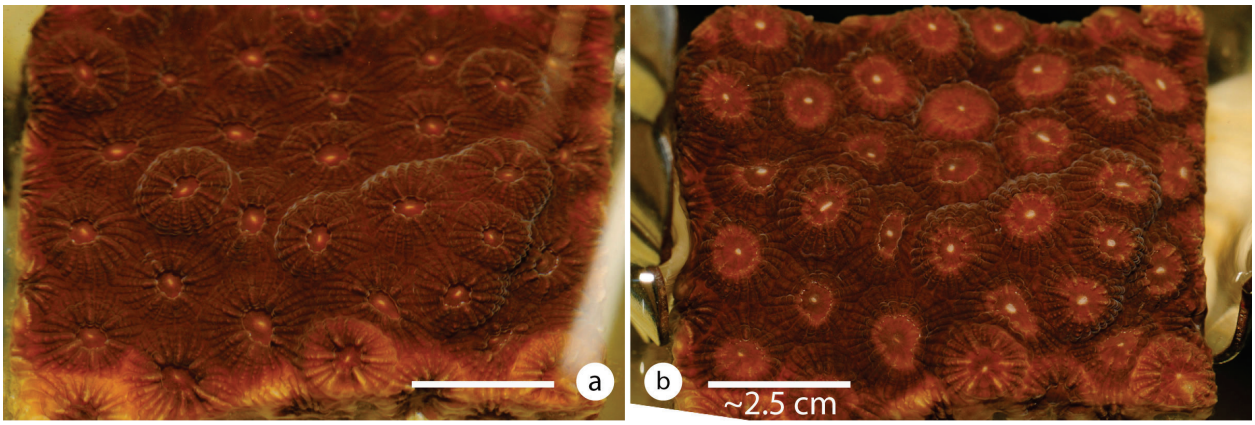

Figure 20. **P2** treated specimen before (*a*) and after (*b*) first bacterial exposure. Notable changes could be observed immediately after exposure but for a few minutes only. Scale bars ~2.5 cm.

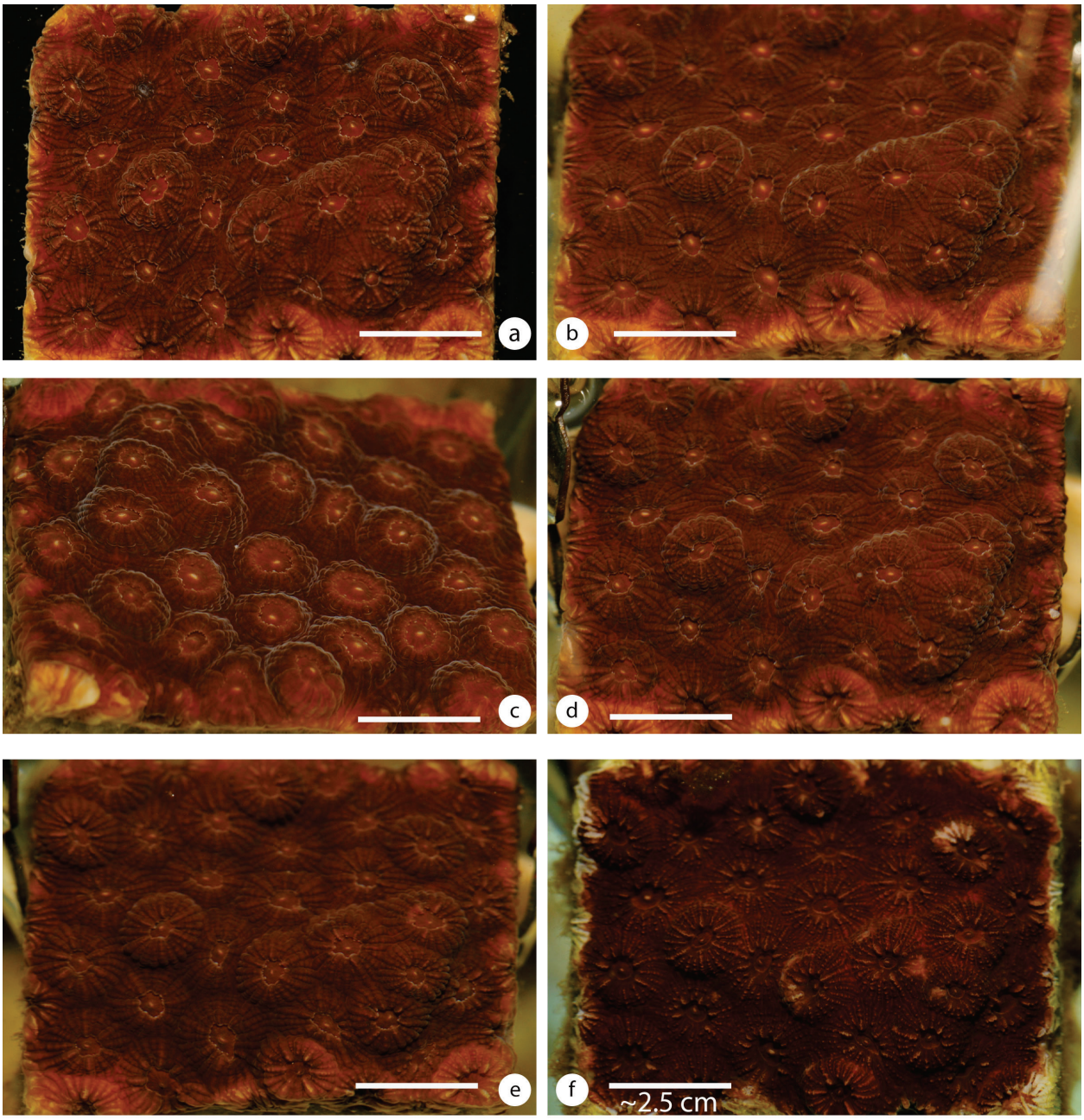

Figure 21. **P2** time series. Photographs taken every 24 h of same specimen at 27°C. Photomicrograph (*a*) T_0, (*b*) T_{24}, (*c*) T_{48}, (*d*) T_{72}, (*e*) T_{96}, (*f*) day 34, note multifocal bleaching. Note pale tissue around the margins at T_0 was lost by d 34 and was accompanied by filamentous and fuzzy macroalgae growth on the skeleton on all sides. Scale bars ~2.5 cm.

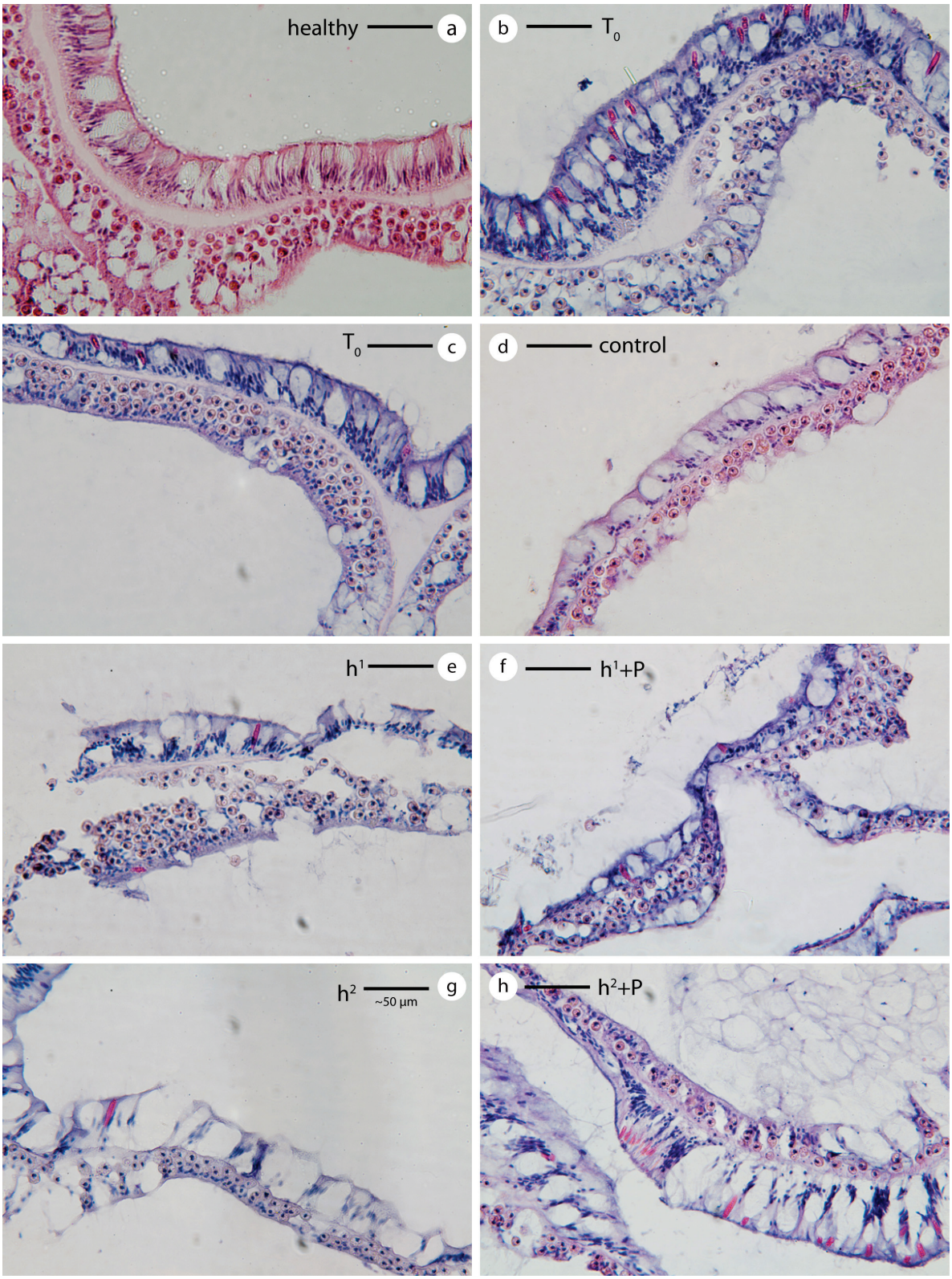

Figure 22. Photomicrographs at 40x of **P2** specimens held at 27°C, sacrificed on day 7. Details of the surface body wall of (*a*) healthy coral collected in 1981, (*b*) and (*c*) T_0 and (*d*) day 7 controls, and (*e, f, g, h*) the four treatment specimens. All scale bars ~50 µm.

In exposed specimens, the SBW exhibited extensive and severe loss of integrity of the epidermis, with less severe integrity loss in the mesoglea and gastrodermis was accompanied by prominent sloughing of the epidermis at multiple foci (Figure 22*e*, 23*f*). In contrast, the epidermis of the control remained mostly contiguous (Figure 24*c, d, e*). Epithelia of the control SBW were in mostly fair to poor condition with mild sloughing of the epidermis at multiple foci and slightly more prominent sloughing of the gastrodermis.

Large particle surface debris was a notable feature in the treated specimens, and a very thick basophilic margin (or a greatly thickened terminal web) at the oral surface of the epidermis, was found where the epidermis remained intact. Cilia of the epidermis were not apparent, which may help to explain the large amount of surface debris. An increase in hypertrophied mucocytes and/or vacuolated cells along with feathery mucus strands spilling outward from the cells of the epidermis were observed (Figure 22*e, f, g, h*; Figure 23*a*). A diffuse increase in mucocytes was also notable in the control specimen (Figure 22*d*; Figure 24*c, d, e*).

Attenuation of the treated epidermis and gastrodermis was occasional in frequency but severe in condition while minimal attenuation of the epithelia was observed in the control SBW. In the control, however, loss of integrity to the SBW gastrodermis and BBW calicodermis was more prominent with no apparent interruptions to the mesoglea, although it is notably attenuated at septa and costae.

The gastrodermis of the challenged specimens was populated with large vacuolated cells or mucocytes at multiple foci (Figure 23*c, d, g, h*) and numerous regions were detached from the mesoglea. The control gastrodermis was also somewhat commonly detached from the mesoglea while the epidermis showed minimal loss of adhesion. Paling nuclei of the epidermis were somewhat prominent as was paling of nuclei in the gastrodermis accompanied by changes in their shape. Karyorrhectic nuclei were abundant and consistently present in the gastrodermis, and present in mostly low numbers and sporadically in the epidermis (Figure 23*a, b, c, f*). Karyorrhectic nuclei were also distinctly present in the control (Figure 24*f*) and degeneration of the host nuclei of the gastrodermis was diffuse, while most nuclei of the epidermis and calicodermis appeared in good condition. Suspect bacteria in the treated specimens were not found present on or near any of the epithelia of the SBW with the exception of minimal amounts along the oral surface of the epidermis.

In challenged specimens, the calicodermis of the BBW did not appear attenuated but was associated with clusters of suspect bacteria at multiple foci throughout the sections, and was vacuolated with a porous, foamy appearance in numerous areas (Figure 23*f, g*). Integrity loss, karyolysis, and lack of adhesion to the mesoglea were patchy features of the calicodermis, but sloughing was not apparent. Enlarged vacuolated cells and loss of integrity of the gastrodermis were prominent (Figure 23*d, g*). In contrast, there was some loss of adhesion and integrity in the calicodermis of the control, but no suspect bacteria were observed along the calicodermis or associated with the endolithic communities.

Pathological changes in the zooxanthellae were moderate in severity but their condition was mostly poor in exposed specimens. They exhibited some deformity in shape, minimal paling, and/or decrease in size. The starch collar and pyrenoid body were somewhat visible and the nuclei appeared to be stretched or trapezoidal in shape (Figure 23*d*). Most of the zooxanthellae had a yellowish-green tint. Exocytosis was observed but not common. Similar changes were observed in the control symbionts with the exception of their cell shape, color, and size, which were only mildly altered from the T_0 specimens. Highly degenerated zooxanthellae in the deep gastrodermis of the BBW had a low prevalence in the exposed specimens, while in the control they were a prominent feature (Figure 24*h*).

Epithelia of the challenged specimens' mesenteries showed multifocal loss in integrity, while in the control the changes were actually more severe. Enlarged vacuolated cells were a prominent feature in exposed specimens, especially in the cnidoglandular bands, but lobe margins remained fairly intact (Figure 23*c*). Gonads in all P2 specimens were present but paling appearance indicated degradation. There was also a notable lack of the large, red, granular pigment cells that were present in the P1 specimens and only a few acidophilic granular gland cells as compared to P1 mesenteries.

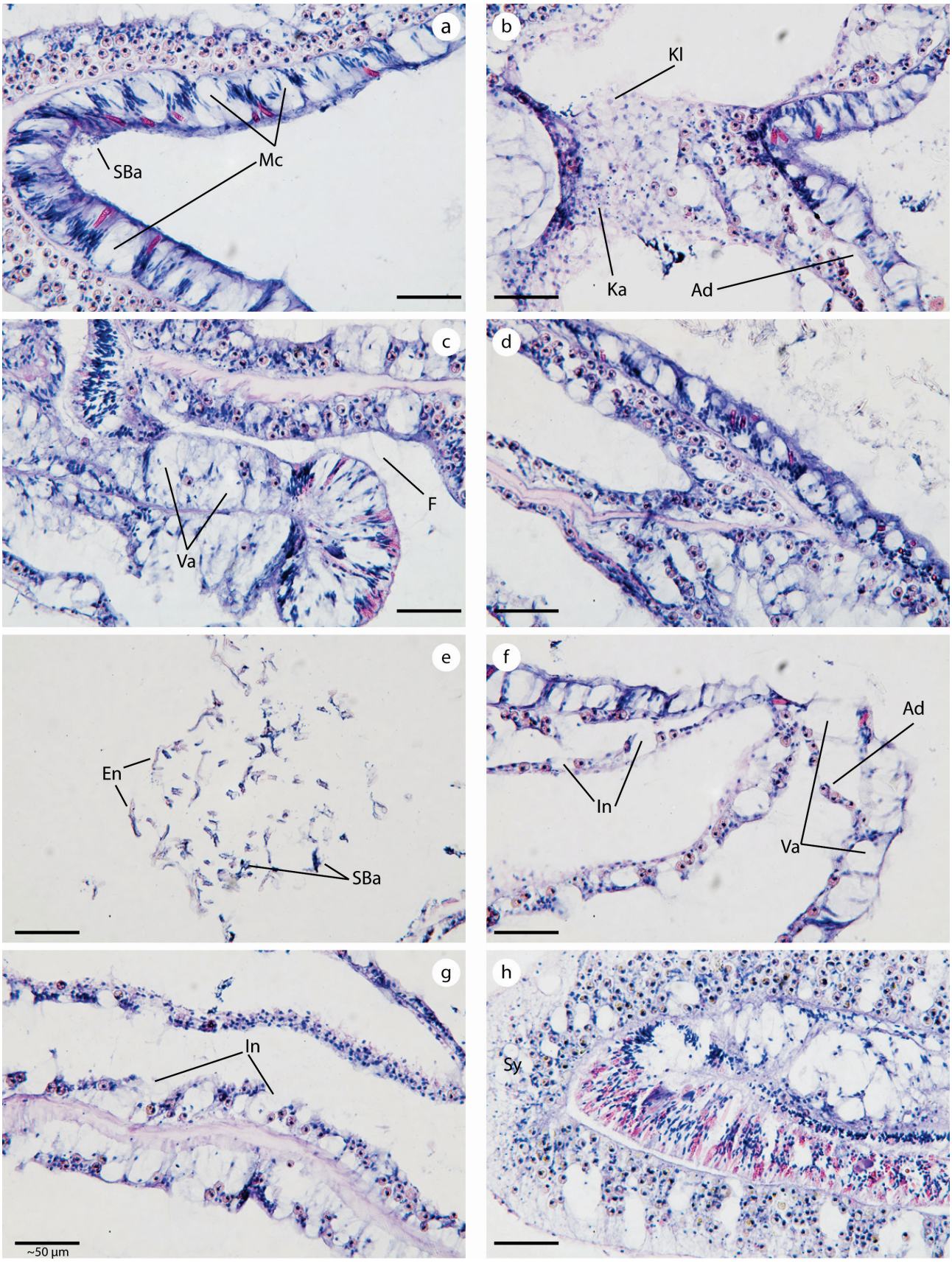
a
SBa
Mc
b
Kl
Ka
Ad
c
F
Va
d
e
En
SBa
f
Ad
In
Va
g
In
~50 µm
h
Sy

Figure 23. Photomicrographs at 40x of **P2** specimen, treated at 27°C and sacrificed on day 7. Photomicrograph (*a*) shows contiguous epidermis with some loss of integrity of the gastrodermis (*b*) loss of adhesion of the gastrodermis and karyolysis and karyorrhectic nuclei, (*c*) enlarged vacuoles of the cnidoglandular band, (*d*) vacuoles in the gastrodermis, (*e*) endolithic organisms with associated suspect bacteria, (*f*) septum with loss in integrity of the gastrodermis and hypertrophied mucocytes in epidermis, (*g*) shows loss of integrity to epithelia of BBW, (*h*) symbiophagy in the deep basal body wall. Mc = mucocytes hypertrophy, F = feathery mucus strands, Va = vacuolated cells (or hypertrophied), Ad = loss of adhesion, In = integrity loss, En = endolithic organisms, SBa = suspect bacteria, Sy = symbiophagy, Kl = karyolysis, Ka = karyorrhexis. All scale bars ~50 µm.

Similar to the P1 specimens, scores for P2 challenged specimens were significantly higher than those for the control, indicating that the challenged specimens were negatively affected by the bacterial exposures (Table 6).

Table 6. Kruskal-Wallis H test comparing **P2** control specimen severity scores to challenged specimen severity scores

All **P2** at 27 ˚C, day 7

Group	N	Median	Min	Max
Control	33	1.0	0.0	5.0
Treated	132	3.0	0.0	5.0

p value: 0.039
Kruskal-Wallis H test statistic: 4.271
degrees of freedom: 1

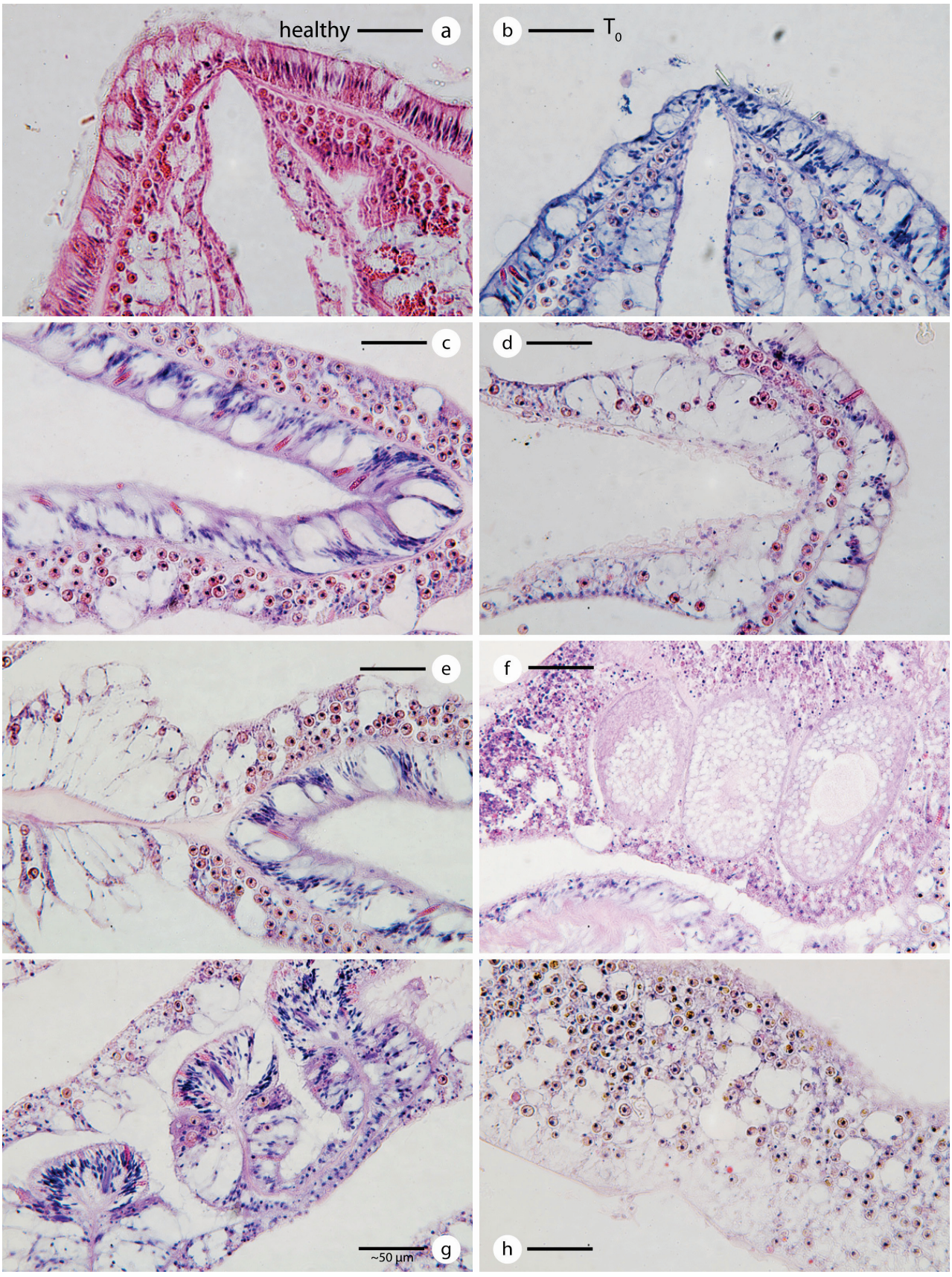
healthy
a
b
T_0
c
d
e
f
g
~50 µm
h

Figure 24. Photomicrographs at 40x of control **P2** specimens held in 27°C tanks and sacrificed on day 7. In (*a*) 1981 ECP healthy sample, and (*b*) T_0 control for visual comparison. Photomicrographs (*c*, *d* and *e*) show details of SBW highlighting hypertrophied mucocytes and/or vacuolated cells, (*f*) shows oocytes surrounded by mesoglea and cell debris accumulated in the gastrodermal cells of this mesentery, (*g*) cnidoglandular bands in contact with the BBW, (*h*) deep region of BBW with large numbers of degenerating zooxanthellae. Note abundance of enlarged mucocytes and/or vacuolated cells in epidermis of the T_0 control specimen (*b*) and lack thereof in the healthy specimen (*a*). All scale bars ~50 μm.

Differential responses of P1 and P2 to bacterial exposures at ambient seawater temperature

Comparative statistical analysis of all severity scores between P1 and P2 held at 27°C yielded results that support the null hypothesis. No statistical differences were found between phenotypes. The tallied mean of each individual specimen's severity scores, which corresponds to an overall pathological response to exposures (evaluated with all non-weighted criteria), and the tallied mean for the group can be viewed in Table 7. The tallied mean of the **P1** treated group's severity scores is 51%, while the **P2** treated group tallied mean was 48%. Individual tallied scores for P1 ranged from 40% to 58% and individual tallied scores for P2 ranged from 45% to 51%. The control specimen severity score for P1 was 25%, and P2 was 32%. The variance from the mean in the P2 group as compared to the P1 group was smaller, as P2 scores tended to cluster closer to the mean than the P1 scores (Table 7).

The overall **P1** *condition* tallied mean score was 55% with individual treatment scores ranging from 45% to 61% and the **P2** treated condition score was 57% with individual specimen scores ranging from 45% to 60%. It should be recalled that condition scores were assigned as a function of the severity scores and as such were used strictly as a guide to understand the *quality* of the pathological change (i.e., how bad) in a coral specimen at the location in which pathological change(s) occurred (Table 7). Condition scores tended to be higher than the severity scores for all specimens, which suggest that the quality of the condition was consistently worse than the frequency of the pathological change itself.

Table 7. Tallied mean scores for P1 and P2 specimens held at 27°C, day 7. Four specimens per phenotype were exposed to bacteria.

SEVERITY	P1	P2	CONDITION	P1	P2
Exposed specimen	**Mean Overall score**		**Exposed specimen**	**Mean Overall score**	
1	58%	51%	**1**	61%	60%
2	52%	50%	**2**	55%	56%
3	52%	45%	**3**	58%	55%
4	40%	45%	**4**	45%	56%
Mean of all exposed	**51%**	**48%**	**Mean of all exposed**	**55%**	**57%**
control	25%	32%	**control**	33%	45%

Table 8. Comparison of all criteria between phenotypes of treated and controls for specimens held at 27°C, sacrificed on day 7.

Treated **P1 and P2**, 27 ˚C, day 7

Pheno type	N	Median	Min	Max
P1	132	3.0	0.0	5.0
P2	132	3.0	0.0	5.0

p value: 0.487
Kruskal-Wallis H test statistic: 0.484
degrees of freedom: 1

Control P1 and P2, 27 ˚C, day 7

Pheno type	N	Median	Min	Max
P1	33	1.0	0.0	5.0
P2	33	1.0	0.0	5.0

p value: 0.523
Kruskal-Wallis H test statistic: 0.408
degrees of freedom: 1

Effects of elevated temperature on P1 specimens

The pathological changes observed in specimens held at 32°C were similar to those held at 27°C with few exceptions. Elevated temperature did not appear to be a contributing factor to the pathology observed in P1 specimens. As in the 27°C treated specimens, the 32°C treated

specimens stained overall very basophilic (purple) while the P1 control specimen stained brightly eosinophilic but not as brightly basophilic.

The SBW of P1 specimens exhibited a very pronounced lack of contiguous epidermis and a diffuse increase in hypertrophied mucocytes throughout the epithelia. (Figure 25*b*). The control also exhibited pronounced multifocal loss in integrity of epidermis and gastrodermis, but with less severity, and a less pronounced increase in hypertrophied mucocytes (Figure 26*c, d, e*). Unlike the 27°C control, the hypertrophied mucocytes in the 32°C control were as large as those in the treated specimens.

Epidermal and mesogleal attenuation, also conspicuous in the coenenchyme in 32°C specimens, were observed at multiple foci. Eosin staining of the tightly coiled tubules in the spirocytes was bright and many appeared to be clumping together with some uncoiled and discharged. Pockets of large aggregates of surface debris were observed in challenged specimens (Figure 25*d*), but mucus debris in the control was slightly more prominent at multiple foci and was made up primarily of suspect bacteria (Figure 26*d*). As in the 27°C treated specimens, karyorrhectic nuclei in the gastrodermis were prominent and degenerated host gastrodermal nuclei were diffuse. The fragmented nuclei were observed in the gastrodermis of the control, but with less frequency.

Symbiophagy appeared more prominently in the deep regions of the BBW in both treated and control specimens at 32°C than at 27°C (Figure 25*e*; Figure 26*g*). Changes to the zooxanthellae were a prominent feature of the 32°C treated specimens as they were in the 27°C specimens, but a great decrease in density of the symbionts throughout gastrodermal epithelia was also noted and is consistent with thermal bleaching. Those observed were very pale at multiple foci, especially at specimen margins, and possessed a generally yellow/green tint in the interior regions of the section (Figure 25*b, c*), whereas control zooxanthellae exhibited prominent degeneration of the nuclei and moderate changes in shape, color and size, but stained brightly eosinophilic, like their 27°C counterparts, with no green or yellow hue (Figure 26*c, d, e*) that suggests breakdown of the cell wall and cytoplasm.

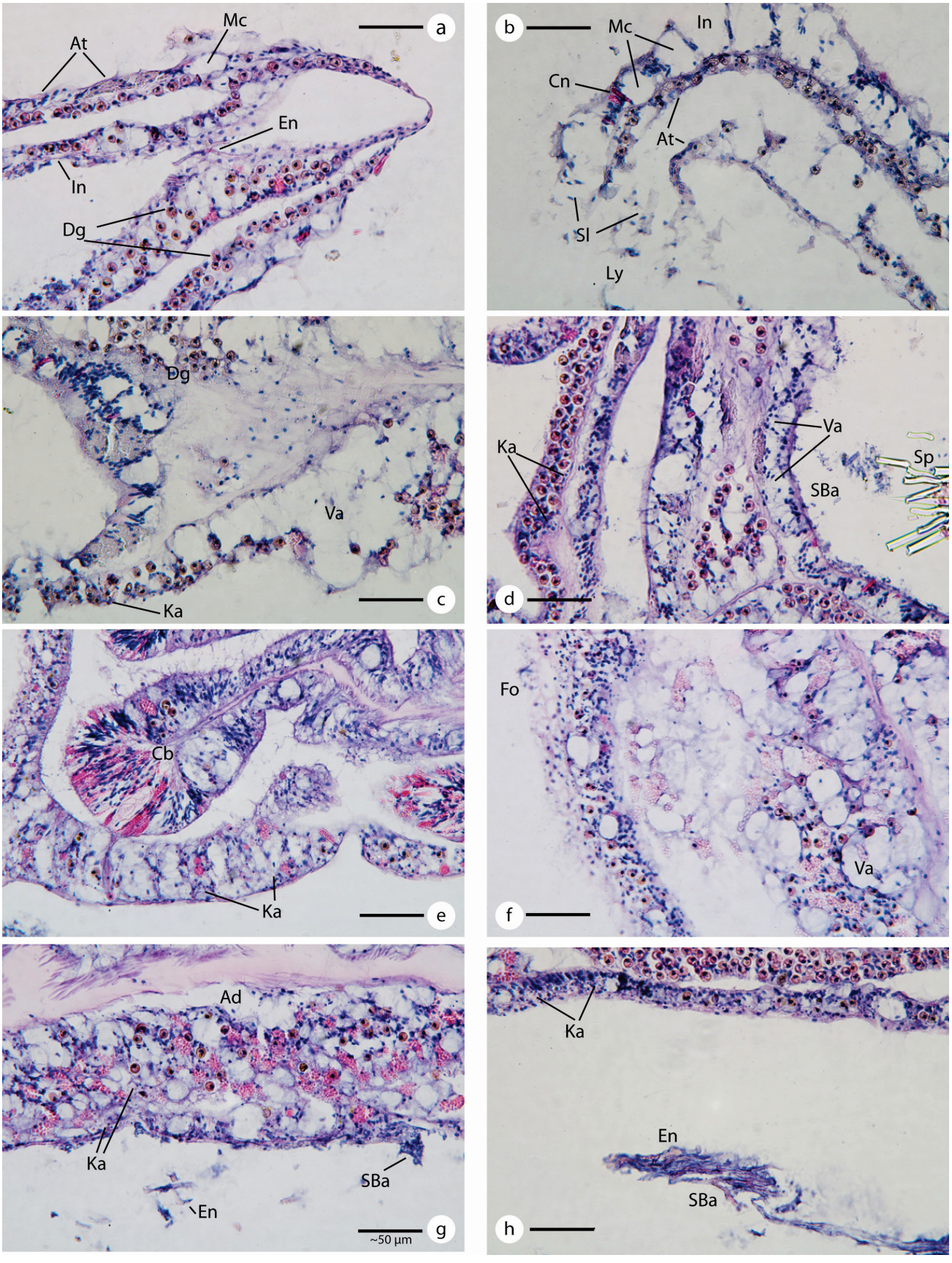
a
Mc
At
En
In
Dg
b
Mc
In
Cn
At
Sl
Ly
Dg
Va
Ka
c
Ka
Va
Sp
SBa
d
Cb
Ka
e
Fo
Va
f
Ad
Ka
SBa
En
~50 µm
g
Ka
En
SBa
h

Figure 25. Photomicrographs at 40x of **P1** treated specimens at 32°C, sacrificed day 7. Photomicrograph (*a*) shows attenuation, hypertrophied cells, and degenerated zooxanthellae, (*b*) sloughing, cell lysis, hypertrophied mucocytes, and reduction in and degeneration of zooxanthellae, (*c*) decrease in density of zooxanthellae, vacuolated cells of gastrodermis, (*d*) vacuolated epidermis, suspect bacteria on oral surface and karyorrhectic nuclei in gastrodermis, (*e*) mesenterial filaments with moderate symbiophagy and vacuolated cells, (*f*) foamy texture of the calicodermis of the deep BBW, (*g*) mesenteries with degenerated zooxanthellae and granular gland cells, suspect bacteria along calicodermis and endolithic organisms, (*h*) BBW replete with karyorrhectic nuclei and endolithic organisms surrounded by suspect bacteria. Cn = cnidocytes (spirocytes), Mc = mucocytes hypertrophy, At = attenuation, Va = vacuolated cells, enlarged (or hypertrophied), Ad = loss of adhesion, In = integrity loss, En = endolithic organisms, SBa = suspect bacteria, Sy = symbiophagy, Dg = degeneration, Ka = karyorrhectic nuclei, Gr = large, raspberry-like granular gland cells, Fo = foamy texture of calicodermis, Ly = cell lysis, Sl = sloughing, Sp = spicules of sponge, Cb = cnidoglandular band. All scale bars ~50 μm.

The zooxanthellae of the P1 specimens exhibited more yellowing at 27°C than at 32°C. The color change in the zooxanthellae is thought to be a manifestation of the breakdown of the cell wall and degradation of the cytoplasm (Esther Peters, pers. comm.) and potentially the chloroplasts of the algal cell. This presumably leaves pigments diadinoxanthin and peridinin—the characteristic pigments of the zooxanthellae—unsheathed and visible. It follows that the more visible the yellow/green color, the more degraded the cell wall and cytoplasm.

Minimal to moderate losses in integrity of the mesenteries were observed in the treated and control specimens (Figure 25*f*; Figure 26*h*) although no regions appeared entirely missing as in the 27°C specimens.

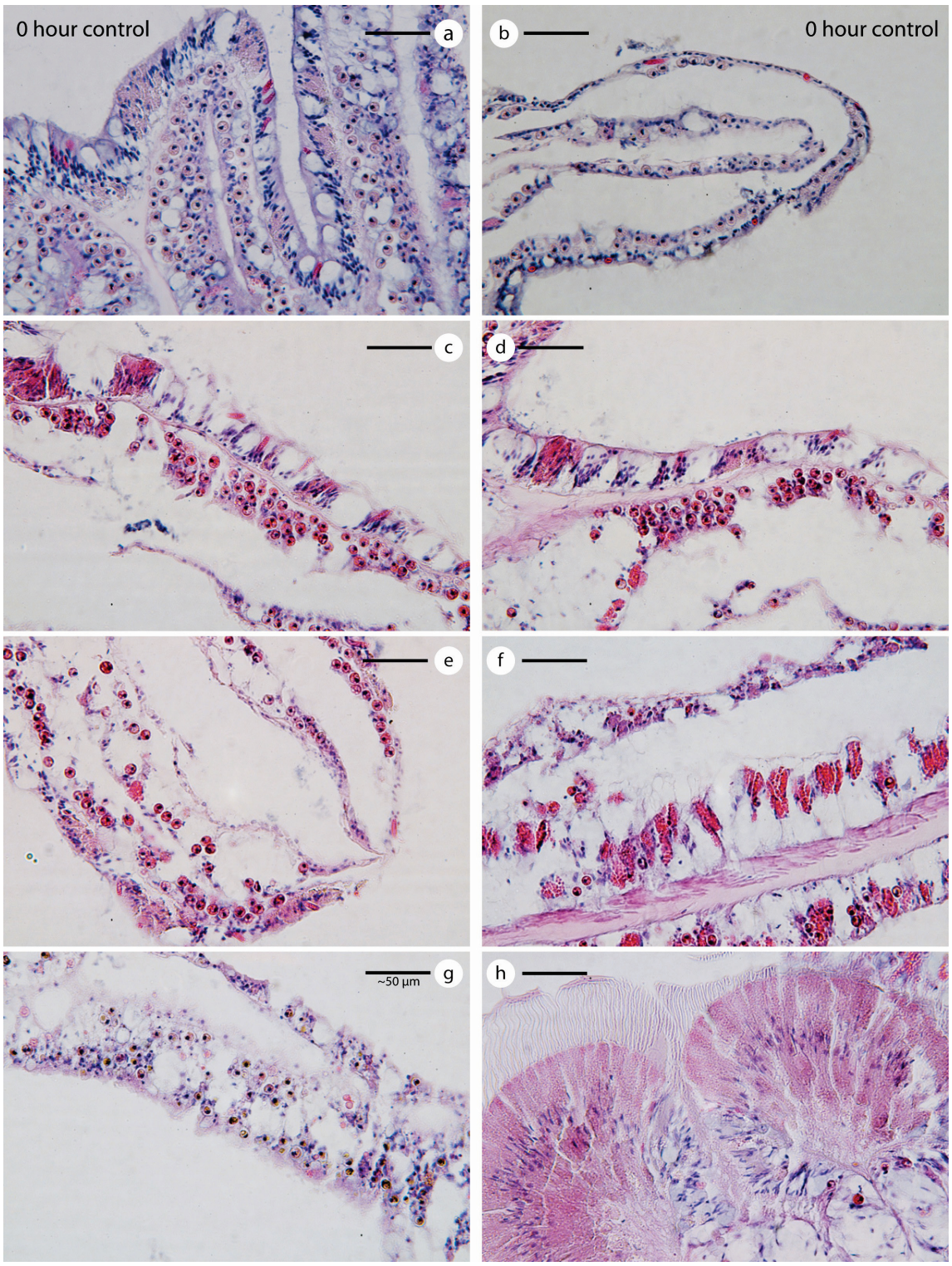

Figure 26. Photomicrographs at 40x of control **P1** specimen held at 32°C. Photomicrograph (*a*, *b*) T_0 control, for visual comparison. Control specimens, (*c, d, e*) show details of the SBW, (*f, g* and *h*) shows details of the BBW and/or mesenteries. Note condition of T_0 control specimen in (*b*)—this particular view of greatly attenuated epithelia of the septa. All scale bars ~50 µm.

The modest differences observed between the P1 specimens at 27 and 32°C were analyzed statistically. The results show that there was no statistical difference between exposed specimens held at 27°C and 32°C, nor for the control specimens. Thus, temperature did not play a significant role in the observed changes (p-values > 0.05; Table 9), although the results for the treated specimens were much closer to significant than the control specimens. All 33 criteria were then scrutinized for temperature effects. The analysis yielded three criteria for which the specimens' scores were significantly different (Figure 27). Significant temperature effects in P1 treated specimens were evident in mucus debris (p = 0.019), suspect bacteria in the calicodermis (p = 0.019) and yellow/green zooxanthellae (p = 0.034). Interestingly, median scores for all three criteria were lower at 32°C than at 27°C.

Table 9. Comparison of **P1** treated and control specimens between two temperatures.

Treated **P1** fragments, day 7

Temp (˚C)	N	Median	Min	Max
27.0	132	3.0	0.0	5.0
32.0	132	2.75	0.0	5.0

p value: 0.087
Kruskal-Wallis H test statistic: 2.928
degrees of freedom: 1

Control **P1** fragment, day 7

Temp (˚C)	N	Median	Min	Max
27.0	33	1.0	0.0	5.0
32.0	33	2.0	0.0	4.0

p value: 0.257
Kruskal-Wallis H test statistic: 1.288
degrees of freedom: 1

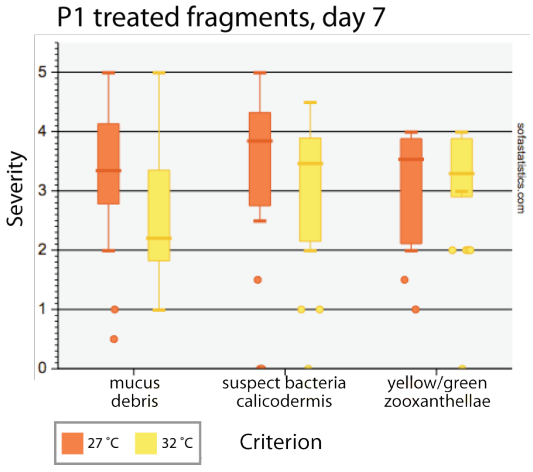

Figure 27. Criteria for which P1 scored significantly different in severity between 27°C and 32°C.

Effects of elevated temperature on P2 specimens

As in the P1 specimens, pathological changes observed in the P2 treated specimens at 32°C were very similar to those observed in the 27°C specimens. A great increase in the size and frequency of hypertrophied mucocytes in the SBW appeared to be the result of cell lysis with a loss of cell membrane integrity, resulting in the expansion of the cells as water was drawn in. The overall effect was that of an expanding epidermis although the terminal web remained largely intact (Figure 28*d*). These differed from P1 specimens in size but not in frequency. The control specimen also exhibited notable amounts of hypertrophied mucocytes (or vacuoles) in the gastrodermis and a loss of integrity as a result.

Discharging mucocytes were diffuse, though surface debris was slightly less prominent than in P1 specimens at 32°C. Increases in mucus and mucus debris in the controls were minimal (Figure 30*c, d, e, f*). Spirocysts in remaining epidermis appeared to be clumping together and multifocal sloughing of the epidermis was observed, especially at septa or costae.

In the BBW, alternating patches of attenuated and foamy-textured calicodermis were prominent in the BBW (Figure 28*a, c*), which differs from the primarily foamy calicodermis of the 27°C specimens. Clusters of suspect bacteria along the calicodermis were diffuse in deep polyps and along the coenenchyme (Figure 28*a*) as in the 27°C specimens but deep regions of the gastrodermis were populated with numerous, enlarged, vacuolated cells and great quantities of zooxanthellae at various stages of degeneration (Figure 28*h*). Minimal symbiophagy was also observed in the control (Figure 30*g*).

As in their 27°C counterparts, zooxanthellae of the 32°C specimens showed prominent multifocal shape, size and color changes to the cells and prominent changes to the nuclei (Figure 28*a, d*) in exposed, but changes in control zooxanthellae were mild and infrequent. Patent yellowing of the zooxanthellae at multiple foci was observed in treated and control specimens and some exocytosis was detected, though it often appeared to be due to disruption of gastrodermal cell membranes. This disruption was not a prominent feature of the 27°C specimens.

Disintegrating oocytes in the mesenteries and lipid-filled patches were apparent in all gonads of the treated specimens. Mesenteries appeared crowded and bulging with numerous

hypertrophied vacuolated cells. The majority of the mesentery regions showed loss of integrity, likely as a result of the hypertrophied or swollen cells. Suspect bacteria were diffuse among the endolithic organisms, which were also present in great numbers (Figure 28*a, c, d, e, f, g*). In contrast, the epithelia and the oocytes in the mesenteries were largely intact in the control but similar to the exposed, suspect bacteria were diffuse among the endolithic organisms.

As with the P1 specimen analysis of severity scores between temperatures, no significant difference was found. These results support the null hypothesis for the P2 specimens as p-values range from 0.636 to 0.932 and again show that temperature was not a major factor affecting or causing pathology in the P2 specimens (Table 10).

Table 10. Comparison between temperatures of P2 treated and control specimens

Treated **P2** fragments, day 7

Temp (˚C)	N	Median	Min	Max
27.0	132	3.0	0.0	5.0
32.0	132	3.0	0.0	5.0

p value: 0.636
Kruskal-Wallis H test statistic: 0.224
degrees of freedom: 1

Control **P2** fragment, day 7

Temp (˚C)	N	Median	Min	Max
27.0	33	1.0	0.0	5.0
32.0	33	1.5	0.0	4.0

p value: 0.932
Kruskal-Wallis H test statistic: 0.007
degrees of freedom: 1

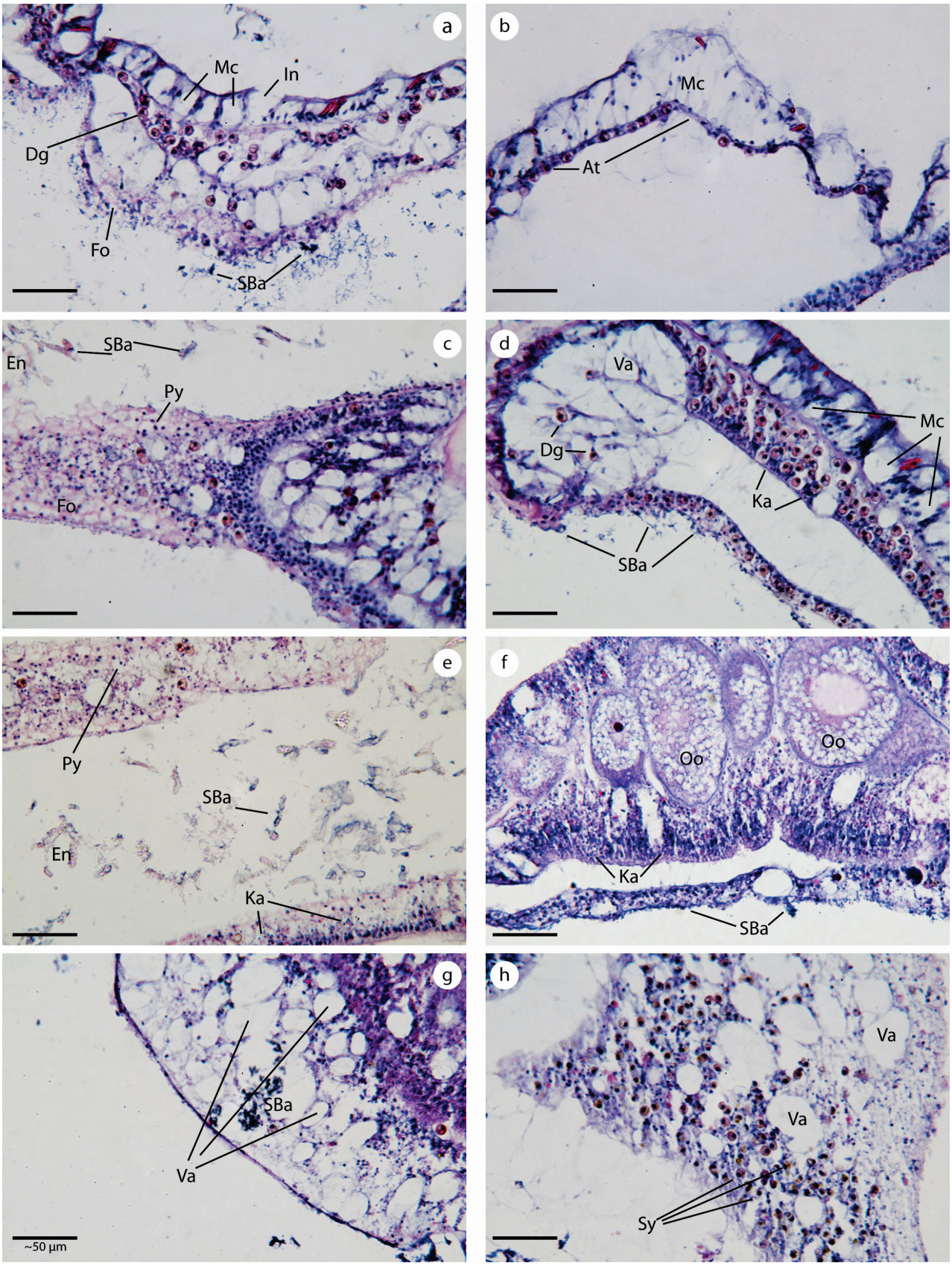
a
Mc
In
Dg
Fo
SBa
b
Mc
At
c
SBa
En
Py
Fo
d
Va
Mc
Dg
Ka
SBa
e
Py
SBa
En
Ka
f
Oo
Oo
Ka
SBa
g
SBa
Va
~50 µm
h
Va
Va
Sy

Figure 28. Photomicrographs at 40x of treated **P2** specimens held at 32°C, sacrificed on day 7. Photomicrograph (*a, b*) SBW detail, (*c*) oblique cut through calicodermis highlighting foamy texture, (*d*) SBW and BBW, (*e*) endolithic organisms with suspect bacteria, (*f*) details of gonads found only in P2 specimens, (*g*) highly vacuolated gastrodermis and prominently intact, thin calicodermis, (*h*) BBW with highly degenerated zooxanthellae and granular gland cells. Mc = mucocytes hypertrophy, At = attenuation, Va = vacuolated cells, hypertrophied, Ad = loss of adhesion, In = integrity loss, En = endolithic organisms, SBa = suspect bacteria, Dg = nuclear degeneration, Ka = karyorrhectic nuclei, Py = pyknotic nuclei, F = feathery mucus strands, Fo = foamy texture calicodermis, Oo = oocytes. All scale bars ~50 µm.

Individual criteria were scrutinized to find outliers that may be diagnostic of bacterial and temperature stresses for P2. The results yielded two criteria: symbiophagy ($p = 0.013$) and endolithic organisms' adherence to calicodermis ($p = 0.011$; Figure 29) for which the severity scores were statistically different. Because there is no overlap in the outlier criteria for both P1 and P2, it is believed that none of these are particularly important temperature-related criteria, although the possibility they are important is not being ruled out for future investigations.

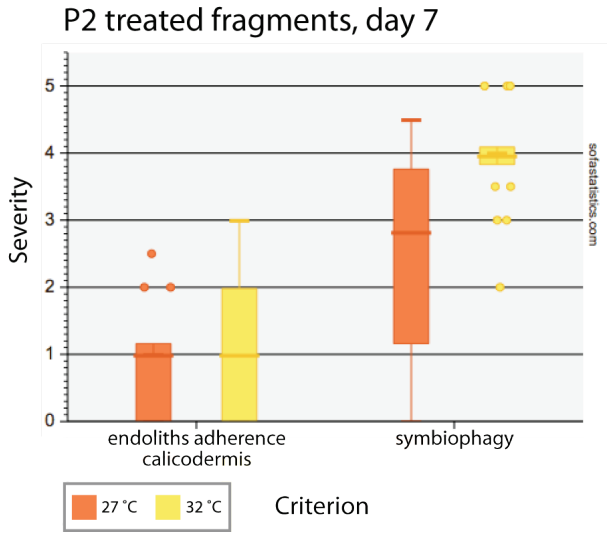

Figure 29. Criteria for which P2 specimens scored significantly different between 27 and 32°C: symbiophagy ($p = 0.013$), endolithic organism adherence to calicodermis ($p = 0.011$).

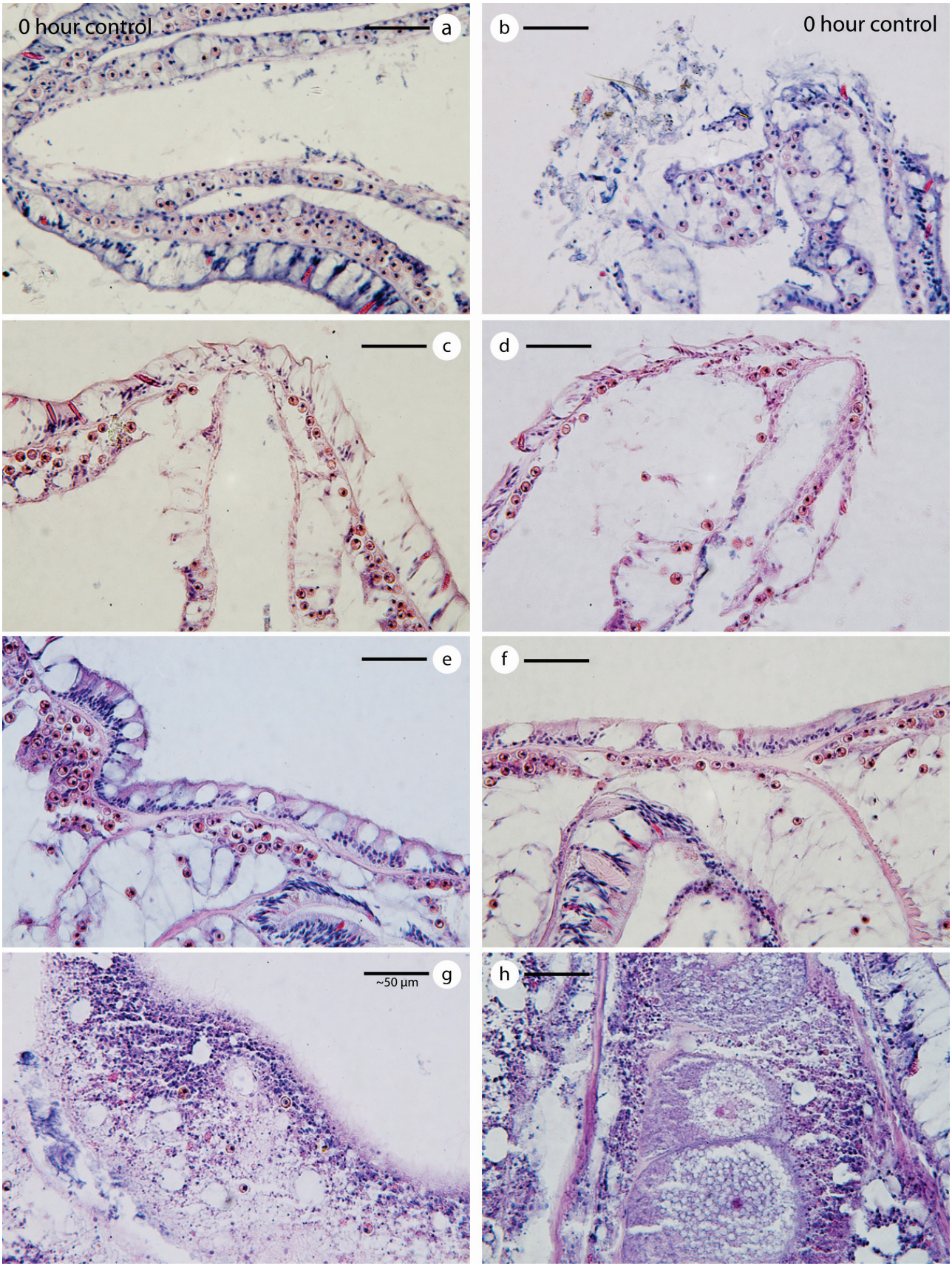
0 hour control
a
b
0 hour control
c
d
e
f
g
~50 µm
h

Figure 30. Photomicrographs at 40x of control **P2** specimen at 32°C, sacrificed on day 7. Photomicrographs (*a, b*) T_0 specimen, (*c*) shows large increase in hypertrophied mucocytes and/or vacuolated cells, (*d*) shows attenuation of the epithelia and a notable decrease in the density of zooxanthellae of the gastrodermis, (*e*) shows contiguous epidermis with increase in hypertrophied mucocytes, (*f*) shows reduction in zooxanthellae and hypertrophied vacuolated cells, (*g*) shows deep BBW with some symbiophagy noted and (*h*) details of mesenteries where oocytes are present and appear to be degenerating. All scale bars ~50 µm.

Differential responses of phenotypes to bacterial exposures at 32°C

Comparative statistical analysis of all severity scores between P1 and P2 at 32°C yielded results that again support the null hypothesis: no statistical differences were found between the phenotypes. The tallied mean of each individual specimen's severity scores, can be viewed in Table 11. As in the 27°C specimens, these scores indicate that the treated corals experienced an increase in the severity of pathological changes and those changes were likely due to the bacterial exposures. Condition scores can also be viewed in Table 11 and as in the 27°C specimens, show that these scores tended to be higher than the severity scores for all specimens. This final comparison of severity scores *between* the phenotypes shows unequivocally that there was no significant difference between their responses to the bacterial challenges. Treated and control P1 and P2 severity scores at both temperatures were statistically the same (Table 12) with p-values ranging from 0.094 to 0.731. Figure 31 provides a side-by-side comparison of the treated and control phenotypes by temperature and emphasizes the close similarities between all scores for all parameters (phenotypes, treated and control, temperatures). The two graphs in Figure 31 are almost exactly the same.

Table 11. Tallied mean scores for P1 and P2 specimens at 32°C, day 7.

SEVERITY	P1	P2	CONDITION	P1	P2
Treated specimens	**Mean Overall Score**		**Treated Specimens**	**Mean Overall Score**	
1	49%	53%	**1**	58%	67%
2	45%	57%	**2**	61%	70%
3	39%	45%	**3**	55%	63%
4	49%	46%	**4**	73%	68%
Tallied mean of all treated	**46%**	**50%**	**Tallied mean of all treated**	**62%**	**67%**
control	35%	32%	**control**	43%	49%

Table 12. Comparison of all criteria between phenotypes for specimens held in 32°C tanks, sacrificed day 7.

Treated **P1 and P2**, 32 ˚C, day 7

Pheno type	N	Median	Min	Max
P1	132	2.75	0.0	5.0
P2	132	3.0	0.0	5.0

p value: 0.094
Kruskal-Wallis H test statistic: 2.808
degrees of freedom: 1

Control P1 and P2, 32 ˚C, day 7

Pheno type	N	Median	Min	Max
P1	33	2.0	0.0	4.0
P2	33	1.5	0.0	4.0

p value: 0.731
Kruskal-Wallis H test statistic: 0.118
degrees of freedom: 1

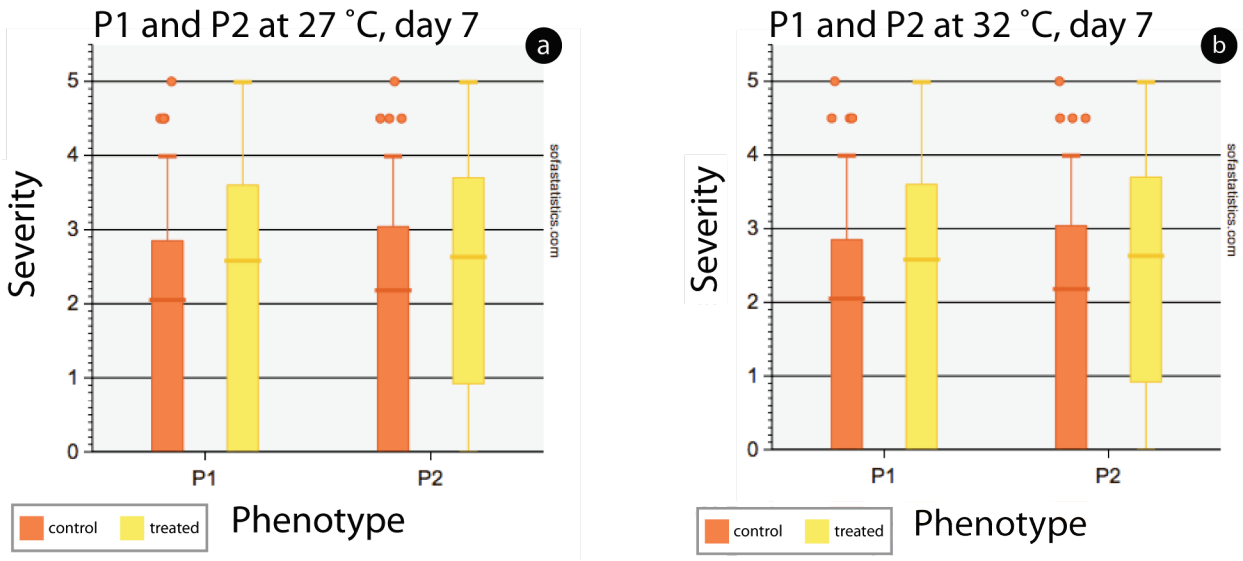

Figure 31. Comparison between control and treated phenotypes at 27°C (*a*) and 32°C (*b*).

Individual criteria were scrutinized to find outliers that may be diagnostic of bacterial and temperature stresses for either phenotype. This analysis yielded two criteria that stood out as significantly different for exposed specimens held at 27°C: adhesion loss in the gastrodermis and symbiophagy (Figure 32*a*). P2 specimens scored significantly higher in adhesion loss of the gastrodermis (P1 median = 0.0, P2 median = 3.5) and P1 specimens scored significantly higher in symbiophagy (P1 median = 3.5, P2 median = 1.0; Figure 32*a*). It is interesting to point out that symbiophagy was also more pronounced for thermally-stressed P2 specimens. At 32°C the treated specimens scored significantly different for four criteria (Figure 32*b*): adhesion loss of the calicodermis (P1 median = 1.0, P2 median = 3.0), nuclei of the calicodermis (P1 median = 4.0, P2 median = 2.0), karyorrhectic nuclei of the gastrodermis (p1 median = 3.0, P2 median = 4.5), and suspect bacteria in/on the calicodermis (P1 median = 1.5, P2 median = 4.0).

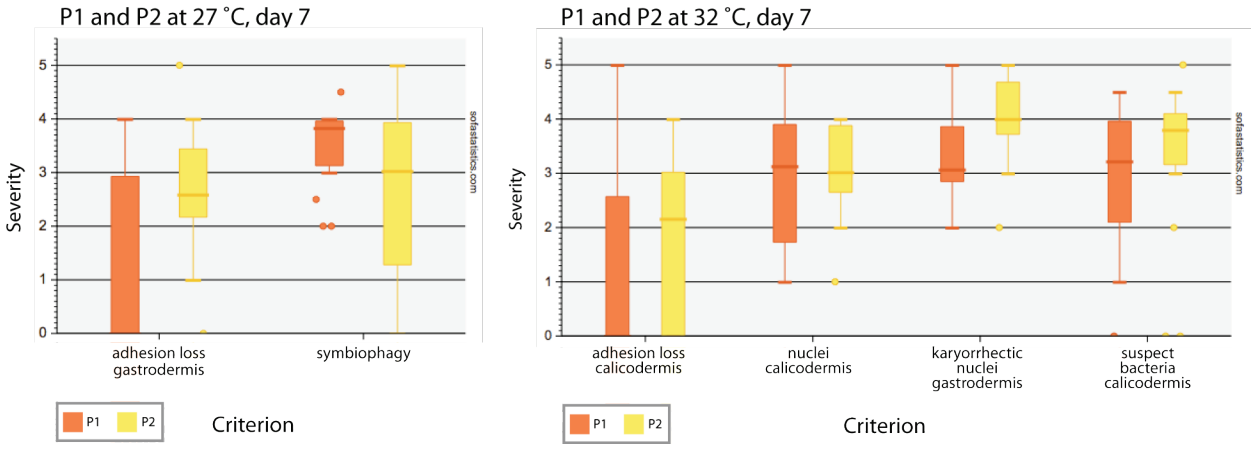

Figure 32. P1 and P2 scored significantly different for two criteria at 27°C (*a*): adhesion loss of the gastrodermis (p = 0.05), symbiophagy (p = 0.03), and four criteria at 32°C (*b*): adhesion loss calicodermis (p = 0.044), nuclei of the calicodermis (p = 0.034), karyorrhectic nuclei gastrodermis (p = 0.036), suspect bacteria calicodermis (p = 0.019).

To understand the potential importance of the statistically different criteria in 27°C specimens, it is important to understand how the pathology affects the coral. Adhesion loss of the gastrodermis indicates changes to the gastrodermal layer where the epithelium is no longer attached to the connective mesoglea. This pathological change often appeared in conjunction with a large number of hypertrophied vacuoles in the gastrodermis and a concomitant loss of zooxanthellae. Exocytosis of zooxanthellae was rarely observed and only found when the integrity of the gastrodermis was compromised, however, large numbers of the algae were often found at various stages of degeneration in the gastrodermis deep in the BBW that also exhibited signs of hydropic degeneration. Cnidoglandular bands with somewhat degenerated zooxanthellae were also often seen connected to the lower BBW providing what may be a mode of transport into the lysosome-laden deep gastrodermis (Figure 33*b, d*). Three of the four criteria outliers at 32°C involved the calicodermis, the health of which is vital, since this epithelium is responsible for accretion of the aragonite skeleton (Figure 34*a*). Building skeleton enables corals to grow larger, thus more able to capture available light and more nutrients from their symbionts, and become better able to compete for reef substrate.

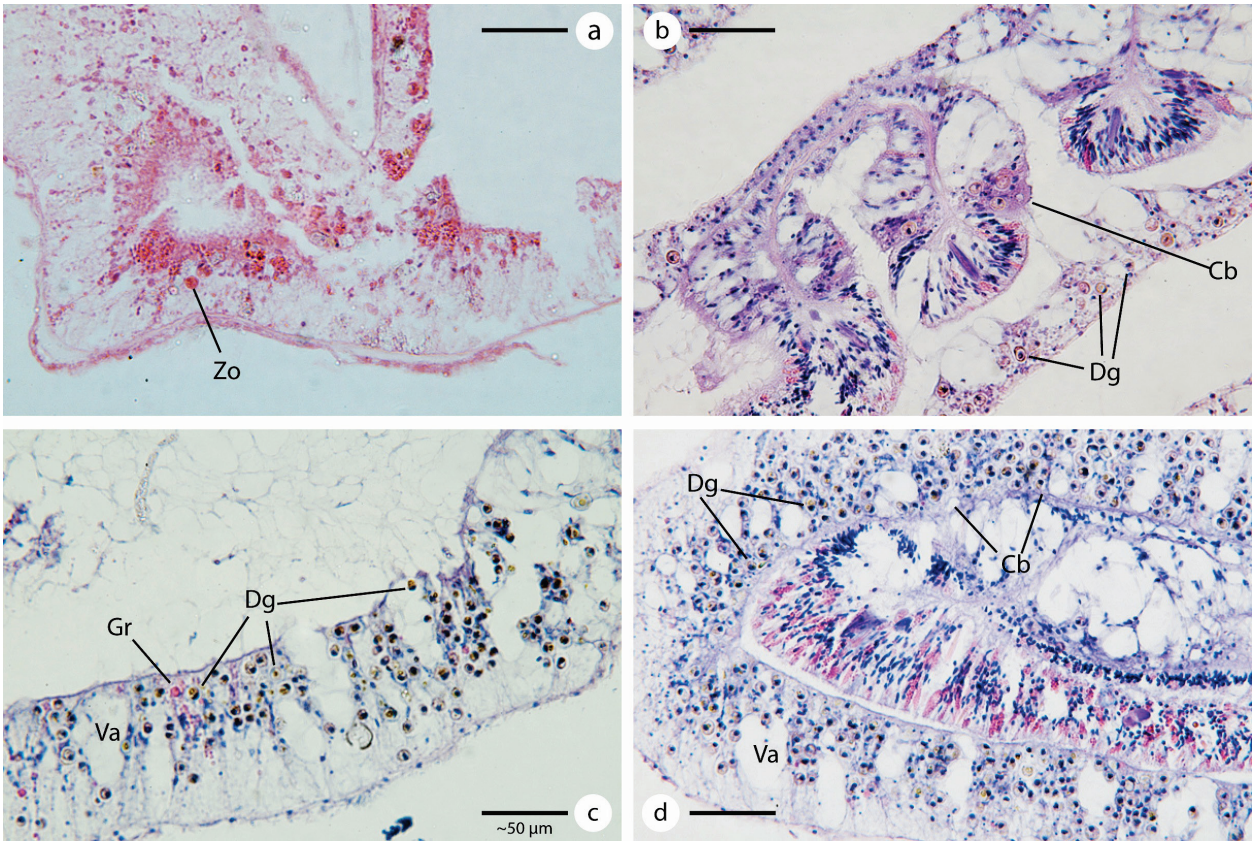

Figure 33. Photomicrographs at 40x of sequestration of zooxanthellae at various stages of degeneration to the deep region of the gastrodermis in the BBW. Photomicrograph (*a*) shows ECP 1981 healthy sample with conspicuous lack of degenerating zooxanthellae, (*b*) shows cnidoglandular band containing zooxanthellae in contact with the gastrodermis of BBW, (*c*) shows numerous degenerating algae in gastrodermis and hydropic degeneration of vacuoles in the gastrodermis, (*d*) shows cnidoglandular band contact with gastrodermis replete with degenerating zooxanthellae. Zo = zooxanthellae, Dg = degenerated zooxanthellae, Cb = cnidoglandular band, Gr = large, raspberry-like granular gland cells, Va = hypertrophied vacuoles. All scale bars ~50 µm.

In addition, suspect bacteria were commonly observed on and around the calicodermis of both phenotypes at 32°C (Figure 34*c, d*). Great clusters of them were present when the calicodermis exhibits a foamy texture, when it was attenuated or stretched, and also when it appeared normal, so it was difficult to determine whether their role is positive or negative for the coral holobiont. Nuclear fading (karyolysis) in the calicodermis is a sign of dissolving chromatin as a result of the release by the cell of hydrolytic enzymes (Figure 34*b*), and is a process that signals necrosis of the cell (Figure 4). The nuclei appear faded because the process leads to the loss of the groups that bind hematoxylin. Karyorrhexis generally precedes karyolysis and was a

prominent feature in many of the specimens from all groups, but was significantly more prevalent in the gastrodermis of P2 treated specimens at 32°C.

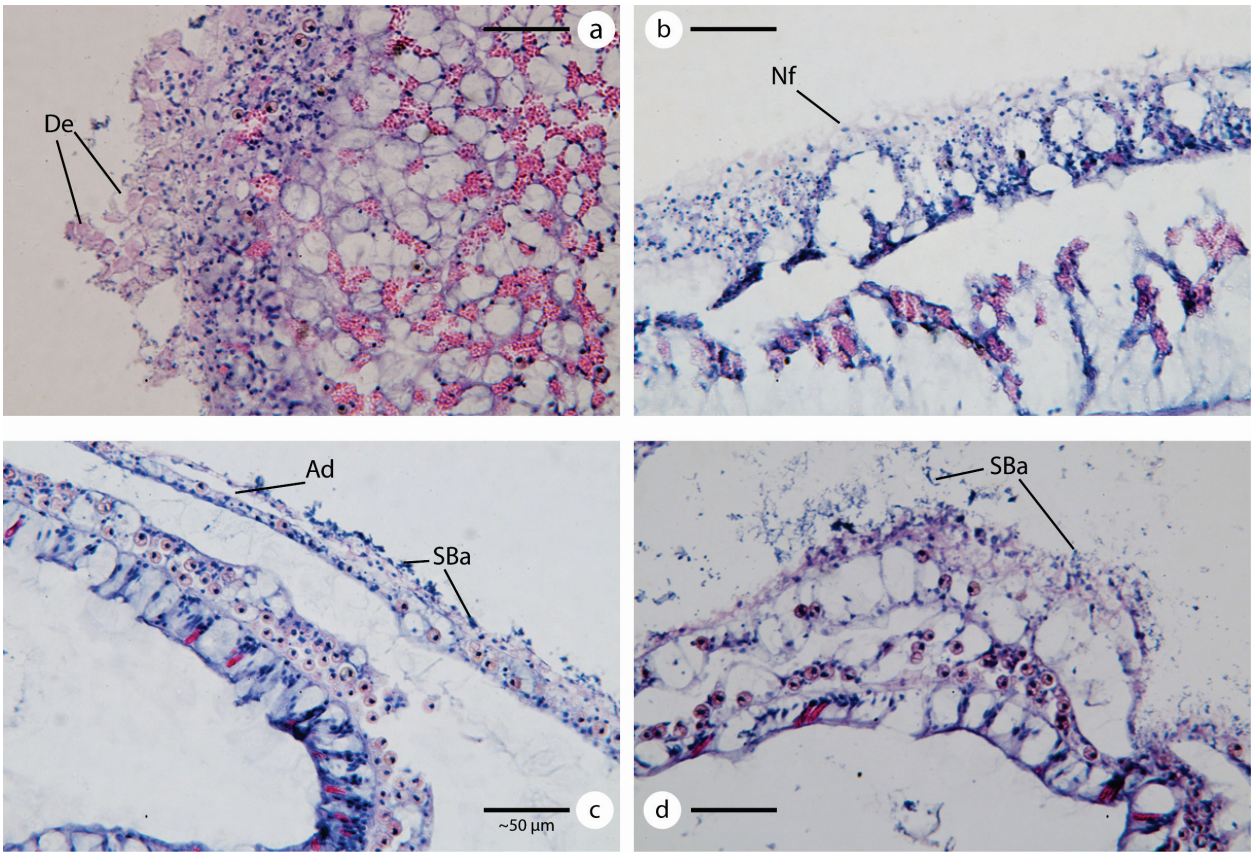

Figure 34. Photomicrographs at 40x of details of the calicodermis for P1 (*a, b*) and P2 (*c, d*) specimens at 32°C. Photomicrograph (*a*) shows T_0 specimen with numerous desmocytes that appear in good condition, (*b*) shows nuclear fading and foamy texture of calicodermis, also large amounts of karyorrhectic nuclei in the gastrodermis, (*c*) shows T_0 specimen with prominent suspect bacteria and area with adhesion loss, (*d*) shows apparent proliferation of suspect bacteria and foamy texture. Ad = adhesion loss, SBa = suspect bacteria, Nf = nuclear fading, De = desmocytes. All scale bars ~50 µm.

Effects of holding time on both phenotypes

Little is known regarding the timeline for development of CYBD lesions, and as none of the specimens had clearly developed one during the exposure period, time in tanks was extended to determine whether specimens would develop lesions, begin repair processes, or neither. At the

conclusion of the extended period (34 d) all tanks had considerable algae floating, growing on the bottom of the tanks and along all sides of the coral skeleton to the margin of live tissue (Figure 35). In no tanks, save one—the 32°C control tank, which also lacked algal growth—was new coral tissue observed growing over the sides of the specimen, a grossly visible indication of repair (Downs et al. 2009). One specimen from a 32°C tank exhibited a pale lesion that was grossly similar to CYBD lesions (Figure 35*b*).

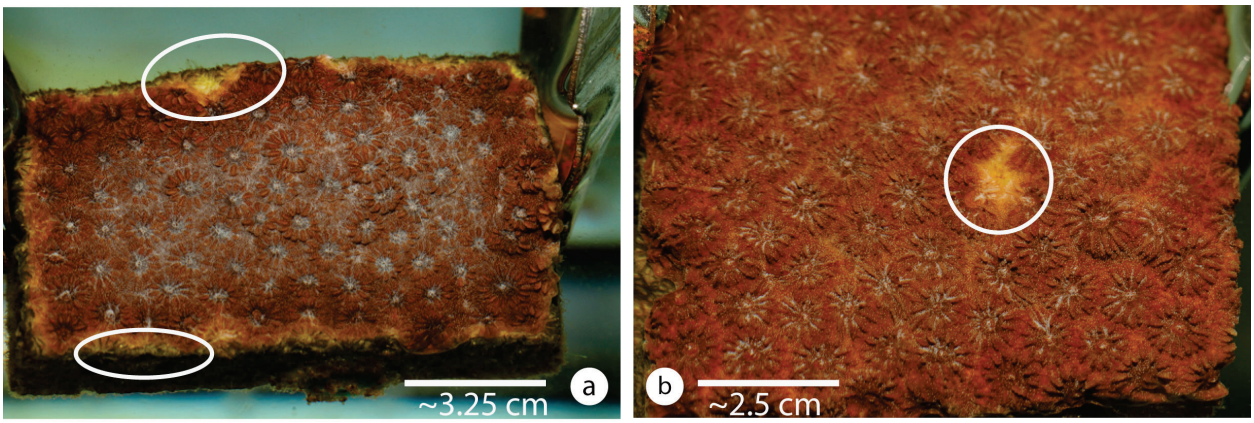

Figure 35. P1 day 34 specimens, (*a*) 27°C specimen exhibiting algal growth along sides of skeletons and directly adjacent to live coral tissue, and (*b*) 32°C specimen with a pale lesion, potentially CYBD-like.

P1 challenged specimens held at 27°C showed significant pathological change over the 34-day time period ($p = 0.004$; Table 13), though the greatest increase in severity scores was between T_0 and day 7 (T_7). Change to the control instead was nearly but not significant ($p = 0.055$). Treated specimens at 32°C also showed significant pathological change ($p = 0.017$) over the 34-day time period, but not for the control specimen ($p = 0.882$). Trends for the treated specimens generally followed a pattern of an increase in pathology from T_0 to d 7 with improvement from d 7 to d 34. Control trends followed a roughly opposite pattern with improvement in pathology from T_0 to T_7 and worsening from T_7 to T_{34} (Figure 36).

Table 13. Effects of incubation time for **P1** specimens at 27°C and 32°C.

Treated **P1** fragments, 27 ˚C

Time (days)	N	Median	Min	Max
0	33	2.0	0.0	4.0
7	132	3.0	0.0	5.0
34	132	2.0	0.0	5.0

p value: 0.004
Kruskal-Wallis H test statistic: 11.205
degrees of freedom: 2

Treated **P1** fragments, 32 ˚C

Time (days)	N	Median	Min	Max
0	33	2.0	0.0	4.0
7	132	2.75	0.0	5.0
34	132	3.0	0.0	4.5

p value: 0.017
Kruskal-Wallis H test statistic: 8.196
degrees of freedom: 2

Control **P1** fragments, 27 ˚C

Time (days)	N	Median	Min	Max
0	33	2.0	0.0	4.0
7	33	1.0	0.0	5.0
34	33	2.5	0.0	4.5

p value: 0.055
Kruskal-Wallis H test statistic: 5.816
degrees of freedom: 2

Control **P1** fragments, 32 ˚C

Time (days)	N	Median	Min	Max
0	33	2.0	0.0	4.0
7	33	2.0	0.0	4.0
34	33	2.0	0.0	4.0

p value: 0.882
Kruskal-Wallis H test statistic: 0.252
degrees of freedom: 2

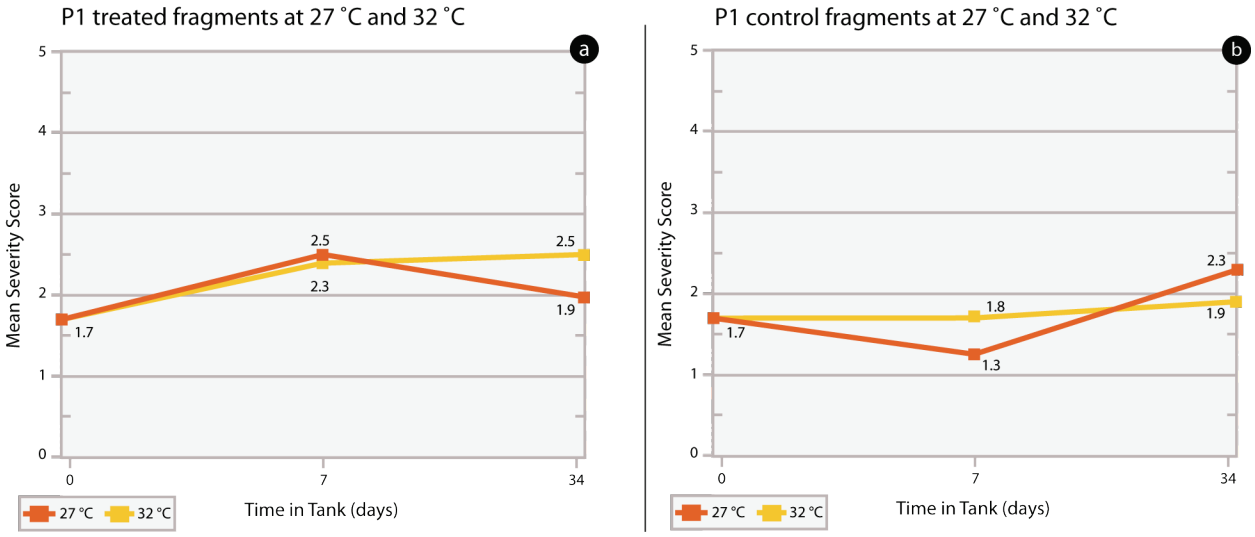

Figure 36. Severity scores trends for **P1** treated (*a*) and control (*b*) specimens at 27°C and 32°C over course of experiment.

Neither P2 challenged specimens held at 27°C or 32°C showed significant pathological change over the course of the 34 d period ($p = 0.203$; Table 14), although the overall trend was a slight increase in pathology for both groups from T_0 to T_{34} (Figure 38). Similarly, the P2 control specimen held at 27°C showed no change over time ($p = 0.493$), whereas the P2 control at 32°C showed significant pathological changes over the 34 d period ($p = 0.049$; Table 14). In contrast to the treated specimens, the trend for the controls was that of a decrease in severity from T_0 to T_7 and a subsequent increase in pathology to T_{34}. The severity score for the 27°C specimen was virtually the same at T_0 (1.9) and at T_{34} (2.0), whereas the 32°C specimen had a severity score of 2.0 at T_0 and 2.5 at T_{34}. This increase in severity score represents the only significant change over time of the P2 specimens and may be the only instance where temperature appears to be an important factor in the pathological changes observed. Some specimens were grossly changed, however, at T_{34}. Multifocal bleaching of polyp regions was observed in 27°C specimens as well as 32°C, but these pathologies did not resemble CYBD lesions (Figure 37) and were likely due to "tank effects" other than those pertaining to water quality.

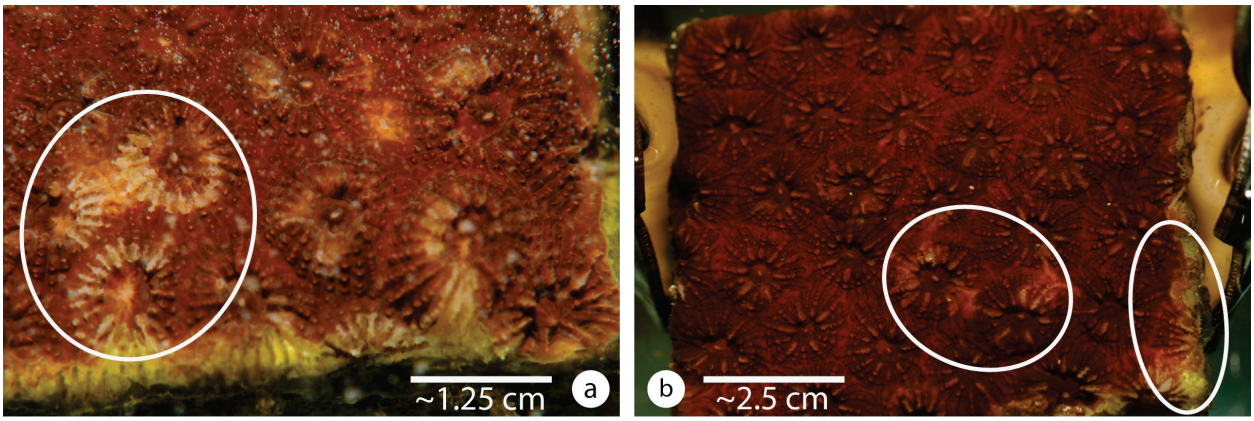

Figure 37. **P2** challenged specimens held at 27°C (*a*) and 32°C (*b*) on d 34. Note presence of bleached polyps, algal growth to tissue margins on both specimens.

Table 14. Effects of incubation time for **P2** specimens at 27°C and 32°C.

Treated **P2** fragments, 27 ˚C

Time (days)	N	Median	Min	Max
0	33	2.0	0.0	4.0
7	132	3.0	0.0	5.0
34	132	3.0	0.0	5.0

p value: 0.203
Kruskal-Wallis H test statistic: 3.187
degrees of freedom: 2

Treated **P2** fragments, 32 ˚C

Time (days)	N	Median	Min	Max
0	33	2.0	0.0	4.0
7	132	3.0	0.0	5.0
34	132	2.25	0.0	5.0

p value: 0.216
Kruskal-Wallis H test statistic: 3.064
degrees of freedom: 2

Control **P2** fragments, 27 ˚C

Time (days)	N	Median	Min	Max
0	33	2.0	0.0	4.0
7	33	1.0	0.0	5.0
34	33	2.5	0.0	4.0

p value: 0.493
Kruskal-Wallis H test statistic: 1.413
degrees of freedom: 2

Control **P2** fragments, 32 ˚C

Time (days)	N	Median	Min	Max
0	33	2.0	0.0	4.0
7	33	1.5	0.0	4.0
34	33	3.0	0.0	4.5

p value: 0.049
Kruskal-Wallis H test statistic: 6.026
degrees of freedom: 2

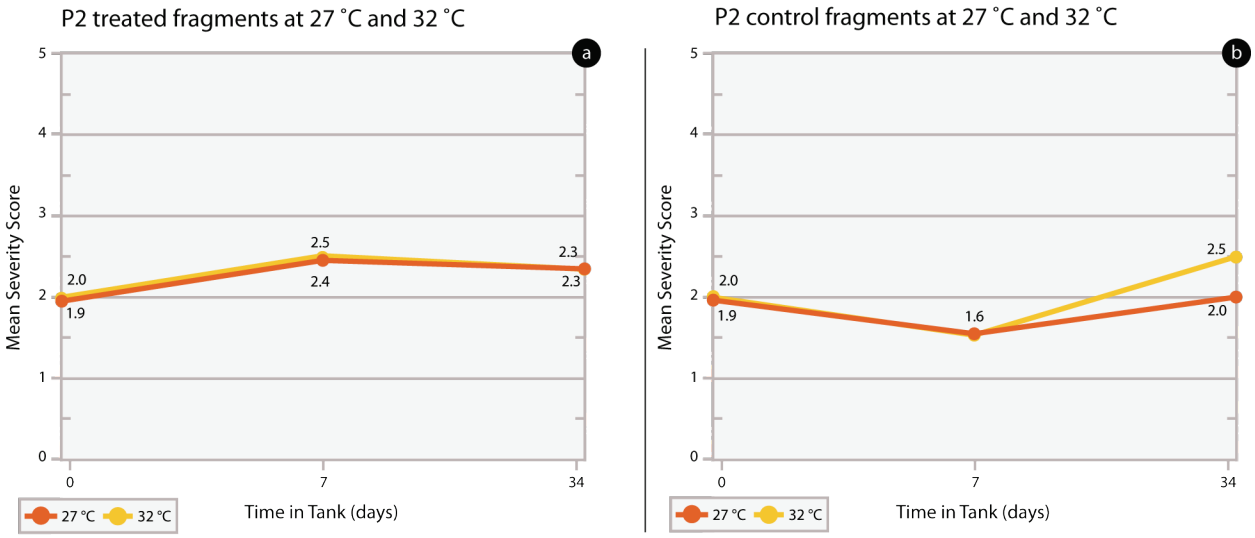

Figure 38. Severity score trends for **P2** treated (*a*) and control specimens (*b*) at 27°C and 32°C over course of experiment.

CYBD and presumed healthy samples

In order to understand whether the exposure experiments induced CYBD-like signs in the P1 and P2 specimens, it is necessary to understand what CYBD-infected coral tissue looks like. To address this knowledge gap, field-collected CYBD-infected and presumed healthy *M. faveolata* samples were evaluated (Figure 39). Lesions were apparent on the diseased samples, but not on the others. No grossly distinguishable differences were observed between the samples taken outside the lesion area and the presumed healthy samples (*or* the experimentally treated and control specimens).

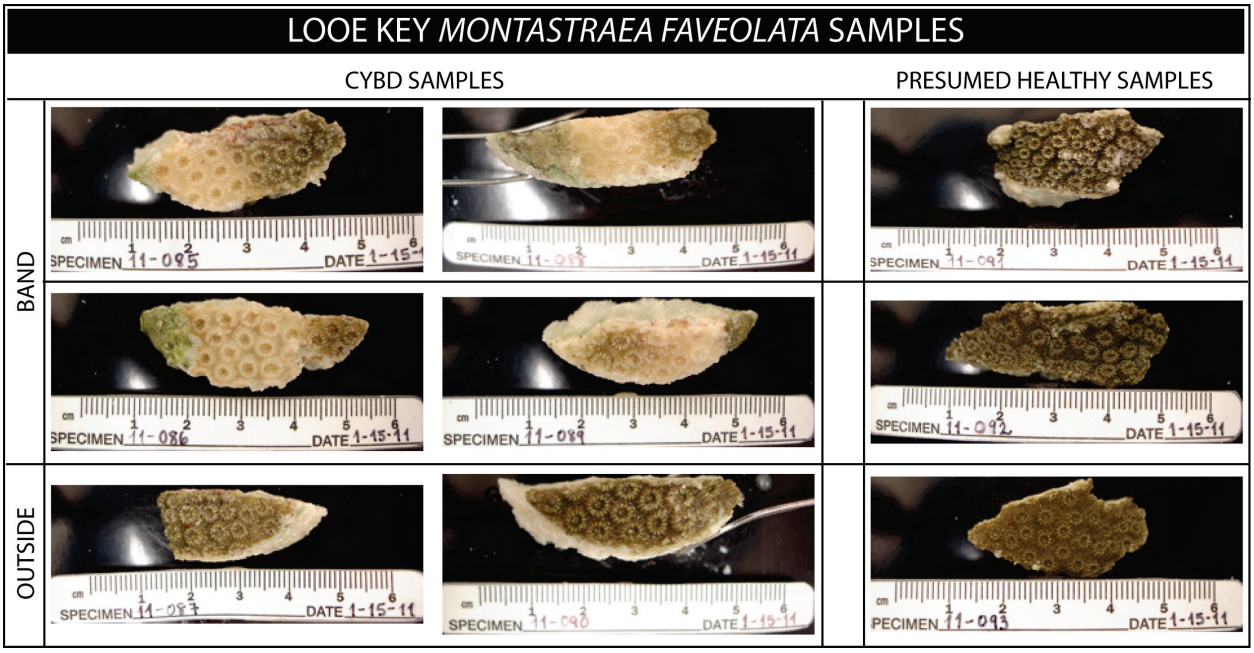

Figure 39. Photographs of fixed Looe Key samples. Photos taken as a part of histological preparation.

Grossly, each diseased specimen showed a fairly stark progression from pigmented tissue to paling tissue to complete loss of tissue (as evidenced by skeletal overgrowth by macroalgae; Figure 39 top left). The bands of paling tissue were approximately 2 cm wide. The paling tissue regions were believed present on the histoslides, but were not perceivable by light microscopy. Assessing the same criteria used to evaluate the experimentally treated and control specimens, the Looe Key-diseased samples (LKDS) scored perplexingly low in overall severity of pathological changes (Table 15). This could be partially explained by the fact that the tissue in

the pale band was not viewable for evaluation, but may also be a reflection of the differences between true diseased specimens from the field and acute exposure and experimentally-induced alterations. In fact, when viewing these samples microscopically, it is abundantly clear the pathology looks very dissimilar to that observed in the treated P1 and P2 specimens.

For most criteria, the severity scores ranged from no change (0) to mild (2) with few exceptions. Changes to the shape, size, and color of the zooxanthellae and the shape of their nuclei were somewhat prominent in severity, while very little yellowing of the zooxanthellae was observed. In the gastrodermis, moderate frequency of changes to the nuclei and a mild increase in karyorrhectic nuclei were observed. Suspect bacteria were observed at few foci on and around the endolithic communities but none were found associated with the calicodermis (Figure 40*a, b, d*). Overall integrity of the epithelia and mesenteries was very good and symbiophagy was not appreciably noted (Figure 40*g*).

Attenuation of the epithelia was found very rarely during the first evaluation. However, upon reexamination it was noted that the most prominent of changes to the epithelia of the diseased samples was a severe and diffuse *reduction* in mucocytes, and attenuation of the epidermis (Figure 40*a, b*) that could have been an example of metaplasia, as evidenced by the presence of dense and basophilic cuboidal cells where pseudostratified columnar epithelium should have been. As a result of this change, pigment cells often extended to the oral surface just below the terminal web. The samples taken distant from the pale band scored consistently higher in severity with few exceptions: a moderate presence of suspect bacteria associated with the calicodermis (none were observed in the LKDS; Figure 40*f, g*) and a notable presence of suspect bacteria associated with the endolithic communities (mild in LKDS: Figure 40*f, g*). Attenuation of the epidermis was again a prominent feature of the evaluated epithelia with multifocal reduction of mucocytes, while at other foci mucocytes were hypertrophied (Figure 40*e, f, g, h*).

Table 15. Tallied mean of scores for all of the Looe Key samples.

SEVERITY	Mean of all scores	CONDITION	Mean of all scores
Looe Key CYBD Band		**Looe Key CYBD Band**	
LKDS 11-085	13%	LKDS 1	18%
LKDS 11-086	16%	LKDS 1	32%
LKDS 11-088	22%	LKDS 2	41%
LKDS 11-089	25%	LKDS 2	37%
Tallied mean of CYBD samples	**19%**	**Tallied mean of CYBD samples**	**32%**
Looe Key Outside Band		**Looe Key Outside Band**	
11-087	26%	CYBD 1	46%
11-090	29%	CYBD 2	46%
Tallied mean outside band	**27.5%**	**Tallied mean outside band**	**46%**
Looe Key Presumed Healthy		**Looe Key Presumed Healthy**	
LKHS 11-091	22%	LKHS 1	31%
LKHS 11-092	28%	LKHS 2	44%
LKHS 11-093	28%	LKHS 3	42%
Tallied mean all LKHS	**26%**	**Tallied mean all LKHS**	**39%**

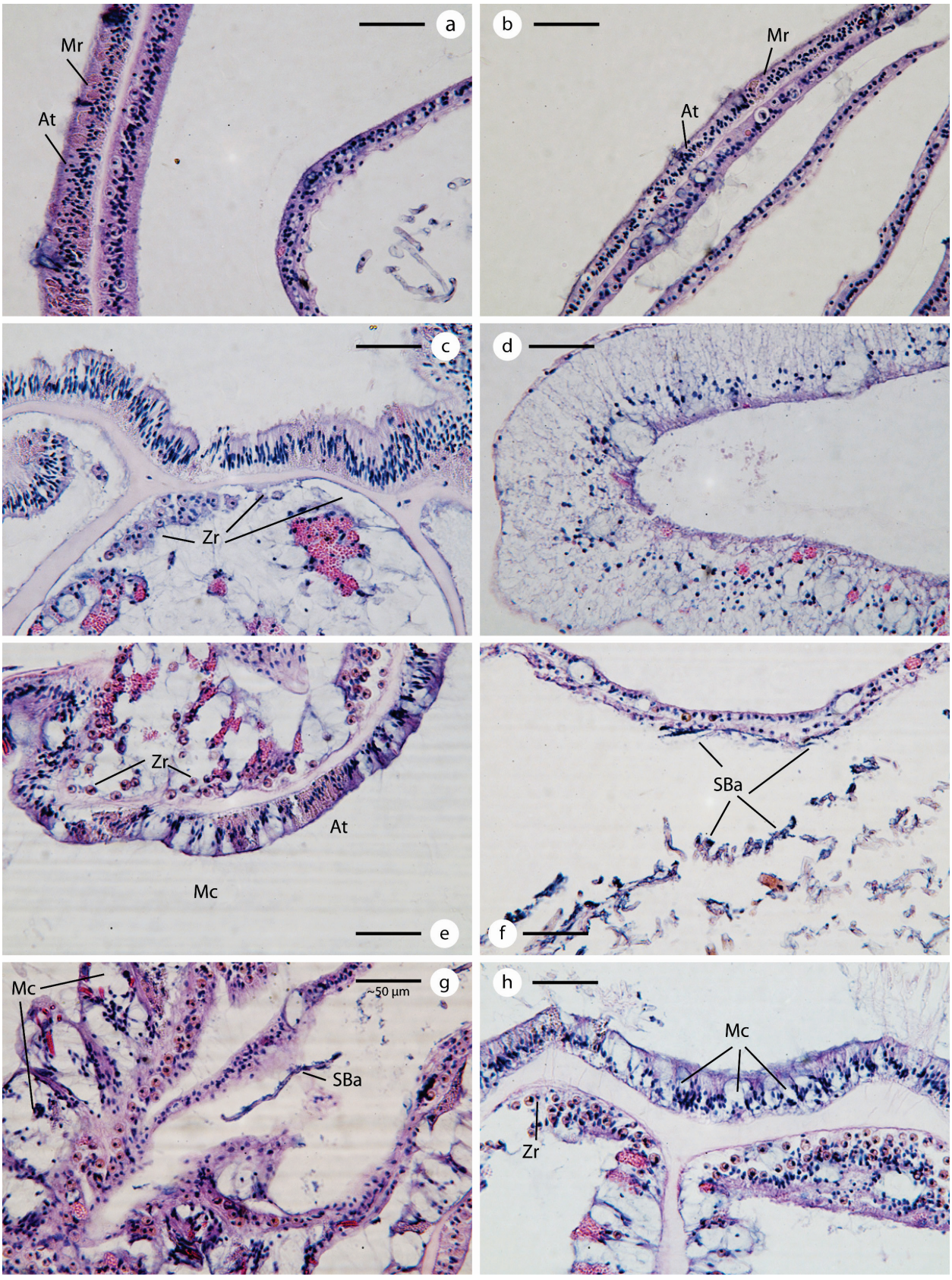
a
Mr
At
b
Mr
At
c
Zr
d
Zr
At
Mc
e
SBa
f
Mc
~50 µm
g
SBa
h
Mc
Zr

Figure 40. Photomicrographs at 40x of Looe Key diseased samples within the lesion (*a, b, c, d*) and outside the lesion (*e, f, g, h*). Photomicrographs (*a*) and (*b*) show contiguous epithelia and reduction in mucocytes and zooxanthellae, (*c*) reduction in zooxanthellae, large raspberry-like granular gland cells in close association with degenerated zooxanthellae, (*d*) basal body wall with no signs of symbiophagy, (*e*) mucocytes present, attenuation of epidermis and reduction in zooxanthellae, (*f*) suspect bacteria lining the calicodermis and endolithic organisms, (*g*) highly enlarged mucocytes or vacuolated cells, suspect bacteria associated with endolithic organisms, (*h*) reduction in zooxanthellae. At attenuation, Mr = reduction in mucocytes, SBa = suspect bacteria, Mc = mucocytes hypertrophied, Zr = reduction in zooxanthellae. All scale bars ~50 μm.

The samples collected from apparently healthy colonies in the vicinity of the diseased colonies, the Looe Key presumed healthy samples (LKHS), looked and scored very similarly in severity and condition to the samples collected from diseased colonies, but distant from the pale lesion (Table 14). These similarities were not just in overall score, but also very specific to the criteria evaluated. This is an important observation because not much is known about the tissue surrounding CYBD lesions and colonies without overt signs of disease are generally considered to be healthy. Again, these samples scored from no change (0) to mild (2) in most criteria for severity with the exception of criteria that involved the zooxanthellae, suspect bacteria and nuclei of the gastrodermis. Pathological changes to the zooxanthellae of the LKHS were diffuse overall. Association of suspect bacteria with the calicodermis was diffuse and occurred in great quantities of clusters. This is in contrast to the calicodermis of the LKDS, with no suspect bacteria observed, suggesting the possibility of a positive role in the holobiont for these suspect bacteria. Alternatively, it may be an early manifestation of the disease.

The LKHS were characterized by a greatly attenuated epidermis throughout the sections; dense, basophilic and cuboidal-appearing cells, and diffuse and greatly reduced numbers of mucocytes were noted throughout the tissue sections (Figure 41 *all*). The epidermis was contiguous throughout most of the section. Pigment cells were prominent and appeared to extend to the oral surface, emphasizing the reduction in height of the supporting cells (Figure 41*a, c*). As a result of the attenuation of the epidermis, a great reduction in the quantities of spirocysts was observed (Figure 41*c*). Another interesting observation is the diffuse occurrence and close association of the large, raspberry-like granular gland cells with degenerating zooxanthellae in the gastrodermis of the SBW (Figure 41*c, d, e, f*).

Many of the pathological changes that characterized the LKHS had not been observed in my experimental specimens, thus many of the exposed specimen criteria were not appropriate for the evaluation of the Looe Key samples, and statistical analyses based on these criteria do not accurately reflect the overall state of the Looe Key samples. The tallied means of the scores for severity and condition of the LKDS are quite low in comparison to the treated samples at 27°C (Table 7; Table 10). For this reason, the Looe Key samples were evaluated separately from the experimental specimens and respective scores were not compared. The importance of these comparison samples, however, cannot be overstated, as they served as clear and unequivocal evidence that some of the processes taking place in CYBD-infected corals were different from those taking place in the exposed P1 and P2 specimens.

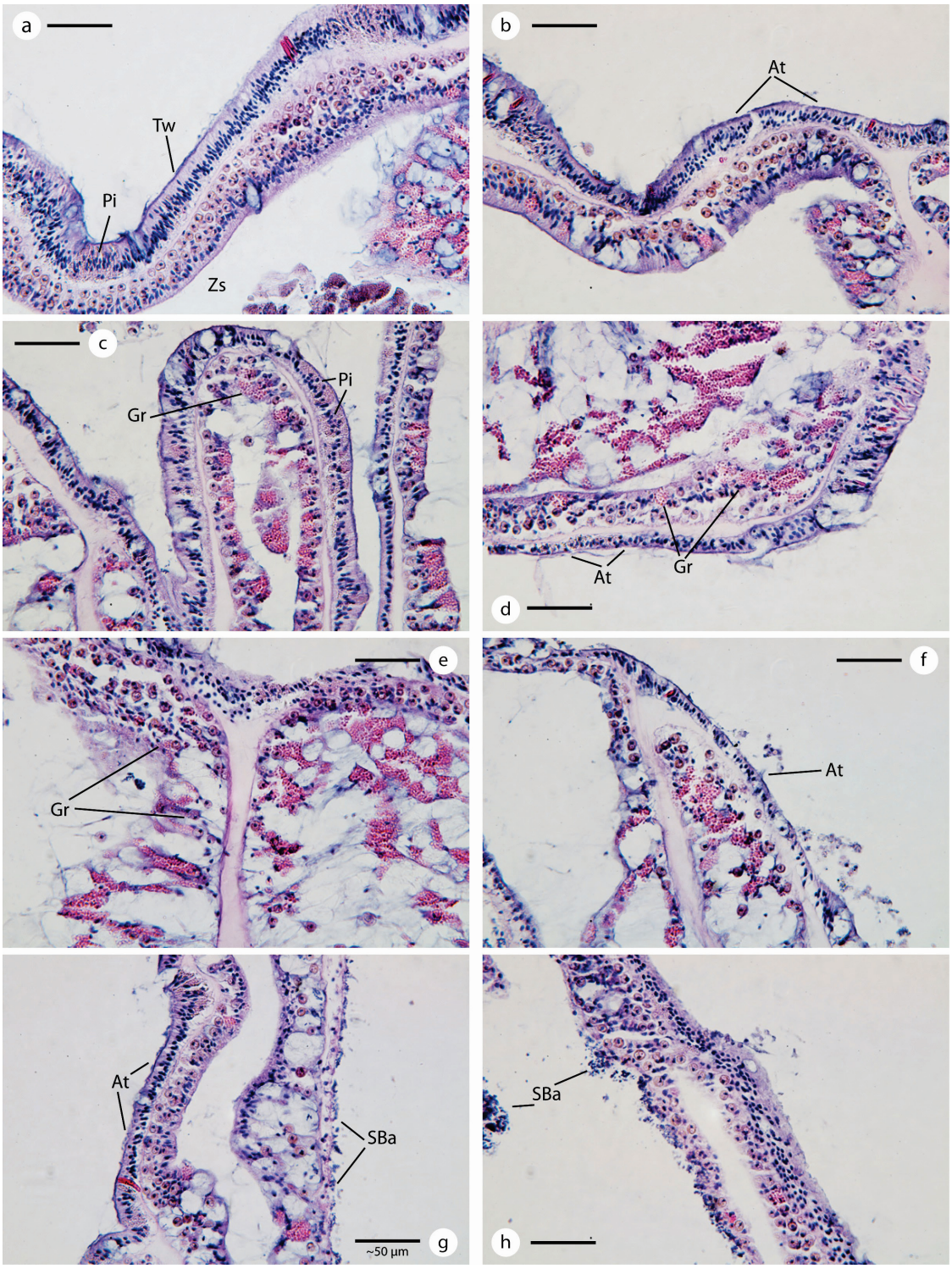

Figure 41. Photomicrographs at 40x of LKHS. All show details of the SBW, (*g* and *h*) also show details of the BBW. *(a)* shows contiguous, attenuated epithelia and lack of mucocytes, *(b)* attenuation of epidermis, (*c, d, e* and *f*) pigment cells extending to oral surface, granular gland cells associated with degenerated zooxanthellae, (*g* and *h*) suspect bacteria along calicodermis. At = attenuation, Pi = pigment cells, SBa = suspect bacteria, Gr = raspberry-like large granular gland cells, Zs = shape changes in zooxanthellae. All scale bars ~50 µm.

Discussion

Use of healthy-appearing *M. faveolata* phenotypes to study coral disease

It is a perplexing observation on a Caribbean reef to see a clearly infected *Montastraea* colony and its apparently healthy neighbor, especially given the immobile nature of corals. It is also unclear why *Montastraea* spp. corals are affected by CYBD pathogens while other genera rarely appear affected. *Montastraea* dominance as a reef-builder in the region may explain its vulnerability, but does not address variability between colonies or the reasons one becomes infected with pathogenic microorganisms while another does not. The *M. faveolata* colonies used for the present experiment, like many colonies in the field, appeared healthy when harvested but were apparently undergoing stress even at T_0. The specimens that actually appeared stressed were swapped for others that did not, thus all specimens at the beginning of the experiment looked grossly similar to many healthy colonies in the field. As the bacterial exposures continued over the one-week period, grossly visible changes were not apparent but histological analyses of the specimens showed great pathological changes in all those exposed. Over the same time period, controls appeared to slightly improve, but no gross morphological manifestations of this were noted. The experimental exposures were acute, lasted between 4 and 12 hours and occurred three times over the course of 7 days. The experimental specimens did not respond to the exposures with visible lesions even after 34 days, which suggests the development of a visible sign of disease is a more gradual process. Thus, healthy-appearing *M. faveolata* colonies on the reef may be undergoing stress from more chronic exposure to bacteria or other stressors. Since this investigation was meant to explore the reasons why certain colonies appeared healthy while others clearly showed signs of disease, it now seems a more prescient and appropriate inquiry involves the level of stress an apparently healthy coral is experiencing at a given time. Neighboring colonies are exposed to similar irradiance, temperature and pathogens or pollutants. Thus, besides intrinsic physiological factors that could not be determined by light microscopy, one possibility that may explain the seemingly random distribution of CYBD lesions among colonies is physical disturbance. Physical contact with fish or other reef organisms, predation, or

human interaction, i.e., fishing equipment and divers, can remove surface mucus and/or damage coral epithelia (Hall 2001) leaving already stressed corals more vulnerable to opportunistic pathogens that are already present in the coral holobiont and/or others that arrive to take advantage of a weakened host. It is also possible that energy devoted by the coral host to managing bacterial populations through xenophagic processes (Downs et al. 2009) combined with a decrease in density of zooxanthellae leads to the inevitable tissue loss that, in CYBD, progresses slowly from a focal pale blotch to a widening yellow band (Santavy et al. 1999; Cervino et al. 2008). Many possibilities exist to explain why certain colonies exhibit signs of disease, but the visible sign of disease is not the only important factor and healthy-appearing colonies in close vicinity to diseased colonies, should perhaps be termed "possibly-diseased" rather than healthy.

The apparently healthy T_0 specimens were managing moderately high levels of stress (mean severity scores ranged from 34% to 40%) compared to the expected condition (nearly or perfectly healthy). Since this was the baseline for all specimens, it is assumed all were equally impaired according to phenotype and temperature, and this impairment likely had a negative effect on the specimens during the experiment. In light of this discovery, investigations employing similar methods should consider the stress levels that recently transplanted and fragmented specimens might be undergoing.

Temperature as a coral stress factor

Statistical analyses of the effects of elevated temperature on the experiment specimens were not able to provide a clear temperature connection with pathological changes in the corals. Temperature is a known factor in coral stress (Glynn 1991; Gates et al. 1992; Baker et al. 2008) and may have had a marginal effect on the experimental specimens, but the expected compounded effect of elevated temperature on challenged corals did not occur. In the field, heat stress weakens corals leaving them vulnerable to disease, and promotes growth and antibiotic resistance in many pathogenic microbes that thrive at elevated temperatures (Baker et al. 2008). *Vibrio harveyi* grows optimally between 30°C and 35°C, which would theoretically give the bacteria an advantage over the coral in the 32°C tanks, if the strains are virulent to the coral or their zooxanthellae. Virulence factors for *V. harveyi* and *V. parahaemolyticus* are still not well understood, but it has been documented that many strains are highly pathogenic whereas others

are not (Owens and Busico-Salcedo 2006). The strains that were used for the experiment were isolated from diseased shrimp *Litopenaeus* sp. (CAIM 1792, CAIM 29) and the oyster *Crassostrea gigas* (CAIM 1075) but their ability to infect coral was unknown. The results of the challenges clearly show these strains were able to negatively affect coral, but the concentrations of bacteria in the inocula were higher than natural exposures thus no conclusions regarding their ability to infect corals in their natural environment can be made at this time.

Important pathological changes

Criteria that scored consistently highest (≥ 3.0) for most specimens (including controls) involved zooxanthellae, increase in and hypertrophy of mucocytes, karyorrhectic nuclei in the gastrodermis and faded nuclei of gastrodermal cells. The importance of zooxanthellae for the coral host has been widely documented and previously discussed in this thesis. Thus it is clear, the degenerative processes taking place in the zooxanthellae of the impaired specimens have important implications for the coral holobiont. Changes in the size, shape and color as well as the nuclei of the zooxanthellae were frequently observed. Density of the symbionts in some specimens also appeared diminished, (although this was not quantified), and symbiophagy was a common observation and could explain the reduction in viable zooxanthellae in the gastrodermis.

The digestion by the coral of its symbionts is a process that is mediated by the vacuolar membrane of the gastrodermis that normally surrounds the algae (Muscatine 1989; Downs et al. 2009). During stress, this membrane is able to transform from medium for nutrient exchange to a digestive organelle (Downs et al. 2009) and uses the same pathways involved in autophagy and xenophagy in coral host cells. Proteins from the Rab family—specifically Rab11 and Rab7, recognized autophagic markers—which under normal conditions are excluded from the algae-containing vacuole, were found by Downs et al. (2009) in phagolysosomes containing dead or degenerated zooxanthellae. This discovery and work done by Dunn et al. (2007) formed the basis for their theory that symbiophagy is a cellular mechanism for bleaching in corals. The loss of zooxanthellae via symbiophagy may result in bleaching (Dunn et al. 2007; Downs et al. 2009) but was not found to be the case in the P1 and P2 specimens, as very few free zooxanthellae were observed in the gastrovascular canals. Most specimens appeared to have sequestered degenerating zooxanthellae in the gastrodermis deep in the BBW (Figure 33). The accumulation of zooxanthellae appears to be a rather novel find and references to similar observations are

absent in the literature, thus this may be the first time symbiophagy resulting in digestion of zooxanthellae in *Montastraea* spp. corals has been reported. Identification of the Rab proteins associated with the degraded zooxanthellae was not a part of this investigation, but it is clear that some process had occurred that results in the amassing of dying zooxanthellae deep in the coral polyp. Downs et al. (2009) showed that *Vibrio* spp. were able to block activation of phagolysosomes and posited that the innate immune response of the coral may become non-specific directing xenophagic responses towards their symbionts. Regardless of whether this is symbiophagy mediated by auto(xeno)phagic mechanisms or the result of some other processes, it is impossible to tell whether the accumulation of lysed zooxanthellae is a response to the bacterial exposures, to elevated temperatures, or both since all of the control specimens also exhibited this pathological change. The sequestration could be a very good method for avoidance of oxidative stress in the gastrodermis of the SBW where healthy zooxanthellae photosynthesize and provide nutrients to its host. Sequestration rather than expulsion of the zooxanthellae suggests the coral host was making use of the degenerating symbiont cells as food during stressful times or starvation. Certainly, the presence of the unique, eosinophilic, granular gland cells containing hydrolytic enzymes in the deep gastrodermis in close association with the necrotic zooxanthellae is a sign that this may be happening. Thus, it cannot be completely ruled out that what is here being termed symbiophagy may actually be beneficial to the coral host though the reasons it occurs are likely otherwise. Symbiophagy was observed in the T_0 specimens indicating it may have already been taking place in the colonies while *in situ* in Key West or it was a response to the initial stress of transplantation and fragmentation. Additionally, no signs of symbiophagy were observed in the LKDS but they were seen in the LKHS, suggesting the symbionts had already been entirely consumed in the diseased samples or this is not an important process during CYBD infection.

The increase in production and secretion of mucus is an early response to environmental stress (Peters et al. 1981; Peters and Pilson 1985; Piggot et al. 2009). In *M. annularis* corals, Piggot et al. (2009) found that seasonal increases in sea surface temperature (SST) coincided with a decrease in zooxanthellae density and an increase in mucocyte density. They showed a pattern of increase in mucus production during summer months accompanied by an increase in mucociliary feeding that effectively supplemented the loss of nutrition from their symbionts. P1 and P2 colonies were collected on May 11, 2010, when local nighttime sea surface temperature

(SST) measured approximately 28°C (NOAA Operational 50 km nighttime SST charts for 2010, available online at http://www.ospo.noaa.gov/Products/ocean/sst/50km_night/2010.html). On May 3, the temperature was approximately 24°C, suggesting an increase of ~ 4°C over the course of the week just prior to their collection. This increase in SST may partially explain the observed proliferation of mucocytes in the experimental specimens and suggests a growing requirement for the experiment colonies to acquire more food from the water column. All P1 and P2 specimens at T_0 (and at subsequent sampling times) showed increases in and enlargement of mucocytes with corresponding severity scores between 3.0 and 5.0. The seawater conditions to which the P1 and P2 colonies were acclimated were light-limited (under docks) and turbid, also suggesting they may have been relying more heavily on heterotrophy of zooplankton and suspended particulate matter (SPM) than their counterparts on the reef. Removal of these colonies to conditions where PAR values were higher and zooplankton and SPM less available would likely have had a negative effect on them. Heterotrophy in healthy *M. faveolata* specimens is not believed to be as important as phototrophy (contributes up to 95% of nutrition; Stat et al. 2006), but in stressed specimens with fewer and impaired zooxanthellae, it may become very important to the coral's nutritional needs. Scleractinian corals are planktivorous carnivores that feed on living zooplankton, small fish, detritus, SPM, and dissolved organic matter, depending on polyp size (Goreau et al. 1971; Anthony and Fabricius 2000). Small amounts of SPM and algal growth in tanks and on specimens were observed but no particles larger than 20 μm were added and it is unclear whether the specimens were making use of those available for food. It seems plausible that SPM for *M. faveolata*—with polyps ~2.4 mm in diameter (Weil and Knowlton 1994)—would be a viable source of nutrients during periods when heterotrophy is increased (Anthony and Fabricius 2000). If SPM in the tanks was insufficient to serve the needs of the coral, reduction in necessary heterotrophic feeding may have also been a contributing factor in the decline of exposed and control specimens. In addition, accumulated SPM on the surface epithelia may have been a source of further stress. The heterotrophic needs of the coral specimens were not addressed during the experiments and conditions in tanks with regards to turbidity were not similar to the environment from which they were removed (Figure 6). Scleractinian corals are known to possess heterotrophic plasticity (Anthony and Fabricius 2000; Piggot et al. 2009) and a lack of available food would not theoretically represent a prolonged threat to the specimen's homeostasis, if normal densities of competent zooxanthellae were

present. The increase in SST may account for the initial increase in mucocytes observed in T_0 specimens, the changes in environment, and bacterial exposures likely caused subsequent increases and hypertrophy in these cells.

Karyorrhectic nuclei in the gastrodermis of the SBW and BBW were diffuse in most specimens, including controls. The high density of these condensed chromatin fragments is likely due to the combined host and symbiont nuclei breakdown. Apoptosis is characterized by nuclear fragmentation, among other things, and may also be occurring in the gastrodermis. This is consistent with the findings of Dunn et al. (2007) where they describe apoptosis and autophagy taking place in alternation in the zooxanthellate anemone *Aiptasia pallida* with bleaching as the final result of these processes. These observations merit further investigation and should be an important focus for future CYBD and other coral disease investigations.

Pathological changes observed in the calicodermis scored high with less regularity, but consisted of some very interesting findings. Clusters of bacteria-sized, sometimes distinguishably coccoid organisms that stained basophilic were commonly found associated with the calicodermis and endolithic organisms of the coral. These were termed suspect bacteria and were observed so often their presence was added as a criterion for specimen evaluation. Their role is unclear and identification of these organisms as bacteria is still pending; however, their presence in association with the epithelium in contact with the skeleton is another novel discovery. Previous to this research, bacteria associated with the calicodermis in this manner have not been reported to the best of this author's knowledge. Specialized cells of the calicodermis called calicoblasts secrete calcium and carbonate ions that are responsible for the accretion of the aragonite skeleton. In *M. faveolata*, most cells of the calicodermis are calicoblasts with the exception of desmocytes, which form finger-like attachments to the skeleton (Figure 34*a*). The processes involved in calcification are in direct competition with photosynthesis for the available stores of inorganic carbon (Jokiel 2011). During daylight hours reef corals exhibit simultaneous high output of photosynthesis and calcification (Jokiel 2011), which suggests a cycling of the available nutrients. Yet, diseased corals such as the challenged specimens exhibit great impairment to the zooxanthellae and the calicoblasts, suggesting a breakdown of the processes that govern photosynthesis as well as calcification. Stressed corals show hierarchal allocation of energy and resources with repair and growth taking precedence over other important processes

(Borger and Colley 2010). Although calcification may be considered a growth process, it is distinct from regeneration of tissue, i.e., at specimen margins, or cell repair and calicoblasts often appeared attenuated, and vacuolated and thus, impaired. Therefore, it is reasonable to infer from the damage observed to the calicodermis, that a number of factors affected the epithelium, resulting in the pathological changes observed including reallocation by the coral of important biological resources. The suspect bacteria may have had some influence on the observed pathologies, but they were also found in the T_0 specimens, the controls and in the non-diseased regions of the LKDS and in the LKHS. Their absence in the CYBD-infected specimens and presence in samples taken outside the lesion area possibly indicates a former presence in the infected areas and a subsequent reduction of these with progression of the disease and loss of tissue. The implications of this discovery are obscured by the fact that identification of these suspect bacteria has yet to be done.

Looe Key CYBD-infected samples differ from bacterial exposed specimens

The observed pathologies within the CYBD-infected Looe Key samples are quite different from those observed in P1 and P2 specimens and appear to be the result of slower processes taking place over a longer period than the 34-day experiment. The differences observed in pathologies can be attributed to the acute nature of the exposures and likely more chronic exposures on the reef. In the LKDS, the epithelia appeared highly condensed and attenuated, mucocytes and zooxanthellae were greatly reduced in density, and organization of cells and epithelia was overly compact. In contrast, the epithelia of the experiment specimens appeared blown out, rarely contiguous, attenuated to the point of breaking and in general, chaotic (P1 Figure 18; P2 Figure 23). Production of mucus is an important function of sessile corals (Ducklow and Mitchell 1979; Piggot et al. 2009) that use it as a primary defense against settlement of unwanted organisms, detritus and sediment. In addition, a reduction in zooxanthellae density results in the reduction of nutrients for the host and thus a greater need to feed. A coral without sufficient nutrition and the ability to produce mucus is functionally impaired, less able to trap food, and vulnerable to pathogenic organisms and other pollutants. From histological examination of the LKDS and LKHS, it seems that visible signs of CYBD may begin as a result of latent infection that is only triggered when some additional stress to the coral provides a weakened host to opportunistic microbes. The rate of tissue death for CYBD-

infected colonies is typically measured in centimeters per month or less (Cervino et al. 2004a, 2008; Weil et al. 2009), which is rather slow compared to other diseases of corals and correlates well with the observed pathologies in the LKDS. The pathological changes resulting from the bacterial exposures, instead, are rapid, extreme, and show the coral specimens were overwhelmed by the bacteria.

The LKHS do share some characteristics with the experiment specimens. Like many of the treated P1 and P2 specimens, these presumed-healthy samples earned high severity scores for criteria that involved changes to the size, shape, and color of the zooxanthellae; nuclei of the zooxanthellae; suspect bacteria in or on the calicodermis; and nuclei of the gastrodermis. In addition, the LKHS exhibited an increase in mucocytes—a characteristic shared with the P1 and P2 specimens—but not with the LKDS. It is thus conceivable that the LKHS are harboring potentially pathogenic microbes that, given the right set of suboptimal circumstances, could eventually lyse the zooxanthellae *in situ* (Cervino et al. 2004a; 2008), and cause lesions and tissue mortality.

New information on the *Montastraea* spp. specimens

The hypothesis that two corals from the same species may have different responses to the same stress was not supported by the results of this research. But what if one of the specimens is actually of a different species? The *Montastraea* spp. complex share many similar morphological characteristics. *Montastraea annularis* is lobate and tends to grow more prolifically in shallower depths (3–8 m) than *M. faveolata*. *M. franksi* apparently shares the same preferences for depth with *M. faveolata*, it grows in boulder form as do the other two species, but is very knobby, often with bleached polyps that appear sprinkled across the bumpy surface of the colony. The coral colonies that were collected for the experiment had originally been removed from a seawall and installed in dockside milk crates in Key West where they remained apparently disease-free for years. Not much else is known about these colonies. At the time they were collected and until very recently, they were believed to be without a doubt, the same species. There is now some doubt as to whether these two colonies are both *M. faveolata.* As mentioned in the methods and materials section, during one of the exposure periods, two specimens—one from each phenotype— were placed directly beside one another. After 4 hours, the mesenterial filaments of at least one of the phenotypes (P2) were extruded and attached to the surface of the P1 specimen

(Figure 9). During a recent conversation with Dr. Judith Lang regarding interspecies aggression, it was noted that P2 has the larger polyps and orange pigmentation common to *M. franksi* colonies (Weil and Knowlton 1994; Szmant et al. 1997). The P2 specimen may be *M. franksi* or it may be *M. faveolata* introgressed with *M. franksi*, which is known to happen at high latitudes (J. Lang pers. comm.; Fukami et al. 2004) in locations such as the Bahamas (and presumably the Florida Keys). This would explain the aggressive behavior and the gross and microscopic morphological differences between the phenotypes.

It may also explain the preference thraustochytrids showed for the P1 specimens. Not much is known about thraustochytrids as they relate to *Montastraea* spp. corals but they are known to associate with other faviid corals (Family Faviidae; Siboni et al. 2010) and the opaque white film on the surface of the tissue in P1 is consistent with reported thraustochytrid appearance in corals. Thraustochytrids produce polyunsaturated fatty acids (PUFAs) and are believed to be an important source of these to corals and other microbes in the coral mucus, especially during stressful events (Kramarsky-Winter et al. 2006; Harel et al.2008; Siboni et al. 2010). Massive corals (like *Montastraea* spp.), which provide plenty of surface area for these eukaryotic microbes to grow, fared better after bleaching events than branching-type corals that do not associate with them (Loya et al. 2001; Kramarsky-Winter et al. 2006). Thraustochytrids were found in the gastrodermis of the stressed massive corals, suggesting they were a source of food for the coral until the zooxanthellae population returned to normal density (Kramarsky-Winter et al. 2006). This is intriguing information and is certainly worth further investigation, but the P1 specimens with presumed dense thraustochytrid presence responded to the exposures similarly and were in similar health after the 34 d experiment as the P2 specimens. If it is true that P2 is in actuality a specimen of *M. franksi*, and thraustochytrids do not associate with *M. franksi* in the same dense numbers as with *M. faveolata*, it still remains that they did not have any differential (positive) effect on the P1 as compared to the P2 specimens. But P2 specimens did have a source of lipids that P1 apparently did not: gonads. Oocyte reabsorption represents a potential source of lipids for the coral (Szmant-Froelich et al. 1980) during periods of nutrient depletion. This is consistent with observations of degenerating oocytes (Figure 24*f*; Figure 29*h*) in the P2 specimens at both temperatures. Thus, it is possible that the lack of PUFAs from thraustochytrids was countered in P2 specimens by the presence and reabsorption of lipids from the oocytes. At this time nothing has been proven with regards to speciation of the two

phenotypes and the information outlined here remains simply an interesting possibility. The frozen specimens that are currently at WHOI may be able to provide the genetic information needed to positively ID these specimens.

Assessment

Every experiment performed has likely had certain aspects of its design (planned or unexpected) that could be improved. Lessons learned from experiments are often great and should assure better preparation and design for subsequent experiments. The following assessments of the current experiment seek to clarify some of the problems discovered before, during, and after the exposure experiment with the intention to guide others (and the author) towards more rewarding future experiments and results. Some aspects of the experimental design, which may seem questionable, are also addressed here.

One area for improvement is scoring and tallying: condition scores only addressed areas of tissue with pathological change and therefore could not be used to describe the overall condition of the specimens. Despite the qualitative nature of a score that describes the condition of a specimen, an improved method that does not tie this score to the severity score would be more useful for statistical analyses. Tallied means of scores allowed a quick overview of the magnitude of the pathological changes occurring in each specimen; however, tallies without assigned weight for the individual criteria give all criteria equal status, regardless of the importance of their effect on the coral. The tally can thus only be used as an indication of the health of the coral, while assuming each criterion has the same negative effect with the understanding that that may not be strictly true.

The results of the entire histological evaluation process are only as accurate as the criteria used. Careful attention was given to the selection of criteria for this research with a focus on those that corresponded to pathological changes that negatively affect the coral's vitality. It is possible, however, that important criteria that could skew the current results exist. The discovery during the evaluation of the LKDS that new criteria were needed to better assess the field-collected samples is a good example of the importance of this selection. Poorly selected criteria can result in incomprehensible scores that do not reflect the true status of the specimen. Additionally, lack of concrete guidelines for the determination of what is histologically normal

for specimens held in captivity further complicates interpretation of the results. The criteria used for the current investigation are believed to be sufficient in scope but were not exhaustive and some may not have had the negative effect assumed.

Bacterial cell densities used in each exposure (10^9 cells/mL) were clearly an exaggeration of exposures likely to occur in a coral colony's natural environment (Table 2). It is also understood that the acute nature of the dose may cause responses that are dissimilar from what would occur on a coral reef subjected to lower chronic exposures. However, since both coral phenotypes P1 and P2, were exposed to the same inocula in exactly the same manner, their responses were expected to be the same unless one individual possessed more robust defense mechanisms. Alternatively, differential responses might emerge if one phenotype began the experiments more impaired than the other. It is not uncommon to find published experiments that used similar concentrations of bacteria. For example, Banin et al. (2000), exposed specimens of *Oculina patagonica* to roughly 10^9 cells per mL of seawater. Certainly, the variability in bacterial concentrations that resulted from the methods used during this research (liquefying agar plates) could be avoided and the protocol improved. An ideal future investigation with similar goals would involve experiments of much longer duration challenging with a series of lower bacterial concentrations in order to discover what is really taking place in the natural environment.

Debris in the surface mucus of the epidermis indicates a breakdown of the capability of the ciliated supporting cells to rid the coral surface of sand or other particles that can reduce irradiance and would-be colonizers. The protocol used during the specimen sampling, in retrospect, may have had some effect on the coral mucus and thus the related criteria. Dripping mucus from the specimen may have caused large particles to stick to the oral surface of the epidermis whereas smaller constituents of the mucus layer likely dripped off with the mucus. This may explain why the specimens were often observed with large diatoms and other debris items attached to the epidermis. It may also have skewed the observations and as a result the severity scores if one phenotype was better equipped to produce mucus quickly, although this is believed unlikely. The ECP 1981 healthy sample tissue sections exhibit thick layers of mucus and no discernible large particles, while this same thick layer was not observed in any of the experimental specimens. The lack of a thick mucus layer may be a result of the challenge

experiments, but since the mucus was dripped off before fixation, conclusions regarding the importance of the mucus and mucus debris to the overall status of these specimens must be made with caution. For future experiments, a different method for collecting mucus should be employed, which allows the coral ample time to produce mucus after it has been sampled.

Furthermore, to avoid tank effects and pathological changes due to factors other than the exposures, a number of improvements could be made to the artificial environment. First, diel measurements of PAR values from the specimen's natural environment should be taken and mimicked in the artificial setting. This was not done for the present study, though efforts to reduce irradiance were made. Tanks were monitored for temperature, salinity, nitrate, nitrite, alkalinity and ammonium, but not for irradiance and algal growth in and under the tanks was obvious. Control specimens appeared to improve during the first week of the experiment, but worsened from d 7 to d 34 indicating changes that can only be explained by unknown tank effects. It is believed that irradiance may have had a negative effect on the coral specimens. Second, importance of heterotrophic feeding of coral specimens should be considered and measures to provide food should be made. Lack of food in the tanks may have been a contributing factor. Finally, the time it takes for coral specimens to acclimate to their new environmental conditions should be studied. Not much is known regarding appropriate time periods and thus a lot could be gained from more broad knowledge on this subject. In addition, numerous specimens from both phenotypes should have been sampled and fixed immediately after fragmentation. Provision of such samples would have made it possible to understand the approximate condition of the phenotypes before they were harvested and the changes that occurred during the acclimation period.

Conclusions

Montastraea reefs (dominated by *Montastraea* spp. corals; Geister 1977) support the largest number of ecosystems and have the greatest biodiversity of all reefs in the Caribbean region (Chollett and Mumby 2012). They are also in great decline across the Caribbean and tropical Atlantic Ocean (Harvell et al. 2007; Pollock et al. 2011), with highly negative implications for Caribbean reef systems in general. As their numbers continue to decrease, it becomes clear that not enough is known about these important reef-builders or what has made them so vulnerable to disease in the past few decades (Santavy and Peters 1997; Knowlton 2001;

Bruno et al. 2007). The results of the experiment showed that there were morphological differences in cells and tissues between colonies, but these did not permit the corals to respond differently to acute doses of bacteria. However, the comparison of the responses between phenotypes was not entirely conclusive since the sample set was small (two phenotypes) and it may be that *these* two colonies did not respond differently. To plausibly conclude that colonies do not respond differently to the same exposure to stress, more similar experiments would need to be carried out.

A lack of overt morphological change does not mean lack of pathology. This is well illustrated by the LKHS, which share some pathological characteristics with the LKDS, and others with the P1 and P2 experiment fragments. Terms that describe the gross observations made during the experiment, i.e., contracted tissue, shrunken tissue, lack of opaque white film appearance, are not terms that describe recognized coral diseases. Most documented coral diseases have names that describe paling, discoloration, or loss of tissue. The accepted terms for grossly visible pathology also specifically describe what is generally termed the "lesion", i.e., yellow band, white band, black band, and dark spot. This investigation has made it clear that a coral need not exhibit overt signs of disease to be undergoing highly damaging processes to its tissues and cells. Necrosis, karyolysis, sloughing, loss of integrity and other signs of disease in advanced stages were observed in P1 and P2 controls and treated specimens, yet none of these excursions from normal could have been predicted from the gross morphology of the specimens as observed at various times during the experiment. Thus, more corals with clear signs of CYBD and presumed healthy neighbors need to be evaluated histologically to gather more information on what each looks like at the tissue and cellular level, and how they compare to one another. Only then can we predict whether a colony will develop a lesion and begin to understand what factors contribute to that development. There is no doubt the challenged specimens were affected by the exposures, but clear evidence of whether they were *in*fected by the *Vibrio* spp. can only be achieved with the use of other tools such as fluorescence in situ hybridization. FISH was attempted for this research but has not yet yielded results that can confirm or disprove the presence of the inoculated bacteria in the coral tissue (see Appendix II).

The coral animal was the primary focus of this research but homeostasis of the host relies heavily on the good health of the holobiont community. The coral host is adversely affected by

any changes that create suboptimal conditions for its symbionts. Expulsion of zooxanthellae (bleaching) is a well-documented example of how a coral may respond to thermal stress and/or stressed symbionts (Glynn 1991; Buddemeier and Fautin 1993; Rowan et al.1997; Jones and Yellowlees 1997; Jones et al. 2008; Baker et al. 2008). Given the nutritional importance of the coral/algae symbiosis, it is safe to assume that the zooxanthellae play a very important role in the coral's ability to defend itself from pathogens, though its role is one of support. Microbial communities that inhabit the coral mucus are beneficial to the coral in many ways including provision of nutrients and defense via antibiotic properties (Knowlton and Rohwer 2003; Ritchie 2006; Reshef et al. 2006; Bourne et al. 2007) but they are not impervious to opportunist-mediated change (Santavy and Peters 1997; Knowlton and Rohwer 2003; Ritchie 2006). The coral host is dependent on its partnerships with other organisms that have made its existence not only possible, but have allowed it to thrive where nutrient availability is greatly limited (Veron 2000; Reshef et al. 2006). These partnerships, while essential to the coral, are also costly since the host must provide conditions for its symbionts that foster their optimal functioning (Veron 2000). In physical terms, this means the coral must continue to build skeleton, grow large, and capture available sunlight. All this must be done while remaining stationary on the reef and thus susceptible to changes in its environment. In the context of a changing global climate and increasing ocean acidification, corals are likely to be susceptible to an increasing number of stress factors. This research has brought to light the possibility that many more coral colonies on reefs may be impaired than is obvious to researchers. It is vital, therefore, that we start to evaluate histologically colonies that appear healthy to determine whether our visual assessments match what is really taking place in coral tissues.

Bibliography

Ainsworth T.D., Fine M., Blackall L.L., Hoegh-Guldberg O. (2006) Fluorescence in situ hybridization and spectral imaging of coral-associated bacterial communities. Appl. Environ. Microbiol. 72(4):3016-3020.

Amann R. I., Binder B. J., Olson R. J., Chisholm S. W., Devereux R., Stahl D. A. (1990a) Combination of 16S rRNA-targeted oligonucleotide probes with flow cytometry for analyzing mixed microbial populations. Appl. Environ. Microbiol. 56:1919-1925.

Amman R.I., Krumholz L., Stahl D.A. (1990) Fluorescent-oligonucleotide probing of whole cells for determinative, phylogenetic, and environmental studies in microbiology. J. Bacteriol. 172(2):762-770.

Amann R., Snaidr J., Wagner M., Ludwig W., Schleifer K.H. (1996) In situ visualization of high genetic diversity in a natural microbial community. J. Bacteriol. 178(12):3496-3500.

Amman R., Fuchs B.M., Behrens S. (2001) The identification of microorganisms by fluorescence in situ hybridization. Curr. Opin. Biotech. 12:231-236

Anthony K.R.N. and Fabricius K.E. (2000) Shifting roles of heterotrophy and autotrophy in coral energetics under varying turbidity. J. Exper. Mar. Biol. Ecol. 252:221-253.

Antonius A. (1977) Coral mortality in reefs: a problem for science and management. Proc. 3 Int. Coral Reef Symp. 2:618-623.

Antonius A. (1981) Coral reef pathology: a review. Proc. 4th Int. Coral Reef Symp. 2:3-6.

Babic A., Loftin I.R., Stanislaw S., Wang M., Miller R., Warren S.M., Zhang W., Lau A., Miller M., Wu P., Padilla M., Grogan T.M., Pestic-Dragovich L., McElhinny A.S. (2010) The impact of pre-analytical processing on staining quality for H&E, dual hapten, dual color in situ hybridization and fluorescent in situ hybridization assays. Methods 52(4):287-300.

Baker A.C. (2001) Reef corals bleach to survive change. Nature 411:765-766.

Baker A.C., Glynn P.W., Riegl B. (2008) Climate change and coral reef bleaching: An ecological assessment of long-term impacts, recovery trends and future outlook. Estuar. Coast Shelf S. 80:435-471.

Banin E., Israely T., Kushmaro A., Loya Y., Orr E., Rosenberg E. (2000) Penetration of the coral-bleaching bacterium *Vibrio shiloi* into *Oculina patagonica*. Appl. Environ. Microbiol. 66(7):3031-3036.

Banin E., Khare S.K., Naider F., Rosenberg E. (2001) Proline-rich peptide from the coral pathogen *Vibrio shiloi* that inhibits photosynthesis of zooxanthellae. Appl. Environ. Microbiol. 67(4):1536-1541.

Barker N.H.L. and Roberts C.M. (2004) Scuba diver behavior and the management of diving impacts on coral reefs. Biol. Conserv. 120:481-489.

Ben-Haim Y., Zicherman-Keren M., Rosenberg E. (2003) Temperature-regulated bleaching and lysis of the coral *Pocillopora damicornis* by the novel pathogen *Vibrio coralliilyticus*. Appl. Environ. Microbiol. 69(7):4236-4242.

Borger J.L. and Colley S. (2010) The effects of a coral disease on the reproductive output of *Montastraea faveolata* (Scleractinia: Faviidae). Rev. Biol. Trop. 58(Suppl. 3):99-110.

Bourne D., Iida Y, Uthick S., Smith-Keune C. (2007) Changes in coral-associated microbial communities during a bleaching event. ISME. 1751-7362/07:1-14.

Brock T.D. and Madigan M.T. (1991) *Jane Ann Phillips/Thomas D. Brock Laboratory Manual. Biology of Microorganisms.* 6th Edn. Prentice-Hall, Englewood Cliffs, NJ.

Bruno J.F., Petes L.E., Harvell C.D., Hettinger A. (2003) Nutrient enrichment can increase the severity of coral diseases. Ecol. Lett. 6(12):1056-1061

Bruno J.F. Selig E.R., Casey K.S., Page C.A., Willis B.L., Harvell C.D., Sweatman H., Melendy A.M. (2007) Thermal stress and coral cover as drivers of coral disease outbreaks. PLoS Biol. 5(6):1220-1227.

Brusca R.C. and Brusca G.J. (2003) *Invertebrates.* 2nd Edn. Sinauer Associates, Sunderland, Massachusetts.

Buddemeier R.W. and Fautin D.G. (1993) Coral bleaching as an adaptive mechanism: a testable hypothesis. BioScience 43(5):320-326.

Bythell J.C., Barer M.R., Cooney R.P., Guest J.R., O'Donnell A.G., Pantos O., Le Tissier M.D.A. (2002) Histopathological methods for the investigation of microbial communities associated with disease lesions in reef corals. Lett. Appl. Microbiol. 34:359-364.

Cervino J.M., Goreau T.J., Nagelkerken I., Smith G.W., Hayes R. (2001) Yellow Band and dark spot syndromes in Caribbean corals: distribution, rate of spread, cytology, and effects on abundance and division rate of zooxanthellae. Hydrobiologia 460:53-63.

Cervino J.M., Hayes R., Goreau T.J., Smith G.W. (2004a) Zooxanthellae regulation in yellow blotch/band and other coral diseases contrasted with temperature related bleaching: *in situ* destruction vs. expulsion. Symbiosis 37:63-85.

Cervino J.M., Hayes R.L., Polson W., Polson S.C., Goreau T.J., Martinez R.J., Smith G.W. (2004b) Relationship of *Vibrio* species infection and elevated temperatures to yellow blotch/band disease in Caribbean corals. Appl. Environ. Microbiol. 70(11):6855-6864.

Cervino J.M., Thompson F.L., Gomez-Gil B., Lorence E.A., Goreau T.J., Hayes R.L., Winiarski-Cervino K.B., Smith G.W., Hughen K., Bartels E. (2008) The *Vibrio* core group induces yellow band disease in Caribbean and Indo-Pacific reef-building corals. Appl. Microbiol. [doi: 10.1111/j.1365-2672.2008.03871.x].

Chollett I. and Mumby P.J. (2012) Predicting the distribution of *Montastraea* reefs using wave exposure. Coral Reefs 31(2):493-503.

Colwell R.R. (2006) A global and historical perspective of the genus *Vibrio*. *The Biology of Vibrios*. Ed. Thompson F.L. pp. 3-11: ASM Press, Washington, D.C.

Constantinides P. (1994) General Cell Injury. *General Pathobiology*. pp. 1-58: Appleton & Lange, Norwalk, Connecticut.

Cunning J.R., Thurmond J.E., Smith G.W., Weil E., Ritchie K.B. (2008) A survey of *Vibrios* associated with healthy and yellow band diseased *Montastraea faveolata.* Proc. 11 Int. Coral Reef Symp. 1:206-210.

Daims H., Bruhl A., Amann R., Schleifer K-H., Wagner M. (1999) The domain-specific probe EUB338 is insufficient for the detection of all bacteria: Development and evaluation of a more comprehensive probe set. Syst. Appl. Microbiol. 22(3):434-444.

Downs C.A., Kramarsky-Winter E., Martinez J., Kushmaro A., Woodley C.M., Loya Y., Ostrander G.K. (2009) Symbiophagy as a cellular mechanism for coral bleaching. Autophagy 5(2):211-216.

Dove S.G., Hoegh-Guldberg O., Ranganathan S. (2001) Major colour patterns of reef-building corals are due to a family of GFP-like proteins. Coral Reefs 19:197-204.

Ducklow H.W. and Mitchell R. (1979) Composition of mucus released by coral reef coelenterates. Limnol. Oceanogr. 24(4):706-714.

Dunn S.R., Bythell J.C., Le Tissier M.D.A., Burnett W.J., Thomason J.C. (2002) Programmed cell death and cell necrosis activity during hyperthermic stress-induced bleaching of the symbiotic sea anemone *Aiptasia* sp. J. Exp. Mar. Biol. Ecol. 272:29-53.

Dunn S.R., Schnitzler C.E., Weis V.M. (2007) Apoptosis and autophagy as mechanisms of dinoflagellate symbiont release during cnidarian bleaching: every which way you lose. Proc. R. Soc. B. 274:3079-3085.

Ferriz-Dominguez N. and Horta-Puga G. (2001) Short-term aggressive behavior in scleractinian corals from La Blanquilla reef, Veracruz Reef System. Rev. Biol. Trop. 49(1).

Fine M., Meroz-Fine E., Hoegh-Guldberg O. (2005) Tolerance of endolithic algae to elevated temperature and light in the coral *Montipora monasteriata* from the southern Great Barrier Reef. J. Exp. Biol. 208:75-81.

Fukami H., Budd A.F., Levitan D.R., Jara J., Kersanach R., Knowlton N. (2004) Geographic differences in species boundaries among members of the *Montastraea annularis* complex based on molecular and morphological markers. Evolution 58(2):324-337.

Galloway S.B., Work T.M., Bochsler V.S., Harley R.A., Kramarsky-Winters E., McLaughlin S.M., Meteyer C.U., Morado J.F., Nicholson J.H., Parnell P.G., Peters E.C., Reynolds T.L., Rotstein D.S., Sileo L., Woodley C.M. (2006) *CDHC Workshop: Coral Histopathology II*. National Oceanic and Atmospheric Administration, Silver Spring, MD. 83p.

Garren M., Walsh S.M., Caccone A., Knowlton N. (2006) Patterns of association between *Symbiodinium* and members of the *Montastraea annularis* species complex on spatial scales ranging from within colonies to between geographic regions. Coral Reefs 25(4):503-512.

Gartner L.P. and Hiatt J.L. (2006) *Color Textbook of Histology*. 2nd Edn. Saunders, Toronto, Canada.

Gates R.D., Bagiidasarian G., Muscatine L. (1992) Temperature stress causes host cell detachment in symbiotic cnidarians: implications for coral bleaching. Biol. Bull. 182:324-332.

Geister J. (1977) The influence of wave exposure on the ecological zonation of Caribbean coral reefs. Proc. 3rd Int. Coral Reef Symp. 2:23-29.

Glynn P.W. (1991) Coral reef bleaching in the 1980s and possible connections with global warming. Trends Ecol. Evol. 6(6)175-179.

Glynn P.W., Maté J.L., Baker A.C., Calderón M.O. (2001) Coral bleaching and mortality in Panama and Ecuador during the 1997-1998 El Niño-Southern Oscillation event: Spatial/temporal patterns and comparisons with the 1982-1983 event. B. Mar. Sci. 69(1):79-109.

Goreau T.F. (1956) *The Study of the Biology and Histology of Corals*. Ph.D. dissertation, Yale University.

Goreau T.F., Goreau N.I., Goreau T.J. (1979) Corals and coral reefs. Sci. Am. 241:124-136.

Goreau T. J, Cervino J.M., Hayes R., Hayes M., Richardson L., Smith G., DeMeyer K., Nagelkerken I., Garzon-Ferrera J., Gil D., Garrison G., Williams E.H., Bunkley-Williams L., Quirolo C., Patterson K., Porter J., Porter K. (1998) Rapid spread of Caribbean coral reef diseases. Rev. Biol. Trop. Vol. 46 Sup. (5):157-171.

Goreau T.J., Hayes R. (1994) Coral bleaching and ocean "hot spots". Ambio 23:176-180.

Hall V.R. (2001) The response of *Acropora hyacinthus* and *Montipora tuberculosa* to three different types of colony damage: scraping injury, tissue mortality and breakage. J. Exper. Mar. Biol. Ecol. 264:209-223.

Harel M., Ben-Dov E., Rasoulouniriana D., Siboni N., Kramarsky-Winter E., Loya Y., Barak Z., Wiesman Z., Kushmaro A. (2008) A new thraustochytrid, strain *Fng1*, isolated from the surface mucus of the hermatypic coral *Fungia granulosa*. FEMS Microbiol Ecol. 64:378-387.

Harvell C. D., Kim K., Burkholder J.M., Colwell R.R., Epstein P.R., Grimes D.J., Hofmann E.E., Lipp E.K., Osterhaus A.D.M.E., Overstreet R.M., Porter J.W., Smith G.W., Vasta G.R. (1999) Emerging marine diseases - climate links and anthropogenic factors. Science 285:505-1510.

Harvell C.D., Markel S., Jordan-Dahlgren E., Raymundo L., Smith G., Weil E., Willis B. (2007) Coral disease, environmental drivers and the balance between coral and microbial associates. Oceanography. 20:36-59.

Hawkins J.P., Roberts C.M., Van't Hof T., De Meyer K., Tratalos J., Aldam C. (1999) Effects of recreational scuba diving on Caribbean coral and fish communities. Conserv. Biol. 13(4):888-897.

Hobbie J.E., Daley R.J., Jasper S. (1977) Use of nuclepore filters for counting bacteria by fluorescence microscopy. Appl. Environ. Microbiol. 33(5):1225-1228.

Huggett M.J., Crocetti G.R., Kjelleberg S., Steinberg P.D. (2006) Recruitment of the sea urchin *Heliocidaris erythrogramma* and the distribution and abundance of inducing bacteria in the field. Aquat. Microbiol. Ecol. 53(2):161-171.

Hyman L.H. (1940) *The Invertebrates, Vol. 1, Protozoa Through Ctenophora*. McGraw-Hill Book Company, New York.

Iglesias-Prieto R., Matta J.L., Robins W.A., Trench R.K. (1992) Photosynthetic response to elevated temperature in the symbiotic dinoflagellate *Symbiodinium microadriaticum* in culture. Proc. Natl. Acad. Sci. USA 89:10302-10305.

Jagoe C.H. (1996) Responses at the tissue level: quantitative methods in histopathology applied to ecotoxicology. *Ecotoxicology: A Hierarchical Treatment*. Eds. Newman M.C., Jagoe C.H., pp. 163-195: CRC Press, Boca Raton, Florida.

Jokiel P.L. (2011) The reef coral two compartment proton flux model: A new approach relating tissue-level physiological processes to gross corallum morphology. J. Exper. Mar. Biol. Ecol. 409:1-12.

Jones R.J. and Yellowlees D. (1997) Regulation and control of intracellular algae (=zooxanthellae) in hard corals. Phil. Trans. R. Soc. Lond. B. 352:457-468.

Jones A.M., R. Berkelmans, M.J.H. van Oppen, J.C. Mieog, Sinclair W. (2008) A community change in the algal endosymbionts of a scleractinian coral following a natural bleaching event: field evidence of acclimatization. Proc. R. Soc. B. 275:1359-1365.

Kiernan J.A. (2010) *Histological and Histochemical Methods: Theory and Practice*. 4th Edn. Scion, Oxfordshire, UK.

Kirk J.T.O. (2011) Light and Photosynthesis in Aquatic Ecosystems. 3rd Edn. Cambridge University Press, New York, NY.

Knowlton N., Maté J.L., Guzmán H.M., Rowan R., Jara J. (1997) Deirect evidence for reproductive isolation among the three species of the Montastraea annularis complex in Central America (Panamá and Honduras). Mar. Biol. 127(4)705-711.

Knowlton N. (2001) The future of coral reefs. PNAS 98(10):5419-5425.

Knowlton N. and Rohwer F. (2003) Microbial mutualisms on coral reefs: The host as a habitat. American Naturalist 162:S51-S62.

Kojis B.L. and Quinn N.J. (1985) Puberty in *Goniastrea favulus*. Age or size limited? Proc. 5th Internat. Coral Reef Congr., 4:289- 293.

Kramarsky-Winter E., Harel M., Siboni N., Ben-Dov E., Brickner I., Loya I., Kushmaro A. (2006) Identification of a protist-coral association and its possible ecological role. Mar. Ecol. Prog. Ser. 317:67-73.

Kumar V., Abbas A.K., Fausto N., Aster J.C. (2010) *Robbins and Cotran Pathologic Basis of Disease*. 8th Edn. Saunders, Philadelphia, Pennsylvania.

Kushmaro A., Rosenberg E., Fine M., Loya Y. (1997) Bleaching of the coral *Oculina patagonica* by *Vibrio* AK-1. Mar. Ecol. Prog. Ser. 147:159-165.

LaJeunesse T.C. (2002) Diversity and community structure of symbiotic dinoflagellates from Caribbean coral reefs. Mar. Biol. 141:387-400.

Lang, J. (1973) Interspecific aggression by scleractinian corals. Why the race is not only to the swift. Bull. Mar. Sci. 23(2):260-279.

Loy A., Maixner F., Wagner M., Horn M. (2007) probeBase – an online resource for rRNA-targeted oligonucleotide probes: new features 2007. Nucleic Acids Res. 35:D800-D804.

Loya Y., Sakai K., Yamazato K., Nakano Y., Sambali H., van Woesik R. (2001) Coral bleaching: the winners and the losers. Ecol Lett 4(2):122–131.

McWilliams J.P., Côte I.M., Gill J.A., Sutherland W.J., Watkinson A.R. (2005) Accelerating impacts of temperature-induced coral bleaching in the Caribbean. Ecology. 86(8):2055-2060.

Muller-Parker G. and D'Elia C.F. (1997) Interactions between corals and their symbiotic algae. *Life and Death of Coral Reefs*. Ed. Birkeland C. pp. 96-113: Chapman and Hall, New York.

Muscatine L. and Cernichiari E. (1969) Assimilation of photosynthetic products of zooxanthellae by a reef coral. Biol. Bull. 137:506-523.

Muscatine L., McCloskey L.R., Marian R.E. (1981) Estimating the daily contribution of carbon from zooxanthellae to coral animal respiration. Limnol. Oceanogr. 26(4):601-611.

Muscatine L., McNeill P.L. (1989) Endosymbiosis in Hydra and the evolution of internal defense systems. Am. Zool. 29:371-386.

Muscatine L., Tambutte E., Allemand D. (1997) Morphology of coral desmocytes, cells that anchor the calicoblastic epithelium to the skeleton. Coral Reefs. 16:205-213.

Nelson C.E., Alldredge A.L., McCliment E.A., Amaral-Zettler L.A., Carlson C.A. (2011) Depleted dissolved organic carbon and distinct bacterial communities in the water column of a rapid-flushing coral reef ecosystem. ISME J. 5:1374-1387.

Owens L. and Busico-Salcedo, N. (2006) *Vibrio harveyi*: pretty problem in paradise. *The Biology of Vibrios*. Ed. Thompson F.L. pp. 266-280: ASM Press, Washington, D.C.

Pearse V.B. and Muscatine L. (1971) Role of symbiotic algae (zooxanthellae) in coral calcification. Biol. Bull. 141:350-363.

Pernthaler J., Glöckner F.O., Schönhuber W., Amann R.I. (2001) Fluorescence in situ hybridization with rRNA-targeted oligonucleotide probes. *Methods in Microbiology: Marine Microbiology, vol. 30*. Ed. Paul J. pp. 207-226: Academic Press, San Diego, California.

Peters E.C., Meyers P.A., Yevich P.P., Blake N.J. (1981) Bioaccumulation and histopathological effects of oil on a stony coral. Mar. Pollut. Bull. 12:333-339.

Peters E.C. (1984) A survey of cellular reactions to environmental stress and disease in Caribbean scleractinian corals. Helgol. Meeresunters. 37:113-137.

Peters E.C. and Pilson M.E.Q. (1985) A comparative study of the effects of sedimentation on symbiotic and asymbiotic colonies of the coral *Astrangia danae* Milne Edwards & Haime, 1849. J. Exp. Mar. Biol. Ecol. 92:215-230.

Peters E.C. (1993) Diseases of other invertebrate phyla: Porifera, Cnidaria, Ctenophora, Annelida, Echinodermata. *Pathology of Marine and Estuarine Organisms*. Ed. Couch J.A. and Fournie J.W. pp. 393-449: CRC Press, Boca Raton, FL.

Peters E.C. (1997) Diseases of coral reef organisms. *Life and Death of Coral Reefs*. Ed. Birkeland C. pp. 114-139: Chapman & Hall, New York, NY.

Peters, E. C., Price K.L., Borsay Horowitz D.J. (2005) Histological preparation of invertebrates for evaluating contaminant effects. *Techniques in Aquatic Toxicology*. Ed. G. K. pp. 653-686: Ostrander: Taylor & Francis, Boca Raton, Florida.

Peters E.C., Price K., Aeby G. (2009) Understanding Anthozoan histology section 4 revised. Course notes for Histotechniques and Histology of the Anthozoans. University of Hawaii, Hawaii Institute of Marine Biology.

Peters E.C. (In press) Anatomy. *Diseases of Corals* Ed. Downs C., Woodley C., Porter J., Bruckner A.: Blackwell Publishing

Piggot, A.M., Fouke B.W., Sivaguru M., Sanford R.A., Gaskins H.R. (2009) Change in zooxanthellae and mucocytes tissue density as an adaptive response to environmental stress by the coral, *Montastraea annularis*. Mar. Biol. 156(11):2379-2389.

Pollock F.J., Morris P.J., Willis B.L., Bourne D.G. (2011) The urgent need for robust coral disease diagnostics. PLoS. Pathog. 7(10): e1002183.

Porter J.W., Dustan P.W., Japp W., Patterson K., Vladimir K., Patterson M., Parsons M. (2001) Patterns of spread of coral disease in the Florida Keys. Hydrobiol. 460:1-24.

Raghukumar S. (2002) Ecology of the marine protists, the Labyrinthulomycetes (Thraustochytrids and Labyrinthulids). Europ. J. Protistol. 38:127-145.

Ramsey F.L. and Schafer D.W. (2002) *The Statistical Sleuth: A Course in Methods of Data Analysis*. 2nd Edn. Brooks/Cole Cengage Learning, Belmont, CA.

Renshaw A.A. and Gould E.E. (2006) Measuring the value of review of pathology material by a second pathologist. Am. J. Clin. Pathol. 125:737-739.

Reshef L., Koren O., Loya Y., Zilber-Rosenberg I., Rosenberg E. (2006) The coral probiotic hypothesis. Environ. Microb. 8(12):2068-2073.

Ritchie K.B. (2006) Regulation of microbial populations by coral surface mucus and mucus-associated bacteria. Mar. Ecol. Prog. Ser. 322:1-14.

Rosenberg E., Koren O., Reshef L., Efrony R., Ziber-Rosenberg I. (2007a) The role of microorganisms in coral health, disease and evolution. Nature 5:355-362.

Rosenberg E., Kellogg C.A., Rohwer F. (2007b) Coral microbiology. Oceanography 20(2):146-154.

Rowan R., Knowlton N., Baker A., Jara J. (1997) Landscape ecology of algal symbionts creates variation in episodes of coral bleaching. Nature 33:265-269

Santavy D.L., Peters E.C., Quirolo C., Porter J.W., Bianchi C.N. (1999) Yellow-blotch disease outbreak on reefs of the San Blas Islands, Panama. Coral Reefs 18(1):97.

Santavy D.L. and Peters E.C. (1997) Microbial pests: Coral disease in the Western Atlantic. Proc 8th Int. Coral Reef Sym. 1:607-612.

Sharp K.H., Eam B., Faulkner D.J., Haygood M.G. (2007) Vertical transmission of diverse microbes in the tropical sponge *Corticium* sp. Appl. Environ. Microbiol. 73(2):622-629.

Siboni, N., Rasoulouniriana D., Ben-Dov E., Kramarsky-Winter E., Sivan A., Loya Y., Hoegh-Guldberg O., Kushmaro A. (2010) Stramenopile microorganisms associated with the massive coral *Favia* sp. J. Eukaryot. Microbiol. 57(3):236-244.

Smith G.W., Hayasaka S.S. (1982) Nitrogenase activity associated with *Halodule wrightii* roots. Appl. Environ. Microbiol. 43(6):1244-1248.

Sokal R.R. and Rohlf F.J. (2001) *Biometry: The Principles and Practices of Statistics in Biological Research*. 3rd Edn. W.H. Freeman and Company, New York.

Stat M., Carter D., Hoegh-Guldberg O. (2006) The evolutionary history of *Symbiodinium* and scleractinian hosts - symbiosis, diversity, and the effect of climate change. Perspect. Plant Ecol. 8:23-43.

Sutherland K., Porter J.W., Torres C. (2004) Disease and immunity in Caribbean and Indo-Pacific zooxanthellate corals. Mar. Ecol. Prog. Ser. 266:273-302.

Szmant A.M. (1991) Sexual reproduction by the Caribbean reef corals *Montastrea annularis* and *M. cavernosa*. Mar. Ecol. Prog. Ser. 74:13-25.

Szmant A.M., Weil E., Miller M.W., Colón D.E. (1997) Hybridization within the species complex of the scleractinian coral *Montastraea annularis*. Marine Biology. 129:561-572.

Szmant-Froelich A., Yevich P., Pilson M.E.Q. (1980) Gametogenesis and early development of the temperate coral *Astrangia danae* (Anthozoa: Scleractinia). Biol. Bull. 158:257-269.

Toller W.W., Rowan R., Knowlton N. (2001) Repopulation of zooxanthellae in the Caribbean corals *Montastraea annularis* and *M. faveolata* following experimental and disease-associated bleaching. Biol. Bull. 201:360-373.

Van Stedum S. and King W. (2002) "Basic FISH Techniques and Troubleshooting." *Methods in Molecular Biology. Vol. 204, Molecular Cytogenetics: Protocols and Applications*. Ed. Fan Y-S. Humana Press, Totowa, New Jersey.

Van Veghel M.L.J (1994) Reproductive characteristics of the polymorphic Caribbean reef building coral *Montastraea annularis*. I. Gametogenesis and spawning behavior. Mar. Ecol. Prog. Ser. 109:209-219.

Veron J.E.N. (2000) *Corals of the World Vol. 1*. Stafford-Smith, Ed. Australian Institute of Marine Science and CCR. Townsville MC, Australia.

Wagner M., Amann R., Kämpfer P., Assmus B., Hartmann A., Hutzler P., Springer N., Schleiger K.H. (1994) Identification and *in situ* detection of Gram-negative filamentous bacteria in activated sludge. System. Appl. Microbiol. 17:405-417.

Weil E. and Knowlton N. (1994) Multi-character analysis of the Caribbean coral Montastraea annularis (Ellis and Solander, 1786) and its two sibling species, M. faveolata (Ellis and Solander, 1786) and M. franksi (Gregory 1895). Bull. Mar. Sci. 55(1): 151-175.

Weil E., Smith G.W., Gil-Agudelo D.L. (2006) Status and progress in coral reef disease research. Dis. Aquat. Organ. [doi:10.3354/dao069001].

Weil E., Cróquer A., Urreiztieta I. (2009) Yellow band disease compromises the reproductive output of the Caribbean reef-building coral *Montastraea faveolata* (Anthozoa, Scleractinia). Dis. Aquat. Org. 87:45-55.

Work T.M. and Aeby G.S. (2006) Systematically describing gross lesions in corals. Dis. Aquat. Org. 70: 155-160.

Young B., Stewart W., O'Dowd G. (2011) *Wheater's Basic Pathology: A Text, Atlas and Review of Histopathology*. 5th Edn. Churchill Livingstone Elsevier, UK.

Appendix I – Methods for assessing individual criteria

Epithelial attenuation, viewed at 40x, 63x, 100x

The epidermis, mesoglea and gastrodermis of the surface body wall and the gastrodermis, mesoglea and calicodermis of the basal body wall were examined and scored. Scores take into account that epidermis and gastrodermis thin somewhat towards the tips of septa (or costae). The assigned score reflects greater than normal attenuation and/or changes in cell types, i.e., from columnar to cuboidal (with light microscopy, it is not possible to determine whether epithelia are attenuated or if cells have undergone metaplastic changes). Gastrodermis was considered attenuated when it was too thin to support zooxanthellae or when it was found housing only one row of zooxanthellae running parallel to the epidermis with gaps of thinned tissue between the algal cells.

Epidermis integrity (40x, 63x, 100x)

The epidermis should be contiguous from one end of a section to the next, with the exception of open, healthy-looking mucocytes. Breaks or tears or regions of epidermis with missing cells were scored. Tips of septa often appeared abraded and were not always scored because this was at times, believed to be caused by handling.

Gastrodermis integrity (40x, 63x, 100x)

The gastrodermis should also be contiguous from one end of the section to the next. Area occupied by gastrodermis usually extends downwards and expands in the valleys between septa. This is also where the surface body wall meets the basal body wall. Zooxanthellae density is generally greater here than along the sides and tips of septa and along the coenenchyme. Only breaks or tears in the gastrodermis of the surface body wall were considered and scored. In addition, areas with a large amount of hypertrophied vacuolated cells, possibly releasing zooxanthellae into the gastrovascular cavity, were scored where breakage was found.

Mesoglea integrity (40x, 63x, 100x)

Mesoglea is the connective tissue layer between the epidermis or calicodermis and gastrodermis and should be contiguous. Loss of integrity of the mesoglea was a condition rarely found in any of the slides, although tissue at the tips of septa was often found entirely ulcerated and abraded. These occurrences were not scored as previously mentioned. Only regions of breakage in the mesoglea that appeared to be the result of processes taking place in the epithelia and NOT the result of handling were evaluated and scored. Most commonly, the mesoglea remained contiguous but attenuated even when the gastrodermis and epidermis did not.

Calicodermis integrity (40x, 63x, 100x)

The calicodermis should be contiguous and have a consistent width except where calicoblasts are actively accreting the calcium carbonate skeleton. The calicodermis was often associated with large amounts of basophilic suspect bacteria, and at times was found broken, or attenuated and torn, or vacuolated with a foamy appearance. Where there were large aggregates, it was often difficult to determine whether the epithelium underneath remained intact. Tissue sections received scores for this criterion only when it was clear there was discontinuity in the calicodermis. Calicodermis that had a "foamy" appearance was scored only when entire breaks in integrity were found. It is unclear what processes were taking place in the foamy-appearing calicodermis.

Loss Of Adhesion (40x, 63x, 100x)

The epidermis and gastrodermis of the surface body wall and the calicodermis were evaluated for this criterion. Loss of adhesion was identified where epithelia were no longer attached to a supporting layer of mesoglea. Loss of adhesion was often also accompanied by loss of integrity, but not always. Regions of tissue that received scores for loss of adhesion were generally short in length.

Epithelial sloughing (40x, 63x, 100x)

Sloughing was evaluated for the epidermis, gastrodermis of the surface body wall and the calicodermis. Epithelia that were no longer contiguous and no longer adhered to the mesoglea or appeared to be debris were scored. Regions of ablation of epithelia were also scored where it was clear the tissue was detached from the skeleton. This important and deleterious pathology was most commonly found affecting the epithelia of the surface body wall, specifically the epidermis, with debris in the mucus layer.

Increase of and/or hypertrophied mucocytes/vacuolated cells (40x, 63x)

Normal epithelia of the surface body wall should have interspersed columnar mucocytes with healthy eosinophilic ciliated supporting cells. An increase in area occupied by mucocytes or vacuolated epidermal cells was scored. It was not possible to differentiate between hypertrophied mucocytes and vacuolated cells. Any regions of tissue with more than a normal amount of mucocytes or open and numerous vacuolated cells were scored (Figure 9*a, b*).

Mucus (40x, 63x, 100x)

Epithelia were assigned scores for this criterion when the amount of mucus seemed greater than normal and the mucocytes appeared hypertrophied. Normal mucus does not generally appreciably pick up the stain used therefore mucus that appeared to have a purple tint streaming from enlarged mucocytes was considered abnormal.

Mucus/surface debris (40x, 63x, 100x)

A small amount of surface debris is considered normal, especially where translucent mucus is found on the apical surface of the epidermis (Figure 9*a, b, c, d*). Epidermis with a greater amount of debris than normal was scored, likely the result of loss of cilia, which aids the coral in removing settling organisms, sediments, or other debris. Large diatoms, sponge spicules, and filamentous algae were commonly found on some of the more degenerated coral specimens.

Endolithic organism adhesion/penetration calicodermis (40x, 63x, 100x)

The occurrence of endolithic algae or fungi, when found clearly attached to or entering the calicodermis, was scored. More commonly, endolithic organisms were found attached or adjacent to the calicodermis. Penetration into the tissue was rare and in the case of calicodermis, difficult to identify clearly.

Endolithic organism adhesion/penetration gastrodermis (40x, 63x, 100x)

Penetration of endolithic organisms into the gastrodermis was rare but more easily identified. Access to gastrodermis was through the calicodermis, unless that layer had sloughed off or had lost integrity and/or no longer adhered to the mesoglea. Adhesion of endolithic organisms to the gastrodermis was more commonly found yet still rare.

Zooxanthellae shape/color/size (40x, 63x, 100x)

Zooxanthellae were scored that had shape, color and size that differed from normal. Normal zooxanthellae are round in shape, and eosinophilic with a purple nucleus that appears as a round cluster of dots due to the permanently condensed chromosomes characteristic of dinoflagellates. Size was evaluated only in conjunction with the other parameters due to the potential presence of different clades which range in size from ~ 5 μm to 15 μm. Changes in size usually occurred together with changes in color and shape. It was common to find zooxanthellae that appeared shrunken, paling and misshapen but individuals were also scored that only qualified for one of the parameters (not size), rendering this criterion very challenging to evaluate.

Zooxanthellar nuclei shape (40x, 63x, 100x)

The nuclei of the zooxanthellae were evaluated separately. Nuclei of healthy zooxanthellae appear as a round (or somewhat square), dark purple cluster of small dots. Nuclei that appeared elongated, trapezoidal, pointed or missing entirely were scored. The further from round the damaged nuclei, the higher the condition score.

Zooxanthellae yellowing/green (40x, 63x, 100x)

Healthy zooxanthellae are constantly undergoing protein synthesis and thus will stain bright pink with eosin. When protein synthesis is reduced, photosynthetic structures within the cell become visible by light microscopy. The frequency of zooxanthellae displaying yellow-

green color was scored; the more prominent the green or yellow tint, the higher the score in condition.

Suspect bacteria epidermis (40x, 63x, 100x)

Clumps of suspect bacteria found present on the epidermis were scored. These suspect bacteria often pooled in the deepest creases of the coral epidermis, where theoretically, more vigorous ciliary action was required to remove surface debris.

Suspect bacteria gastrodermis (40x, 63x, 100x)

Clumps of suspect bacteria were scored when viewed in the gastrodermis of the surface and basal body walls, although they were very rarely found here.

Suspect bacteria calicodermis (40x, 63x, 100x)

Suspect bacteria were often found adhering to the tissue of the calicodermis, more commonly deep in the skeleton at the base of the polyps, but also close to the surface below the septa. These occurrences were scored. The larger clumps scored higher in condition, especially where the tissue was visible and deemed compromised.

Suspect bacteria endolithic organisms (40x, 63x, 100x)

Occurrence of suspect bacteria found among the endolithic organisms was scored. At times, there was difficulty in determining bacteria from exudate that had stained acidophilic. Unless coccoid or rod shapes were clearly delineated, no score was assigned. When found on the endolithic organisms, these suspect bacteria were extremely numerous (as was what appeared to be exudate). Condition of the filamentous endolithic organisms was scored based on the amount of paling that occurred and amount of suspect bacteria present.

Mesentery integrity (10x, 20x, 40x)

Viewed with low magnification, sections were examined grossly to determine whether mesenteries were generally intact. Mesenteries with hypertrophied and/or vacuolated cells and discontinuous or indistinguishable epithelial surfaces were scored. At times, it was clear that damaged regions of epithelia were a direct result of handling, such as when the breaks spanned an entire polyp. Changes in integrity caused by handling were not scored.

Karyorrhexis nuclei gastrodermis (40x, 63x, 100x)

Fragmentation of the nuclei (karyorrhexis) as evidenced by the presence of small purple pinpoints of condensed chromatin (presumably from zooxanthellae and host nuclei, perhaps degraded bacteria) in the gastrodermis of the surface body wall, was scored. Condition scores were given for the gastrodermis where karyorrhectic nuclei were found but not for the condition of the nuclei themselves.

Karyorrhexis nuclei epidermis (40x, 63x, 100x)

Rarely, fragments of condensed chromatin from nuclei were found in the epidermis and scored. Condition of the epidermis where these nuclei were found was scored, but not the condition of the karyorrhectic nuclei.

Nuclei epidermis (40x, 63x, 100x)

Normal nuclei should generally be elongated or ovoid in the predominantly columnar cells of the epidermis. They should also be stained somewhat darkly and uniformly but with a visible nucleolus. Pale, strangely shaped (possibly pyknotic) or differently sized nuclei were scored. Nuclei with a grainy appearance were also scored. Condition of the nuclei was scored based on their overall appearance and how far from elongated, purple, and correctly proportional in relation to the cell size they appeared.

Nuclei gastrodermis (40x, 63x, 100x)

Nuclei of the gastrodermis were the most consistently poor-looking nuclei in the tissues. They were often seen as hypertrophied, misshapen, very pale, and grainy. It was challenging to score these nuclei because they were numerous, paler than nuclei of the epidermis or calicodermis, often tightly spaced, and in various stages of necrosis. Condition scores were assigned based on overall appearance of the nuclei.

Nuclei calicodermis (40x, 63x, 100x)

Normal nuclei of the calicodermis are generally round and somewhat darkly stained. Nuclei that looked pale, and/or exaggeratedly elongated were scored. Interestingly, even when surrounded by the suspect bacteria, the nuclei often appeared to be in fair or good condition.

Symbiophagy in basal body wall (40x, 63x)

Zooxanthellae found in the very deepest regions of the polyps in the mesenteries were often very misshapen, shrunken, and discolored and assumed to be digested by the coral. In the ECP 1981 presumed healthy corals these necrotic zooxanthellae were not found. Symbiophagy also occurred in the lobes of the cnidoglandular bands to a lesser extent. Granular gland cells in the vicinity of these degraded zooxanthellae were a necessary attribute for scoring. Those at more advanced stages of necrosis or where they were more numerous in a given area scored higher in condition.

Appendix II – Fluorescence in situ hybridization

Detection of Vibrios within tissues of exposed corals (FISH and spectral imaging)

The challenge experiment and subsequent histological analysis were components of the current research from the inception. The ability to determine whether the *Vibrio* spp. were able to penetrate the coral tissue was a strongly desired outcome of the research and was an added component after the termination of the challenge experiment. Unfortunately, at this time, results of FISH are inconclusive, as it is still unclear whether the probes were correctly hybridized with the bacterial DNA in the coral tissues.

The corals were fixed in a zinc-formalin solution, later determined to be incompatible with FISH (Kiernan 2010; Fan 2002), although there was a report that countered the incompatibility viewpoint (Babic et al. 2010). It was this latter report that guided the decision to attempt FISH with zinc-formalin fixed samples. In addition, the immense autofluorescence from the coral tissue and symbionts rendered analysis by epifluorescence more than a little challenging. Spectral imaging was deemed necessary to tease out probe signals from autofluorescence since the technology was able to differentiate fluorescent signals to within 10 nm. Numerous hours were spent on spectral imaging numerous FISH-prepared slides in an effort to gain better understanding of the presence and spatial distribution of the *Vibrio* spp. used for the experiment as well as the basophilic bacteria-sized structures termed "suspect bacteria" in this thesis. Work will continue on the FISH slides until it can be determined with certainty whether the protocol worked. They remain at the NIST facilities in Maryland with Dr. David Allen and Dr. Jeeseong Hwang who are actively working on new methods to use the technology in order to get the results needed.

Protocol for preparation of slides for FISH

Fluorescence in situ hybridization provides a means to identify and enumerate certain known bacteria. Coral specimens left in control tanks allowed the verification of the presence of bacteria in unexposed tissue. The assumption was that bacteria found in control specimens are either symbiotic or generally not to be considered to be pathogenic, whereas an increase in *Vibrio* spp. within the tissue of exposed specimens would be considered confirmation that *Vibrio* inocula have been able to proliferate inside the coral tissue. Since CYBD is an infection of the coral host's symbiotic algae that causes lysis of the algal cell *in hospite* (Cervino et al. 2004a), evidence of lysis of the zooxanthellae in the presence of high concentrations of bacteria and absence of such evidence in control specimens guided this aspect of the investigation.

Coral tissue, embedded in paraffin wax and sectioned to 5 μm, were placed onto Tissue Path SuperFrost Plus microscope slides (Fisher Scientific, Pittsburgh, PA) and dried for fluorescence-*in situ*-hybridization (FISH) procedures (Amman et al. 1990; Pernthaler et al. 2001). The "Genus *Vibrio*" (VIB572a) FISH probe with probeBase accession number pB-01188

specific for the genus *Vibrio* was used to detect the presence of *Vibrio* spp. in the coral tissue. This tested probe targets 18 bases of the 16S rRNA gene at position 572-589 (5′–ACC ACC TGC ATG CGC TTT–3′; Huggett et al. 2006; Loy et al. 2007). AlexaFluor® 660 fluorescent label was attached to the probe (Invitrogen; scale of synthesis 50 N, purity HPLC) at the 5′ end. In addition, the general bacteria probes EUB338 I–III were used with Cy3 fluorescent label to detect most other bacteria in the tissue sections (Daims et al. 1999). This 18-base oligonucleotide probe has a G+C content of 56%, and will theoretically dissociate in a hybridization buffer containing ~ 30%–40% formamide at 46°C (Pernthaler et al. 2001). As per probeBase specifications, EUB338 probes required 30% formamide and Genus *Vibrio* probe required 40% formamide for maximum hybridization efficiency. The following protocol was developed after numerous consultations with others who have done FISH on paraffin slides as well as on filters.

Careful preparation of hybridization buffer (HB) and washing buffers (WB) is an important step for the success of FISH, as is adherence to the correct stringency in formamide for each probe that will be added to the HB. Ten mL of HB was prepared just before use and consisted of 2.16 mL 5M sodium chloride (NaCl), 0.24 mL 1M Tris-hydrogen chloride (HCl) titrated to pH 7.4, 3.2 mL formamide (30% for EUB338 probe) or 4.2 mL formamide (40% for Genus *Vibrio* probe), 5 mL sterile DIH_2O (SDW; for EUB 338 probe) or 4 mL (for Genus *Vibrio* probe HB), and 0.025 mL sodium dodecyl sulfate (SDS) 10% added last to avoid precipitation. Fifty mL of the WB consisted of 1.02 mL (for 30% formamide in HB) or 0.56 mL (for 40% formamide in HB) 5M NaCl, 1 mL 1M Tris-HCl 7.4 pH, 0.5 mL ethylenediaminetetraacetic acid (EDTA) pH 8.0, 46.5 mL SDW, and 0.025 mL SDS 10% added last to avoid precipitation. Solutions' pH were titrated using either HCl or NaOH. Volumes of 50 mL of each individual component solution were prepared first and filtered through syringe-mounted a 0.2–µm Millipore filters, then stored in sterile Falcon tubes. In addition, 500 mL of 20 mM Tris-HCl at pH 8.0 was prepared, filtered as above.

Working quickly and in dim light, aliquots of the Genus *Vibrio* probe were prepared. First, the lyophilized probe was reconstituted with 1000 µL of molecular grade H_2O. Next, stock solutions of 100 mL and 50 mL of the probe solution were made and pipetted into 500 µL Eppendorf tubes and kept in the dark at -20°C. Working solutions with concentrations of 50 ng/µl were then prepared: for 100 µl total working solution (W), 19.8 µl of stock solution was added to 80.2 µl of molecular grade H_2O; for 50 µl total working solution, 9.9 µl of stock solution was added to 40.1 µl of molecular grade H_2O. Working solutions were stored at 6°C.

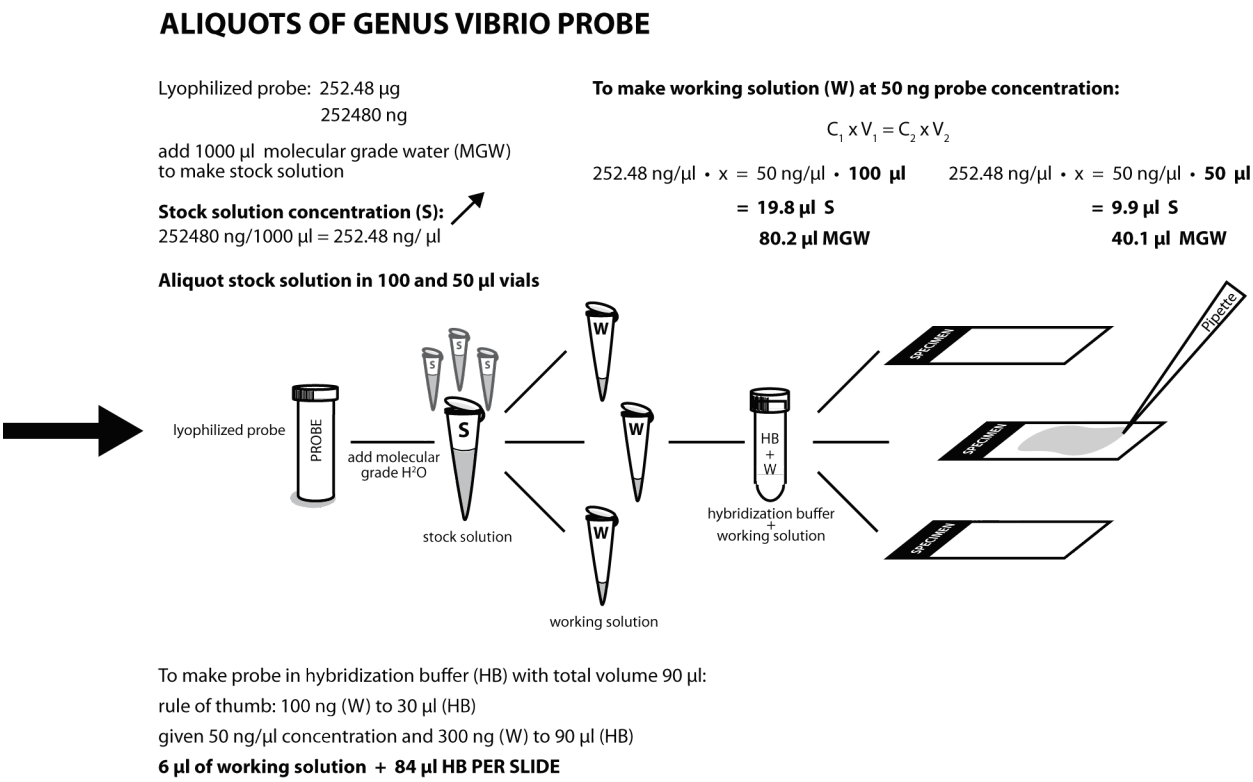

Figure 42. Illustration of protocol for aliquots of Genus *Vibrio* probe.

Slides were pre-selected for FISH that had interesting characteristics such as presence of suspect bacteria in regions of the coral tissue, lack of suspect bacteria throughout the section, control specimens, field-collected diseased specimens, or field-collected apparently healthy specimens. The hybridization oven (Boekel Scientific InSlide Out, Feasterville, PA) was preheated to 46°C. Four slides at a time were de-paraffinized in histological grade xylene (Sigma-Aldrich, St. Louis, MO) two times (2x) for 15 min each using a small ~40 mL slide case with sealable screw cap and gentle agitation. Under the hood, xylene was poured into the slide case and gently agitated. At the termination of the first 15 min, used xylene was replaced by a fresh volume. Next, the xylene was replaced by a graded series of EtOH: 100% for 10 min followed by 95%, 85% and 50% ETOH for 5 min each. 20 mM Tris HCl at pH 8.0 was added to the slide case for 10 min then discarded. Four Eppendorf microcentrifuge tubes containing 90 µl HB and probe (6 µl of W and 84 µl of HB) were prepared just prior to the termination of the 20 mM Tris HCl immersion.

Next, slides were placed flat on a slide rack and the HB/probe solution was distributed to cover the desired area to be hybridized. The slide tray was then covered and placed in the hybridization chamber at 46°C for 3 h. The washing buffer was prepared just before the conclusion of the hybridization and pre-warmed to 48°C in a water bath. Slides were returned to the slide case with the pre-warmed washing buffer and placed in the 48°C water bath for 15 min three times (3x). During the third washing buffer immersion, the HB for the second probe was prepared. At the conclusion of the third wash, the slides were removed from the water bath, air-

dried, and the process for the second probe was repeated. After the final wash, the washing buffer was removed and SDW at room temperature was added to the slide case for 5 min. The slides were then carefully removed from the slide case and placed flat on a paper towel and allowed to just barely dry. Approximately 6 drops of VECTASHIELD® H-1000 mounting medium (Vector, Burlingame, California) was added to each slide and cover-slipped. Clear nail polish was sparingly applied to all edges of the slide to seal and the slides were placed to lay flat in a slide case in a 6°C refrigerator.

Hybridization and washing procedures for the Genus *Vibrio* probe were conducted first since the required percentage of formamide (stringency) is higher, followed by hybridization and washing procedures for the EUB338 I-III probe (Wagner et al. 1994).

Staining control measures

Two selected slides were de-paraffinized and hydrated in a graded EtOH series (100% for 10 min, 95% for 5 min and 80% for 5 min) then left in 80% EtOH to avoid microbial contamination until further use. These slides and those next described were processed as FISH probe staining controls in the event the FISH stained slides viewed by laser scanning confocal microscope yielded inconclusive results. In addition, four selected slides were stained with DAPI, a fluorescent stain that binds to DNA, as a means to detect the presence of all bacteria. Naturally, the stain will bind to all DNA present in the slide, including that of the coral host and its symbionts. Accordingly, DAPI-stained slides were viewed under UV light (emission maximum at ~450 nm) and an effort was made to differentiate bacterial DNA from other DNA. 90 µl of DAPI stain with concentration of 1 µg/mL was prepared for each de-paraffinized slide from a 0.1 mg/mL stock solution and filtered SDW. The solution was pipetted onto the slides and incubated at room temperature in the dark for 3 min. Slide were rinsed briefly with filtered SDW and then briefly rinsed with 80% EtOH and left to air dry. VECTASHIELD® H-1000 mounting medium was applied to dry slides, then coverslipped.

Spectral imaging

The presence of extensive autofluorescence in the tissues prepared for FISH, necessitated the use of spectral imaging and confocal microscopy to differentiate between fluorescent emissions from the tissues and the FISH probes. Lambda scans, which record a series of distinct images within predefined wavelength ranges, were used to determine the excitation and emission maxima of the autofluorescence in the coral tissues. Non-stained *M. faveolata* slides yielded significant autofluorescence signals for presumed green fluorescent proteins (GFPs) or GFP-like proteins and chlorophyll (Dove et al. 2001). These presumptions were made based on emission spectra and spatial distribution of spectra and known ranges for endogenous GFPs, GFP-like proteins and chlorophyll. Lambda scans were also used as a guide for the choice of fluorescent labels for FISH (Figure 12). The AlexaFluor® 660 fluorescent label with excitation maximum at 660 nm and emission maximum at 690 nm, was chosen for hybridization with the *Vibrio* spp. bacteria based on the results of these scans.

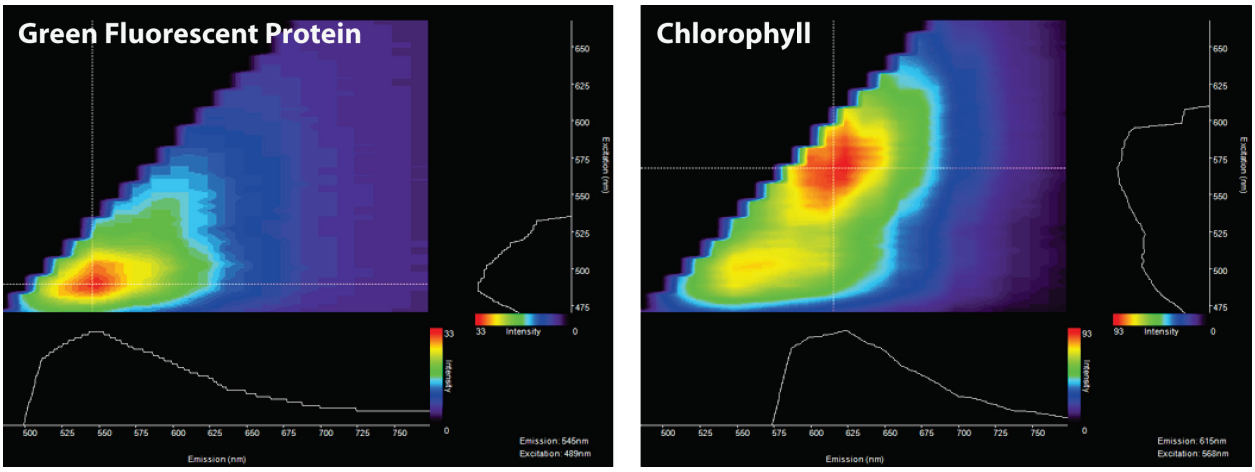

Figure 43. Lambda-lambda scans of presumed GFPs or GFP-like proteins and chlorophyll for *M. faveolata* slides used to determine optimal spectra for FISH fluorescent labels.

All spectral imaging and use of laser scanning confocal microscopy was done at the National Institute of Standards and Technology (NIST) in Gaithersburg, MD under the supervision of Dr. Jeeseong Hwang and Dr. David Allen.

Spectral imaging by confocal scanning microscopy is a powerful tool because it is capable of resolving spectra of various auto-fluorescent tissues and probes without the need to switch optical filters. When used in conjunction with FISH it allows determination of which wavelengths constitute an autofluorescent signal and those wavelengths known to correspond to the chosen fluorophores of the probe. In essence, spectral imaging makes it possible to determine not only the presence of the organisms for which the probe was designed, but also their location in the tissues (Amann et al. 1996; Ainsworth et al. 2006). Pixel-by-pixel spectra were captured during scanning and each pixel corresponded to a fluorescent wavelength resolved to within 10 nm intervals. Scanning confocal microscopy was done with a Leica Microsystems TCS SP5 X system, which used white light laser (WLL) and allowed the tuning of excitation wavelengths to precisely match the fluorophores used. In addition, the system functions at reduced laser power, which minimizes sample damage. This last feature is important when scanning slides for extended periods of time.

Slides were first scanned with green light excitation at 10x to locate regions of interest. Four spectral detection channels—CY3, AlexaFluor 660, backscatter and forward scatter (transmission image)—were simultaneously used to scan regions of the surface body wall and the basal body wall for each slide. One unstained slide, one treated slide, and one control slide for each coral phenotype were analyzed. Images were captured, and 3D analysis of the region captured in each photomicrograph was done.